Natural Resources Canada
Ressources naturelles Canada

Jasper Wildfire Complex 2024 Fire behaviour documentation, reconstruction, and analysis

Information Report NOR-X-433

Northern Forestry Centre
Canadian Forest Service

2025

Canada

The Northern Forestry Centre is one of five centres of the Canadian Forest Service, which has its headquarters in Ottawa, Ontario. This centre undertakes the regional delivery of national projects.

The Canadian Forest Service's main objective is research in support of improved forest management for economic, social, and environmental benefits to all Canadians.

Natural Resources Canada
Ressources naturelles Canada

Jasper Wildfire Complex 2024 Fire behaviour documentation, reconstruction, and analysis

Information Report NOR-X-433
Northern Forestry Centre
Canadian Forest Service

2025

Canada

Library and Archives Canada Cataloguing in Publication

Main entry under title: Jasper Wildfire Complex 2024: Fire behaviour documentation, reconstruction, and analysis.

Aussi disponible en français sous le titre : Complexe d'incendies de Jasper 2024 : Documentation, reconstruction et analyse du comportement du feu.

Issued also on the Internet. Subtitle varies.

Cat no: Fo133-1/433E-PDF
ISBN 978-0-660-78323-9
ISSN: 0831-8247

Canadian Forest Service Information Report NOR-X-433. Northern Forestry Centre, Edmonton, Alberta.

KEYWORDS: Jasper National Park, wildfire, fire behaviour, fuel management, firebrands.

The information contained in this publication is available for public use under the Open Government Licence—Canada version 2.0. You are encouraged to use the data and information available under this licence with only a few conditions. Refer to the Open Government Licence for more information, available at https://open.canada.ca/en/open-government-licence-canada.

Cover photo: The Jasper South Fire on the evening of July 23, 2024, as it advanced northward into the Valley of Five Lakes and toward Mount Tekarra, left background (photo courtesy of Parks Canada, © 2024).

© His Majesty the King in Right of Canada, as represented by the Minister of Energy and Natural Resources, 2025

Natural Resources Canada
Canadian Forest Service
Northern Forestry Centre
5320 – 122 Street
Edmonton, AB T6H 3S5

Information contained in this publication or product may be reproduced, in part or in whole, and by any means, for personal or public noncommercial purposes, without charge or further permission, unless otherwise specified.

You are asked to:

- exercise due diligence in ensuring the accuracy of the materials reproduced;
- indicate the complete title of the materials reproduced, and the name of the author organization; and
- indicate that the reproduction is a copy of an official work that is published by Natural Resources Canada (NRCan) and that the reproduction has not been produced in affiliation with, or with the endorsement of, NRCan.

Commercial reproduction and distribution is prohibited except with written permission from NRCan. For more information, contact NRCan at copyright.droitdauteur@nrcan-rncan.gc.ca.

Recycled paper

Preface

This report on the behaviour of the Jasper Wildfire Complex was undertaken with a clear recognition that the impacts of wildland fire reach far beyond data, models, and scientific understanding. Fire reshapes not only the landscape, but also the lives of the people it touches. We understand that many people in the community of Jasper and beyond were deeply affected by this fire.

First responders and support staff from many communities and agencies came together under extremely difficult circumstances to protect the lives, homes, and livelihoods of the people of Jasper and the visitors to Jasper National Park.

We especially honour the memory of Alberta firefighter Morgan Kitchen, his family, and all the members of the Alberta Wildfire Rocky Mountain House fire base. Morgan died on August 3, 2024, during firefighting operations on the Jasper South Fire. His sacrifice and life of service will always be remembered.

Morgan Kitchen 2000–2024

It is with deep respect for all those affected that we present this report—their experience drives our ongoing efforts to better understand fire behaviour.

Citation

Jasper Fire Documentation, Reconstruction, and Analysis Task Team. 2025. Jasper Wildfire Complex 2024: Fire Behaviour Documentation, Reconstruction, and Analysis. Northern Forestry Centre Information Report NOR-X-433, Natural Resources Canada, Edmonton, AB.

The members of the Jasper Fire Documentation, Reconstruction, and Analysis Task Team are the following:

Field Deployment:
Stefana Dranga, Geoff Goetz, Ginny Marshall, Brett Moore, Daniel Perrakis, Steve Taylor, Dan Thompson

Technical Analysis and Writing:
Matthew Ansell, Luke Collins, Mark de Jong, Rachel Dietrich, Stefana Dranga, Geoff Goetz, Ginny Marshall, Brett Moore, Daniel Perrakis, Steve Taylor, Dan Thompson, Derek Van Der Kamp.

Acknowledgments

Many individuals and organizations assisted in facilitating fieldwork and/or providing data and other materials that helped make this report come together. We acknowledge Al Westhaver (retired), Landon Shepherd, Scott Murphy, Gregg Walker, Elyse Reynolds, and Kris Johnson from Parks Canada; Greg Van Tighem from the municipality of Jasper; Jonathan Boucher, Jean Marchal, Natalie Maslowski, Richard Carr, and Sam Lacarte from Natural Resources Canada; Tanya Letcher from Alberta Forestry and Parks; Brandon MacKinnon from FPInnovations Wildfire Operations Group; Delia Mo and Enoch Leisure from MoLeisureXVentures; various staff members at Marmot Basin and Jasper Park Lodge; and Laura Chasmer, Tristan Skretting, and Emily Jones at the University of Lethbridge, Department of Geography and Environment. We also extend thanks to Marty Alexander, Kelvin Hirsch, and Ian Pengelly for their thoughtful reviews of an earlier draft of this report.

Abstract

Following a highly destructive 2024 wildfire in Jasper, Alberta, a study was completed to describe the behaviour and environmental factors associated with this event. On July 22, 2024, lightning ignited multiple fire starts in the upper Athabasca valley in Jasper National Park following a month-long drought. Three ignitions merged as the South Fire and advanced rapidly toward the Jasper townsite. A separate incident closer to the community initially drew most attention and suppression resources.

Crown fire activity on the South Fire was observed within less than 10 minutes of ignition, indicating that there was no opportunity for effective suppression. Over the next 50 hours, the South Fire exhibited severe to extreme fire behaviour during most daytime hours despite low surface wind speeds. Very high fuel consumption was measured in research plots, partly due to the effects of mountain pine beetle (MPB)–driven mortality 7 years earlier. Plume-driven fire dynamics were evident, including tornado-force fire-generated winds. On the afternoon of July 24, the fire reached steep terrain near the confluence of the Athabasca and Miette rivers. A suspected convection column collapse event occurred as the fire reached treeline and encountered cross-valley winds, sending smoke and embers to the northeast toward the Jasper townsite. The first structures ignited shortly afterward, and the fire ultimately destroyed 358 structures. Hazard reduction treatments successfully reduced crown involvement, particularly treatments implemented less than 10 years before the fire.

This report integrates operational interviews and photographs, field measurements, management records, and modelling to reconstruct the sequence and drivers behind this event. Key contributing factors include drought conditions, rapid ignition and acceleration, continuous and MPB-affected fuels, sustained high intensity, plume-driven behaviour, convection column collapse, and ember transport. The 2024 Jasper Wildfire Complex illustrates the increasing challenge of managing extreme wildland fire events in Canada's evolving fire landscape. By documenting and analyzing this event, this report provides insights into the need for improved understanding and predictive models and to enhance landscape and community resilience to future wildfire threats.

Résumé

À la suite d'un incendie très destructeur en 2024 à Jasper, en Alberta, une étude a été réalisée pour décrire le comportement et les facteurs environnementaux associés à cet événement. Le 22 juillet 2024, la foudre a déclenché plusieurs allumages dans la vallée de la haute Athabasca dans le parc national Jasper après un mois de sécheresse. Trois incendies ont fusionné en un seul, nommé « South Fire », qui a avancé rapidement vers le lotissement urbain de Jasper. Un incident séparé plus proche de la collectivité a initialement attiré le plus d'attention et de suppression de la plupart des ressources.

Une activité de feu de cime a été observée moins de dix minutes après l'allumage du South Fire, indiquant qu'aucune suppression efficace n'était possible. Au cours des 50 prochaines heures, l'incendie South Fire a présenté un comportement de feu sévère à extrême pendant la plupart des heures de la journée malgré des vitesses de vent faibles en surface. Une consumation de combustible très élevée a été mesurée dans les parcelles de recherche, en partie en raison des effets de la mortalité causée par le dendroctone du pin ponderosa (DPP) sept ans plus tôt. La dynamique de l'incendie dirigée par la colonne de convection était claire, y compris des vents générés par les incendies dont la force était comparable à celle d'une tornade. L'après-midi du 24 juillet, l'incendie a atteint un terrain escarpé près de la confluence des rivières Athabasca et Miette. Un effondrement présumé de la colonne de convection s'est produit lorsque l'incendie a atteint la limite des arbres et a rencontré des vents transversaux dans la vallée, projetant de la fumée et des tisons vers le nord-est en direction du lotissement urbain de Jasper. Les premières structures ont pris feu peu après, et l'incendie a éventuellement détruit 358 structures. Les opérations de réduction des risques ont réussi à diminuer l'implication des cimes, en particulier les opérations mises en œuvre moins de 10 ans avant l'incendie.

Ce rapport intègre des entretiens opérationnels et des photographies, des mesures prises sur le terrain, des registres de gestion ainsi que des modélisations afin de reconstruire la séquence des événements et éléments ayant mené à cet incident. Parmi les facteurs contributifs clés figurent les conditions de sécheresse, l'allumage et l'accélération rapides de l'incendie, les combustibles toujours présents et affectés par le DPP, une intensité élevée soutenue, un comportement dirigé par la colonne de convection, l'effondrement de la colonne de convection et le transport de tisons. Le complexe d'incendies de Jasper 2024 illustre le défi croissant de la gestion des événements de feux de végétation extrêmes dans le paysage incendiaire en évolution du Canada. En documentant et en analysant cet événement, ce rapport fournit des renseignements sur la nécessité d'avoir une meilleure compréhension des événements et de leurs modèles prédictifs, ainsi que de renforcer la résilience du paysage et des communautés face aux futures menaces d'incendies.

Contents

List of Figures

List of Tables

Executive summary

Background

On the evening of July 22, 2024, three lightning strikes ignited fires in the Athabasca valley within Jasper National Park, 23 km south of the community of Jasper, Alberta. These fires quickly accelerated and coalesced into the "South Fire," producing a smoke column that was visible from Jasper within an hour. Simultaneously, a fourth ignition was detected about 7 km east of the Jasper townsite, and quickly became the "North Fire," drawing most attention and suppression resources due to its proximity to the community. The rapid acceleration and growth of these fires, especially of the South Fire, prompted an evacuation order for the Jasper townsite and all of Jasper National Park that night.

During the following ~50 hours, the South Fire rapidly progressed northward toward Jasper. Persistent severe to extreme wildfire behaviour made direct suppression efforts impossible. Fire behaviour was most intense when influenced by strong and gusty winds but remained active even when surface winds were light. The fire reached the Jasper townsite in the late afternoon of July 24 during the fastest spread event, following a column collapse event as the fire ascended steep slopes near the Miette-Athabasca valley confluence. This event sent strong surface winds, smoke, and embers downslope toward the townsite; the first structures ignited shortly thereafter. Structure protection measures enabled firefighters to protect two-thirds of the townsite and all critical infrastructure. A total of 358 structures were destroyed, with estimated damages marking this as one of the most destructive wildfires in modern Canadian history.

This report presents the findings of a scientific examination of the 2024 Jasper Wildfire Complex commissioned by Parks Canada and conducted by the Canadian Forest Service (CFS) of Natural Resources Canada to analyze the physical and ecological factors that influenced the 2024 Jasper Wildfire Complex and led to the destruction in the Jasper townsite. The effort incorporated a combination of field observations, documentary evidence from fire management staff, and a multi-faceted modelling and analysis effort.

Key contributing factors

1. Drought: Lack of rainfall and a heat wave in the month before the fire significantly reduced fuel moisture, making nearly all surface fuels available for combustion. This level of aridity increased the spread rate and intensity of the fire.

2. Continuous and beetle-killed fuels: Uninterrupted mature conifer forest created a wind-aligned corridor for fire spread in the upper Athabasca valley. Tree mortality caused by the mountain pine beetle (MPB) altered the structure and availability of the fuel complex. The loss of foliage caused accelerated drying of the surface fuels, and tree mortality led to an abundance of dry woody fuel, greatly increasing fuel consumption and fire intensity.

3. Rapid ignition and acceleration: Three wildfires were ignited concurrently by lightning 23 km south of Jasper on the evening of July 22. Strong convective winds and dry fuels facilitated rapid fire spread. High-intensity crown fire behaviour developed within minutes, beyond the capacity of initial attack resources. Within a few hours, the fires had merged and surpassed 3,500 ha in extent.

4. Sustained fire intensity and growth: The fire spread steadily down the Athabasca River valley over the course of 50 hours, with several prolonged periods of intense fire behaviour. Significant burning persisted overnight due to severe drought and fuel conditions.

5. Plume-driven fire behaviour: High fuel consumption, moderate surface winds, and steep slopes promoted towering convection columns with strong updrafts. Fire-generated wind speeds near the main column are estimated to have reached up to 200 km/h. Ambient winds outside the active fire area remained light to moderate.

6. Column collapse and ember transport: A powerful convection column persisted as the fire spread up steep slopes west of Jasper until it collapsed near the tree line and the junction of the Athabasca and Miette valleys. The column collapse likely transported embers more than 2 km into receptive fuels in and near the Jasper townsite, igniting spot fires and possibly leading to the urban fire. However, the precise origin of the structure-igniting embers remains uncertain.

7. Fuel treatments: Hazard reduction treatments around Jasper, implemented since 2003, moderated fire behaviour in fuel patches surrounding the townsite. In treated areas, crown involvement, fuel consumption, and estimated fire intensity were lower. This reduced ember production and limited the exposure of nearby structures to ignition from nearby crown fire activity; treatments also reduced the exposure of firefighters in the townsite to extreme fire intensity levels.

8. Complex mountain winds: Although strong winds were observed intermittently at ridgetop and higher elevation stations, surface wind speeds in the valley

bottom remained relatively low, as measured by standard wind sensors. This makes this event somewhat unique among recent fire disasters. Atmospheric influences such as fire-induced convection and complex vertical wind profiles may have played a significant role in accelerating fire spread but are difficult to observe and incorporate into prediction models.

Conclusions and management implications

This report documents the 2024 Jasper South Fire as a case study of a complex wildfire event associated with major losses. Several management considerations emerged from this analysis.

Increasing hazard: Over a century of fire exclusion in the upper Athabasca valley shifted the landscape from a mix of open and closed forests to a more uniform, fire-prone structure susceptible to forest health concerns, increasing the potential for large and uncontrollable fires.

Rapid growth and response limits: Although most wildfires are contained quickly, the Jasper South Fire exemplifies how rapidly worsening conditions can exceed response capacity. Success in limiting losses depended on early recognition of extreme fire potential, which enabled a timely evacuation.

Extreme intensity and plume dynamics: Complex meteorological interactions caused a downburst that transported embers into Jasper, highlighting gaps in current predictions of such events.

Enhancing community resilience: Wildfire disasters are driven by a common sequence of factors—severe fire potential, extreme burning conditions, multiple ignitions within communities, and rapidly developing fire behavior exceeding firefighting resources. Strengthening resilience requires an integrated approach, including landscape risk assessment and management, increasing fire-resistance in the built environment, and effective pre-response planning.

The Jasper South Fire exemplifies the increasing challenge of managing extreme wildfire events in Canada's evolving fire landscape. By documenting and analyzing this event, this report provides insights to improve predictive models, refine fire management strategies, and enhance resilience to future wildfire threats.

1. Introduction

1.1 Overview and background

On July 22, 2024, four separate ignitions were detected upper Athabasca River valley in Jasper National Park (JNP), Alberta. Three of these were lightning-caused and merged within minutes to form the Jasper South Fire, which spread 23 km northward down the valley over the following 2 days and into the municipality of Jasper (**Figure 1**). The evening the fires were discovered, approximately 25,000 people were evacuated from the area; 358 structures were ultimately destroyed.

Initial estimates of economic loss make the 2024 Jasper Wildfire Complex the second most destructive wildfire in modern Canadian history, surpassed only by the 2016 Horse River Wildfire in Fort McMurray, Alberta [1]. This event followed the unprecedented 2023 wildland fire season, which broke multiple Canadian records for area burned, the number of large fires, evacuees, and carbon emissions [2]. The 2024 fire season began more slowly, but by late July, a heat wave and lack of rainfall created deep drying conditions and elevated fire danger levels across Jasper National Park and surrounding areas.

On July 29, 2024, following the initial damage assessment, Parks Canada requested assistance from the Canadian Forest Service (CFS) of Natural Resources Canada (NRCan) to document fire behaviour on the Jasper Wildfire Complex. The CFS Wildfire Intelligence and Predictive Services (WIPS) unit (**Box 1**) quickly assembled a Documentation, Reconstruction, and Analysis Task Team (DRATT) comprising researchers and analysts with expertise in fire behaviour and wildfire operations. The team deployed to Jasper in early August to commence a reconstruction of the fire behaviour associated with these events while the fire was still active and most personnel associated with the initial fire spread and community impingement were still present.

Box 1. The Canadian Forest Service Wildfire Intelligence and Predictive Services unit

In 2023, the Canadian Forest Service established the Wildfire Intelligence and Predictive Services (WIPS) unit. Although the CFS is not a land manager or primary wildfire response agency, the WIPS unit was created to coordinate and formalize the science-based fire management resources that the CFS has historically provided on an ad hoc basis to Canadian fire management agencies. The WIPS unit focuses on developing and maintaining advanced fire information and modelling systems and offers operational support such as wildfire detection, prediction, and fire behaviour analysis. The unit also provides technical support to the Canadian Interagency Forest Fire Centre (CIFFC), facilitating operational planning and resource sharing.

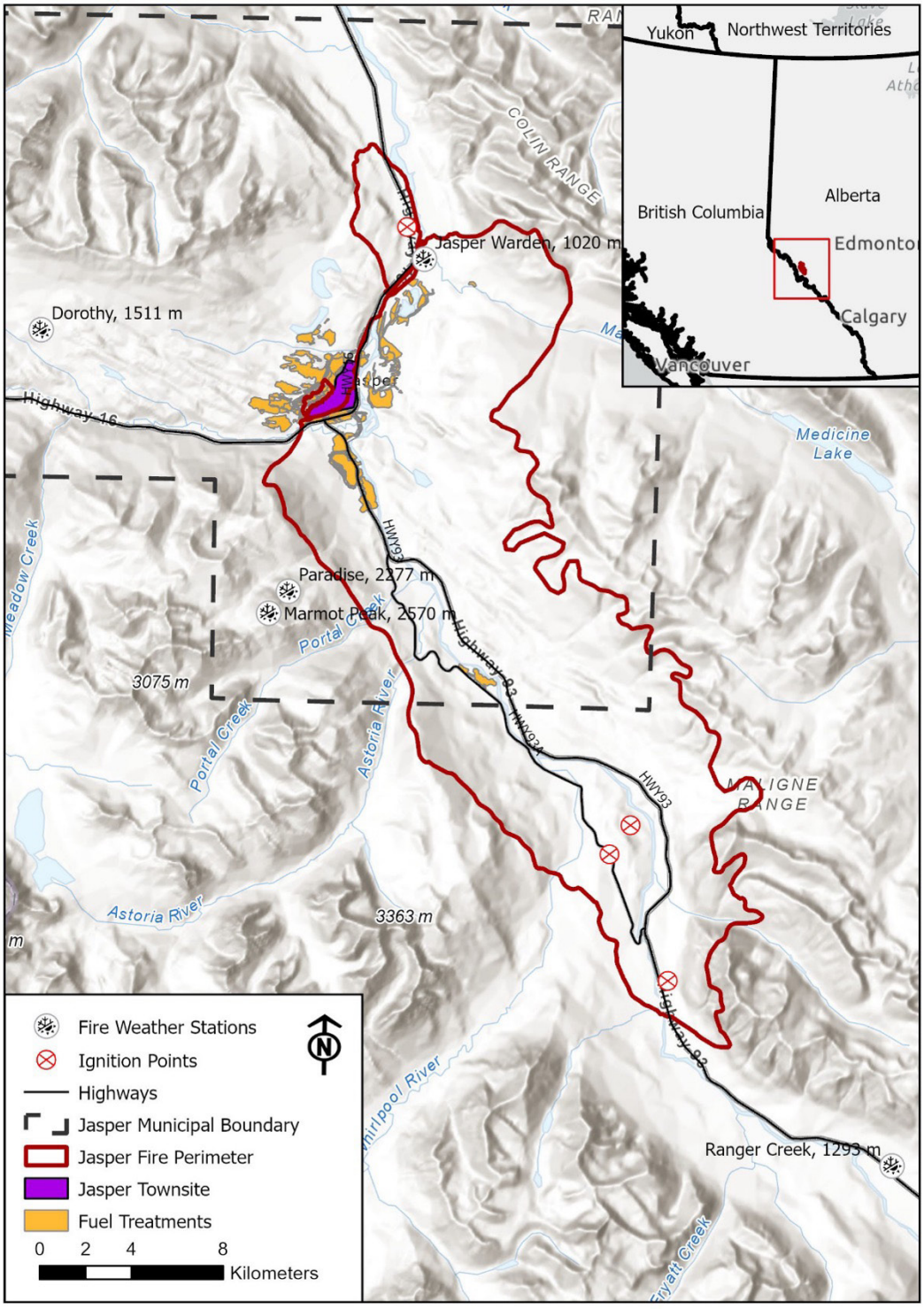

Figure 1. Overview map of the Jasper Wildfire Complex. The perimeter shows the combined extents of the South and North Fires as of August 2, 2024 (the fires merged on July 24, 2024). The townsite, key weather stations, and the extent of hazard reduction treatments are denoted.

1.2 Fire behaviour and fire environment objectives

The objectives of the Jasper Wildfire Complex DRATT were as follows:

1. **Identify ignition and spread factors:** Analyze the environmental and situational factors contributing to the ignition, acceleration, and spread of the fire until it reached the Jasper townsite on July 24, 2024.
2. **Document fire behaviour evidence:** Assemble and analyze photo and video evidence collected by fire management personnel, in addition to satellite imagery, to map fire spread patterns and direction.
3. **Examine fuel-related impacts:** Investigate the role of mountain pine beetle (MPB)–caused tree mortality and mechanical fuel hazard reduction treatments in influencing fire behaviour.
4. **Analyze wind patterns:** Study wind speed and direction using weather station data, reanalysis, and modelling products, including wind profiles with altitude.
5. **Identify extreme fire phenomena:** Document signs of extreme fire behaviour, including fire-induced winds, fire whirls, pyro-cumulonimbus clouds, and long-range ember transport.
6. **Reconstruct fire behaviour near the townsite:** Provide a detailed account of fire behaviour as the fire approached the Jasper townsite on July 24, 2024.

1.3 Structure and scope of the report

The reconstruction and analysis is based on documentation collected after the majority of the area burned and damage occurred, including:

1. Interviews with fire personnel present during the critical events from July 22 to 24, 2024: Information was requested related to fire management timelines including evacuations, aviation operations, and suppression efforts and personal observations of weather and fire-related phenomena, including smoke, atmospheric inversions, and turbulence. Approximately 8,700 photo and video files were acquired for analysis
2. Field observations related to fuel consumption, spread direction, canopy involvement, and ember sampling conducted from August 1–14, 2024
3. Analysis of vegetation and climate data sets provided by Parks Canada
4. Information acquired from academic researchers and public data repositories.

The structure of the report is as follows:

Section 2. Fuel Complex and Condition describes the fuel types present within the Athabasca River valley, the impact of the 2013–2020 MPB outbreak on fuel conditions, and the mechanical fuel treatments that were carried out from 2003 through 2022 to address the fuel hazard.

Section 3. Fire Weather describes the antecedent weather conditions leading up to the fire and provides an overview of fire weather during the main fire spread event.

Section 4. Fire Growth Chronology documents detailed weather, fire spread, and behaviour in 5 half-day intervals during the critical 50-hour period based primarily on analyses of weather station data, photographic evidence, and satellite imagery.

Section 5. Fire Severity and Behaviour Analyses presents the findings from several detailed analyses: fire severity analysis from satellite imagery, fuel consumption measurements, and a discussion of overall calculated fire behaviour characteristics.

Section 6. Summary and Conclusions assembles the findings and evidence together to summarize the most probable fire behaviour processes associated with the incident. The main findings and interpretations relevant to fire managers are also provided in this section.

An extensive Appendices section includes **Appendix A—Methodology**, containing detailed methods related to the analyses. Additional information related to the reconstruction is in **Appendix B—Supplementary Information**.

Although the Jasper North Fire is referenced, it is not the primary subject of this report. It was quickly established that the South Fire was the event that ultimately affected the Jasper townsite and caused the majority of the damage. Throughout this document, references to "the fire" denote the South Fire, except where noted.

An analysis of structural damage, evacuation efforts, and fire management tactics was beyond the scope of this report. Separately, the FPInnovations Wildfire Operations Group (https://wildfire.fpinnovations.ca/) examined fire behaviour in the interface between the Athabasca and Miette Rivers and Jasper townsite and structure losses within the wildland-urban interface and townsite. Although the CFS DRATT and FPInnovations teams shared some personnel and observations, their analyses were conducted independently.

Although Parks Canada and other partners supplied essential data and documentation to support the analysis, all scientific interpretation was carried out by the DRATT. This report emphasizes firsthand observations and

measurements of wildfire behaviour (**Box 2**), supplemented by references to scientific studies and reports where appropriate. Certain transient fire phenomena—such as wind gusts, convection column collapse, and ember deposition—were not fully captured by photographs, sensors, or other measurement devices. In these cases, the most likely mechanisms have been inferred using established physical principles based on eyewitness accounts by on-site personnel.

Key fire behaviour metrics, including spread rate, intensity, and crowning tendency, are presented along with comprehensive descriptions of weather and fuel conditions. Quantitative measures, such as head fire intensity (expressed in kW/m), are used to support accurate interpretation for wildland fire professionals and researchers. The basis for most terminology specific to forest fire science in this report is the Canadian Forest Fire Danger Rating System (CFFDRS), a standard framework for assessing fire danger and predicting fire behaviour across Canada [3], [4], [5] and defined in the CIFFC Glossary (https://glossary.ciffc.ca/). Some background on predicting fire behaviour in mountainous terrain is discussed in **Box 2**. For an introduction to fire behaviour prediction, the User Guide to the Canadian Forest Fire Behavior Prediction System [6] is recommended.

For the convenience of the reader, a list of abbreviations used in the text can be found in Appendix B11. All times are given in mountain daylight time (MDT), unless otherwise noted.

Box 2. Fire behaviour, mountain weather, and modelling limitations

Wildfire behaviour describes how wildland fuels ignite, flames develop, and fires spread [7]. Wildfire behaviour research draws on interdisciplinary insights from forestry, ecology, meteorology, climate science, thermodynamics, fluid mechanics, and other fields [7] to help identify the mechanisms driving wildfire activity and enable predictions of how fires spread through complex landscapes. Traditionally, fire behaviour has been viewed through the interactions of three key elements comprising the fire environment: fuels, weather, and topography, often referred to as the "fire behaviour triangle". A single factor can dominate in some situations – extreme weather, for example, tends to override variations in fuel type [8], while in low wind situations, fuel conditions may be most influential. However, these factors do not exist in isolation and many interactions between separate fire environment variables are important. Surface fuel moisture, for example, is highly sensitive to the effects of fuel structure and topography on the microclimate within forest stands [9], [10], [11]. Interactions between the three factors and the fire itself also provide continuous feedbacks to atmospheric processes, such as fire-induced winds [12]. Some of these interactions are currently only implemented in complex fire-atmosphere models [13] and are not well validated [14] or implemented operationally [15].

Fire behaviour prediction is particularly challenging in mountainous terrain, where complex variations in slope, aspect, and elevation exert strong influences on air currents and fire spread [16]. Valleys can channel winds, increasing speed and turbulence. There is a tendency for local winds to blow upslope during the day, and downslope at night due to diurnal heating and cooling. Higher elevations are generally cooler, but temperature inversions can trap cool air (and smoke) in valley bottoms overnight. As inversions lift due to daytime heating, sudden increases in fire intensity can occur [17].

Temperature, relative humidity (RH), and fuel moisture vary with elevation. Temperature and RH typically decrease with elevation and increase on south- and west-facing aspects, especially with direct sunlight, whereas fuel moisture increases with elevation and on north- and east-facing aspects. However, nighttime RH recovery can be poor at upper elevations, keeping fuels dry overnight. Fires spread faster upslope due to preheating of fuels above the flames, which may contribute to convection column development. However, fire spread direction and spread rate are influenced by the interaction of wind and slope. Furthermore, although burning debris can roll down steep slopes, steep slopes and wind patterns can also carry embers ahead of the main fire.

Canada's highest-resolution operational weather forecast model has a horizontal resolution of 2.5 km near the surface [18], although an experimental version used in this report has a resolution of 1 km. Although these models may capture the effects of topography on wind channeling, they do not resolve upslope and downslope winds or microclimate variations in complex terrain.

2. Fuel complex and condition

2.1 Fire history and fuel dynamics of the upper Athabasca valley

The composition and characteristics of live and dead biomass that combust to sustain a wildland fire are collectively referred to as the fuel complex [19]. The loading (quantity of combustible material per unit area), composition (species mix and condition for dominant vegetation), structure (arrangement in space), continuity (vertical or horizontal gaps), chemistry, and moisture content (greatly influenced by weather) of fuels all are known to influence wildland fire behaviour [10]. Fuel properties are dynamic. The moisture content in dead fuels changes daily to hourly with weather, whereas live fuel moisture varies seasonally. Over years to decades, ecological processes including vegetation growth, natural mortality and decomposition, natural disburbances such as wildland fires, and insect outbreaks alter fuel loading, structure, and species composition.

The fuel complex involved in the Jasper South and North Fires (Section 2.3) was typical of vegetation communities in the central Canadian Rocky Mountains, Eastern Continental Ranges ecoregion [20]:

- Montane zone (approximate elevation, 1000–1350 m): dominated by uneven-aged Douglas-fir (*Pseudotsuga menziesii*), interior lodgepole pine (*Pinus contorta*), and trembling aspen (*Populus tremuloides*) in valley bottom locations, with white spruce (*Picea glauca*) found in well-drained riparian areas.
- Lower subalpine zone (approximate elevation, 1350–1600 m): characterized by lodgepole pine, Engelmann spruce (*Picea engelmanii*), and subalpine fir (*Abies lasiocarpa*) in lower- and mid-slope locations.
- Upper subalpine zone (approximate elevation, 1600–2200 m): primarily Engelmann spruce and subalpine fir, in mid- and upper-slope locations

The treeless alpine tundra zone is found at higher elevations and along ridgelines. All forest stands were experiencing the effects of varying degrees of fire suppression and exclusion, a pronounced change affecting vegetation in dry forests across North America during the past century.

Before the 19th century, fire activity in the Canadian Rocky Mountain National Parks was historically frequent, driven by both lightning and Indigenous burning practices [21], [22]. A pattern of frequent, mixed-severity fires maintained a diverse vegetation mosaic with lower fuel loading and susceptibility to large crown fires, particularly in montane forests. Sampling of charcoal in Little Trefoil Lake near Jasper Park Lodge indicated evidence of 55 fires in the past 3500 years, with stand-replacing fire return intervals of approximately 50–115 years [23]. A separate study used evidence from fire scars and post-fire cohorts in a site 12 km north of the Jasper townsite, and identified a mixed-severity regime with mean fire return intervals of 14–165 years, or approximately 1 fire within the study area every 20 years [24]. The forests of the upper Athabasca valley originated primarily from fires in 1889 and 1906, although isolated older trees were common, particularly in the montane zone [24], [25]. Historical photographs from the 1915 M.P. Bridgland survey, recaptured by the Mountain Legacy Project, provide visual evidence of the mosaic of mature forests and younger regenerating stands after these fires [26]. This vegetation mosaic was disrupted by the fire control mandate enacted in the 20th century, which has led to denser, more continuous forests across the Rocky Mountains and nearby cordilleran regions [27], [28], [29], [30].

Beginning in the 1980s, Parks Canada began to restore natural fire regimes, primarily via prescribed burning, which helped reduce fuel loading and connectivity in treated areas [31]. Despite these efforts, no prescribed fires occurred within the Jasper South Fire perimeter area in recent decades. Since 2000, fuel management has primarily focused on hazard reduction around the Jasper townsite and campgrounds (Section 2.4 and Section 5.2).

2.2 Mountain pine beetle attack extent and severity

The mountain pine beetle (MPB) outbreak that began in central British Columbia in the early 2000s represents one of the most significant continental-scale shifts in forest vegetation and fuel conditions in the past century. It continues to influence ecosystem dynamics in northern British Columbia (BC), Alberta, and the Rocky Mountain National Parks [32], with the potential to spread into the boreal and subboreal forests of central and eastern Canada [33]. Although scientific debate persists regarding the influence of the outbreak on fire danger and behaviour [34], extreme fire seasons in BC have revealed highly flammable landscapes in the wake of extensive pine mortality [2], [35]. One recent study found that MPB-affected areas in BC experienced 1.7 times more large lightning-caused fires than unaffected areas; however, there was a reduced likelihood of large human-caused fires [36].

Ecologists and fire modellers generally recognize MPB-affected trees in categories based on time since beetle attack: the red attack stage (1–5 years), grey attack stage (5–15 years) and post-epidemic attack stage (>15 years) [37], [38]. **Figure 2** shows the estimated distribution of year of attack based on aerial Forest Insect and Disease surveys conducted by NRCan in Jasper National Park [39], extracted to the extent of the Jasper Wildfire Complex perimeter on August 2, 2024. Peak outbreak severity around the Jasper townsite and in the upper Athabasca valley occurred from 2016 through 2018. As a result, most MPB-affected forest stands within the fire perimeter were in the early grey stage, 6 to 8 years post-attack. In these stands, most pine foliage had fallen to the forest floor, while the majority of branch structure remained intact in the canopy [40], [41].

Although canopy changes following MPB have been documented in previous studies, the consequences for fire behaviour remain varied and difficult to predict [42], [43]. This unpredictability stems from competing feedback between altered fuel structure and microclimate (Appendix A1) as well as limitations in how most fire models represent the combustion of woody debris [44], [45]. Finally, few studies have assessed MPB effects using representative field-scale experiments.

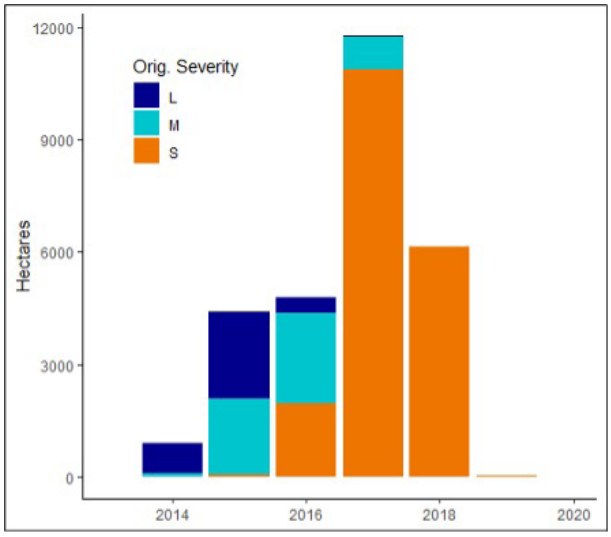

Figure 2. Annual distribution of mountain pine beetle (MPB) outbreak area, 2014–2020, within the Jasper South Fire perimeter on August 2, 2024. Area affected was calculated from annual aerial survey data [39]. Colours represent originally mapped outbreak severity (L-low, M-moderate, S-severe), though many low and moderate patches subsequently increased in severity by 2017 or 2018. By 2019, the MPB outbreak had collapsed throughout the park, and the newly affected area remained small (<500 ha) from 2020 through 2022.

2.3 Vegetation and fuel complex

Fuels can be assessed in detail through field measurements, but they are frequently mapped more broadly using vegetation-based classification systems [3], [46]. Detailed forest inventory information was provided by Jasper National Park's Vegetation Resource Inventory (VRI) program. This dataset combines interpretation of high-resolution orthorectified imagery with ground-based surveys to assess and map forest attributes. The most recent VRI map, derived from July 2022 imagery, includes a range of stand-level forest attributes such as species composition, mortality, canopy closure, tree height, basal area, age, disturbance history, understorey characteristics, and landform. Stand characteristics are mapped at the polygon level, with an average size of approximately 5 ha. For this analysis, vegetation types within the Jasper Wildfire Complex perimeter were extracted from the VRI layer and reclassified for interpretation and display.

A simplified VRI vegetation cover map is shown in **Figure 3**, combining vegetation inventory and tree mortality data. Forest stand types are described by the leading live species, defined as a single species composing 75% or more of the basal area. Engelmann spruce and subalpine fir were grouped (spruce-balsam) due to their frequent overlap and similar crown structure. Mixed species stands include mixedwood (>25% of basal area of both live conifer and deciduous species) and mixed-conifer (>75% conifer, split between 2 or more live species, excluding spruce-balsam); however, both mixed types represented only a small portion of the total vegetation cover. Detailed vegetation descriptions within the Jasper Wildfire Complex perimeter area are provided in **Table 1.**

Before the fire and MPB disturbances, lodgepole pine was the dominant species across the landscape, occurring in both pure and mixed stands. At the time of the fire, approximately 90% of the area within the perimeter was forested, with lodgepole pine– and spruce-balsam–leading stands each comprising about 43% of the forested area. Douglas-fir–leading stands accounted for roughly 8% of the total area (9% of the forest), whereas deciduous stands, non-forest (defined as canopy cover <10%, excluding dead pine) and non-fuel zones (water bodies, etc.) each made up about 5% of the landscape. Dead pine resulting from MPB mortality was a significant component of the fuel complex, with standing dead pines in various states in most stands; the majority (59%) of conifer and mixed forest area are estimated to have been in a pre-fire state of moderate (35–64% dead) or severe (≥65% dead) mortality (**Table 1**). Note that these classifications reflect higher levels of pine mortality than those used in earlier MPB studies in western Canada [47], [48].

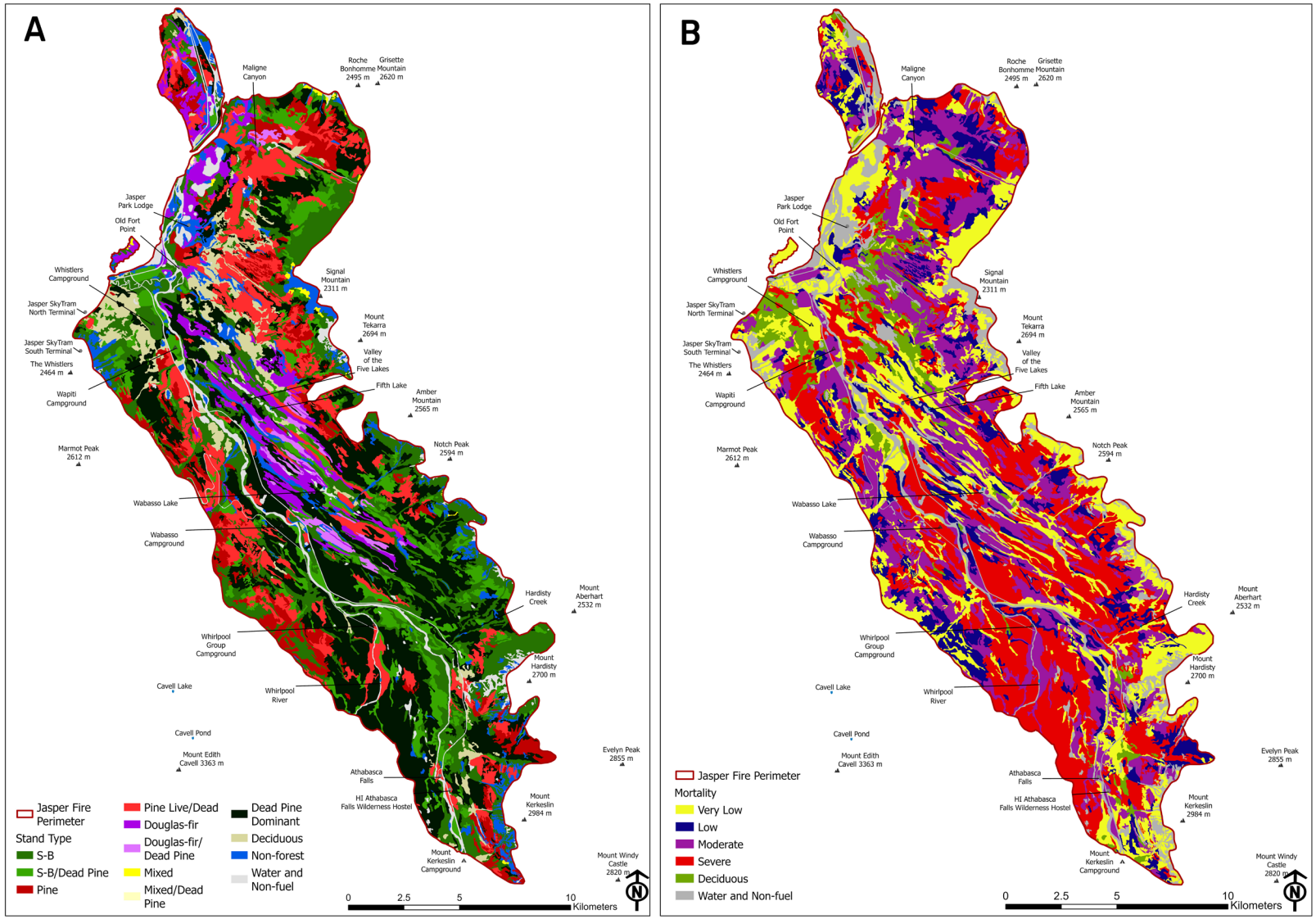

Figure 3. Pre-fire vegetation cover type for the Jasper Wildfire Complex based on classified overstorey species and mortality. **A**, Forest stand type map, in which Engelmann spruce and subalpine fir (balsam) were grouped as a single vegetation type (S-B) due to their frequent overlap and similar crown structure. S-B, lodgepole pine, and Douglas-fir refer to pure (>75% by percent cover) stands of each of these based on leading species, with very low or low (≤34%) overstorey mortality (by dead basal area and stems/ha, equally weighted). Mixed refers to mixed-species stands (≤75% cover by dominant live species). S-B/dead pine, pine live/dead, Douglas-fir/dead pine, and mixed/dead pine indicate the same species classes with intermediate levels of pine mortality (35–64%). Dead pine dominant indicates any forest stand with ≥65% overstorey mortality. **B**, Overstorey tree mortality map, showing very low, low, moderate, and severe overstorey mortality classes, indicating 0–9%, 10–34%, 35–64%, and ≥65% mortality, respectively. Deciduous stands include those where trembling aspen or other broadleaf species represent >75% of overstorey cover. Non-forest stands were those with <10% canopy cover, excluding dead pine. Dead Pine-Dominant polygons in panel A are identical to Severe polygons in panel B.

Table 1. Pre-fire stand type and mountain pine beetle (MPB)-caused mortality class within the Jasper Wildfire Complex perimeter. See **Figure 3** for MPB mortality classes.

Vegetation Type (leading species)	MPB Severity Class (ha, % of affected)				Total area (ha)	% Area
	Very Low 0 – 9%	Low 10 – 34%	Moderate 35 – 64%	Severe ≥65%		
Lodgepole pine	540 (2)	1,843 (7)	4,265 (16)	5,815 (21)	12,463	39
Spruce-Balsam	5,233 (19)	1,802(7)	2,850(10)	2,403 (9)	12,288	38
Douglas-fir	1,331 (5)	361 (1)	472 (2)	364 (1)	2,528	8
Mixed species	74 (0)	0	9 (0)	4 (0)	87	0
MPB affected forest						
Area (ha)	7,178	4,006	7,596	8,586	27,366	85
Percent	26	15	28	31	100	
Deciduous [a]	-	-	-	-	1,564	5
Non-forest	-	-	-	-	1,741	5
Water and non-fuel	-	-	-	-	1,510	5
Total Area					32,281	100

[a]Deciduous type stands include unspecified proportions of dead trees, mostly in the 0–9% mortality class.

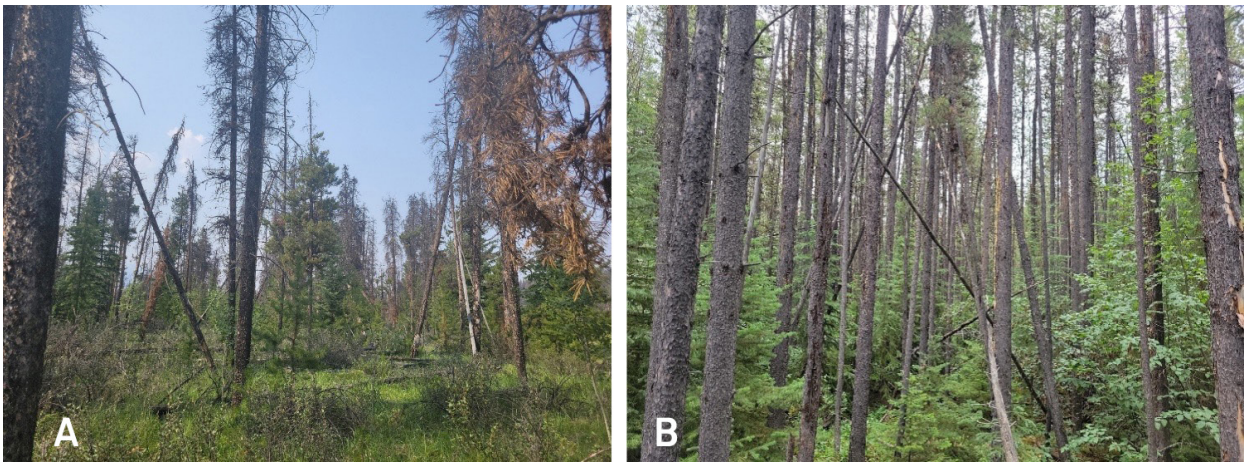

Figure 4. Fuel structure in the upper Athabasca valley. **A**, Typical, low-density, grey attack stage pine stand at lower elevations near Highway 93 South. This location was unburned due to an adjacent gravel pit. Most needles have dropped from mature pine trees, but fine branch structure remains mostly intact. **B**, Typical pre-fire structure of a lower subalpine zone (elevation, ~1450 m) mixed lodgepole pine–spruce-balsam stand with minimal overstorey mortality, outside the fire perimeter. In addition to the overstorey conifers, there is a dense spruce and subalpine fir understorey that can act as ladder fuel for crown fire initiation.

For operational fire behaviour assessment, vegetation and biomass are frequently classified into fuel types. The Canadian Fire Behaviour Prediction (FBP) System is a sub-system of the CFFDRS (noted in Section 1.3) that generates quantitative fire behaviour outputs (rate of spread, fire intensity, etc.) based on fuel type, weather, and topographic inputs. The FBP System fuel types [4], [5], [49] are discussed further in Section 5, in the context of fire behaviour calculations, and a sample FBP fuel type map is shown in Appendix B1.

Figure 4 shows photos of forest stands representative of the state of lodgepole pine and spruce-balsam forests prior to the fire. As noted previously, overstorey breakdown was underway among dead pines: foliage had largely disappeared from the canopy and become decomposing litter; dead branch wood and bole wood fuels were beginning to shift from the canopy to the forest floor.

During the August DRATT deployment, the team conducted crown fire and fuel consumption surveys within the fire perimeter (Section 5.5). This work made use of a highly fortuitous dataset of fuel structure plots collected by students and faculty from the University of Lethbridge [41]. Remeasuring these plots resulted in a dataset that formed the basis for the estimation of fuel consumption, a major determinant of overall fire intensity.

2.4 Fuel treatments

To address wildland fire threats, managers are increasingly implementing fuel management treatments such as thinning and prescribed fire. These projects attempt to alter forest stand structure by reducing the loading of certain components of the fuel complex, generally to reduce potential fire activity. Thinning treatments involve partial harvesting of canopy trees. Thin-from-below treatments (also called low thinning), target high-density stands to reduce the continuity of ladder and canopy fuels and create conditions less conducive to crown fire [50], whereas thin-from-above treatments (also called crown thinning) involve selective removal of dominant and co-dominant trees to increase spacing, reduce crown density, and lower active crown fire hazard by lowering the canopy bulk density [41]. In wildfire risk reduction, thin-from-above treatments are commonly applied to stands experiencing high mortality, with aggressive removal of standing dead trees and highly flammable species, such as spruce. Given limited opportunities for experimental fire research, much of our current understanding of how thinning treatments influence fire behaviour in North American conifer forests is derived from wildfire case studies or from modelling with limited validation [51], [52], [53]. Ultimately, conifer fuel management treatments aim to reduce the potential for crown fire initiation and spread, thereby reducing fire intensity, spread rate, and spotting behaviour. The overall goal is to enhance the safety and effectiveness of suppression operations and improve overall public safety and community resilience in high-risk areas. Mechanical fuel treatments involve the selective removal of trees (living or dead) and woody debris; prescribed fire can also be a type of fuel treatment, and thinning and burning can be combined. However, no treatments involving prescribed fire were conducted within the Jasper South Fire perimeter since park establishment.

From 2003 through 2022, a total of 1,518 ha of mechanical fuel treatments were implemented to reduce fire hazard in the Jasper townsite and adjacent wildland-urban interface (campgrounds, developments, road corridors; (**Figure 1**). Treatment specifications varied somewhat over time but overall, were a mix of thin-from-below and thin-from-above mechanical treatments aimed at reducing the potential for extreme crown fire behaviour and improving fire suppression opportunities. Ladder and canopy fuels were cut by hand or machine to reduce stand density and canopy fuel loads. Forested stands with significant forest health issues (i.e. mortality due to MPB) were prioritized. Additional objectives were frequently specified, including enhancing wildlife habitat, ecosystem integrity, cultural values, and visual quality.

Analysis of fuel treatment impacts on fire behaviour, including crown fraction burned, char height, and fuel consumption, can be found in Section 5.2.

3. Fire weather

3.1 Conditions preceding the fire

The snowpack across the region during the winter of 2023–2024 was generally below average. At Yellowhead Pass, approximately 800 m higher and 30 km west of the Jasper townsite, a notably low snowpack was recorded based on observations from 1996 through 2023. Despite this, snow disappeared only a week earlier than average. In contrast, at the Marmot Basin ski hill, 925 m above and 8 km south of the Jasper townsite, the late 2023–2024 season snowpack was approximately 90% of the average. At the Jasper Warden station, a snow depth of more than 1 cm was last recorded on March 29.

During the month of June 2024, typically the wettest month of the year, very little rain fell. Dry conditions and warm temperatures (**Figure 5A**) led to an elevated Buildup Index (BUI; **Box 3**) during that month relative to a 62-year climatological record (**Figure 5B**).[1] However, in late June and early July, a significant amount of rain fell at the Jasper Warden station, reducing the BUI to a near-median level. In early July a large blocking high-pressure system formed over western North America, as evidenced by a large positive anomaly in the 500 mbar geopotential height shown in **Figure 6A**. These synoptic conditions led to sustained warm and dry weather in the region as indicated by a strong negative anomaly in the daily precipitaton rate (**Figure 6B**). No daily rainfall greater than 2 mm was recorded at the Jasper Warden Station or nearby stations from July 1–22, 2024, while record-high temperatures were recorded in the days leading up to the fire (**Figure 6A**). During that 23-day span, the BUI increased rapidly from a near-median value to an extreme level (BUI of 169), the highest value recorded for that time of year (**Figure 6B**) and above the 99th percentile for all fire season values (May–September). On July 22 there were 55 uncontrolled fires in Alberta and 149 uncontrolled fires in British Columbia.

Because the BUI is calibrated to conditions in closed conifer forests (**Box 3**), it is likely that the fuel drying was even greater than expected due to the canopy loss from the MPB attack discussed in Section 2.2. Loss of canopy cover is associated with increased wind speeds and solar radiation at the forest floor [54]. A modelling exercise was undertaken to simulate the change in the forest floor microclimate to generate an "enhanced BUI" (**Figure 5B**). This analysis suggested that a further 38% increase in the effective BUI was due to this loss of cover (Appendix A1).

In the days preceding ignition, the persistent high-pressure system that led to dry and warm conditions began to break down as a low-pressure system moved inland from the Pacific Ocean. This system generated significant instability throughout the region as indicated by high values of Convective Available Potential Energy (CAPE; Figure S-6 in Appendix B3) CAPE is a measure of how unstable the atmosphere is, that is, how supportive the atmosphere is to vertical convective activity and the development of thunderstorms. Unstable atmospheric conditions can promote extreme fire behaviour [55].

Regional smoke also affected the area at this time, from fires south of Jasper National Park in eastern BC, and across the western boreal forest region from Saskatchewan to northeastern BC.

[1] This section uses the full 1962–2023 fire weather record when discussing Fire Weather Index System components since the longer record captures infrequent but important droughts. The 1991–2020 climatology is used when discussing monthly anomalies of temperature and precipitation in accordance with Environment and Climate Change Canada's best practices.

Box 3. The Canadian Forest Fire Weather Index System

The Fire Weather Index (FWI) System [56] is a major sub-system of the CFFDRS (Section 1.3) that is designed as a bookkeeping system to track fire danger throughout a wildland fire season. The system uses three primary codes (unitless) that react at different speeds to changes in weather: the Fine Fuel Moisture Code (FFMC), Duff Moisture Code, (DMC) and Drought Code (DC). These codes are calculated using physical principles to approximate drying and wetting processes and are empirically calibrated to boreal pine forests with a closed canopy. The FFMC is the fastest-reacting component, suitable for estimating the flammability and reactivity of conifer needle litter at the top of the forest floor, whereas the DC is the slowest-changing component, tracking the gradual buildup of drought over weeks to months, requiring significant rainfall to decrease. These three indices are combined with wind speed to generate indices of overall fire spread and danger, the Initial Spread Index (ISI), Buildup Index (BUI) and Fire Weather Index (FWI). The system is traditionally based on a single daily calculation at noon local standard time, but can also be applied to hourly observations, or a combination of daily components with hourly winds [57]. Since its development, the FWI System components have been found to perform well as predictors of fuel moisture in Canadian forests [58] and are routinely mapped as decision support tools for Canadian fire management agencies [59]. The FWI System has also been adopted or adapted in several other countries. Refinements are presently underway for a significant update the system, due to be released in 2025 [60].

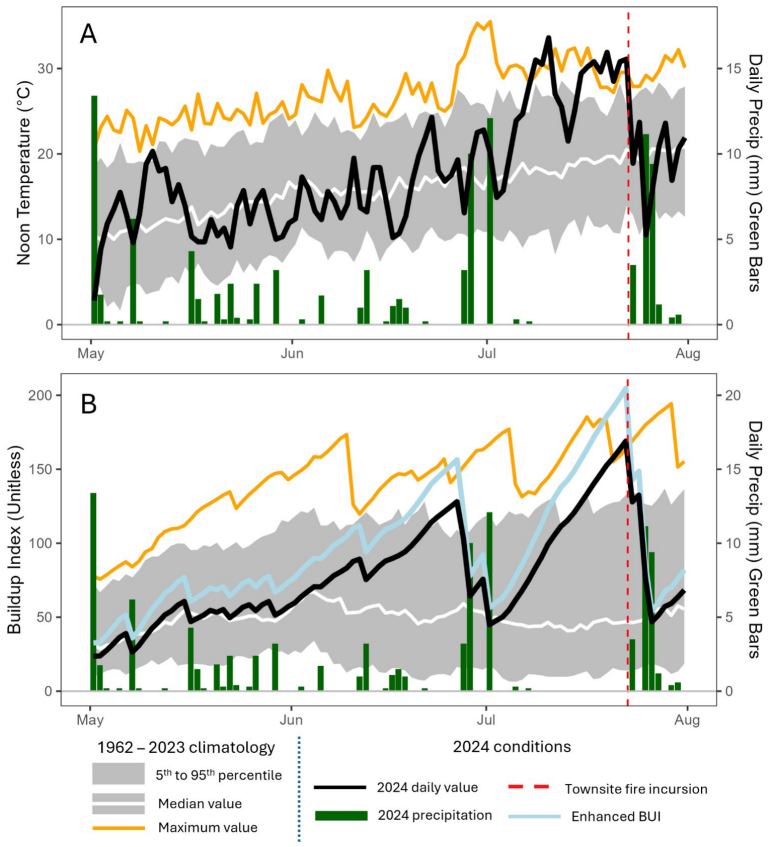

Figure 5. May–July 2024 weather from the Jasper Warden Station compared with 1962–2023 climatology. **A**, Noon air temperature. **B**, Daily BUI. The enhanced BUI includes the impact of MPB-driven defoliation on fuel drying. For periods when the Jasper Warden weather station was not recording, interpolated values from nearby stations are used.

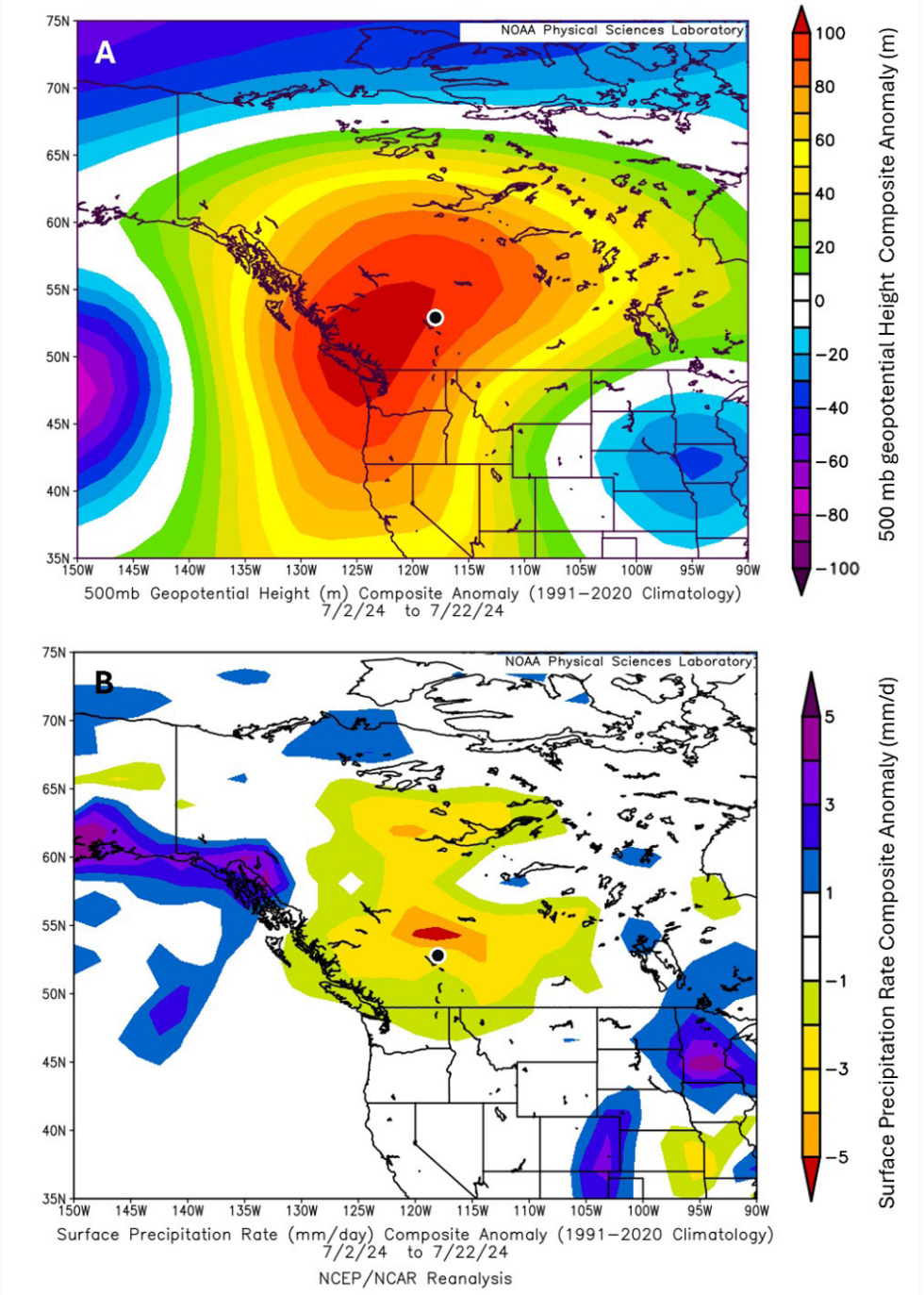

Figure 6. Weather maps of western Canada showing the persistent high-pressure ridge and lack of rain during the 22 days prior to ignition. **A**, The 500-mbar geopotential height anomalies. **B**, Daily precipitation anomalies. Anomalies are defined as the difference between the 2024 conditions and the 1991 to 2020 long-term average. The location of Jasper is indicated by the black and white dot. Source: Images are from the National Oceanic and Atmospheric Administration Physical Sciences Laboratory, Boulder Colorado: https://psl.noaa.gov/.

3.2 Conditions during the burn period

Figure 7 and **Figure 8** show summary weather graphics ("meteograms") for 4 nearby surface weather stations, each useful for representing surface conditions on part of the fire during the spread event. Similar figures for additional stations of interest can be found in Appendix B5.

The Ranger Creek Station was well situated to record valley bottom conditions near the ignition points and southern end of the Jasper South Fire. It recorded very light winds throughout the incident except for isolated gusts, particularly around the time of ignition. Although the Jasper Warden Station was the closest to the community and the most representative of the lower montane zone fuels (Section 2), it had power outages during the July 22–24 period that limited its usefulness.[2] The Dorothy Station, approximately 12 km northwest from and 500 m higher in elevation than Jasper, represented conditions in the east-west–oriented Miette valley, the other major feature channeling winds near the townsite. In addition, higher elevation stations were useful for representing ridgetop conditions, less influenced by local terrain and vegetation. The Paradise Station operated by the Marmot Basin ski hill captured upper subalpine zone conditions near the treeline, reporting cooler conditions but much more active winds at the time of ignition the evening of July 22, and all through the evening, overnight, and morning of July 23. The Tangle Station, near the Columbia Icefield Discovery Centre (Appendix B5), was useful for capturing alpine conditions with much cooler but windier conditions than in the forests below.

FWI System component values are shown in **Table 2** for three weather stations. All three stations indicated critically dry conditions and extremely dry forest floor conditions though the Athabasca valley at the time of ignition, with FFMC of 94–96 and BUI of 153–169. The maximum ISI was calculated with the daily FFMC and the maximum hourly windspeed. On July 22 this value peaked at 28.4 at Ranger Creek, suggesting the potential for significant fire growth at the time of ignition.

[2] The first power outage occurred during the convective storm associated with the South and North Fire ignitions, and may have been due to a lightning strike according to Jasper National Park staff (Marmot Basin reportedly lost power near the same time). The station had power restored on the evening of July 23 but lost power again shortly before the fire entered the Jasper townsite the following afternoon (July 24); this outage was associated with final evacuation of the Jasper National Park operations building.

Table 2. Standard FWI values[a] from the 3 nearby weather stations immediately before and during the main burn period of the Jasper Wildfire Complex, July 21–24, 2024

Day	Temp (°C)	RH (%)	WS (km/h)	Max WS (km/h)	WD (deg)	24 h Rain (mm)	FFMC	DMC	DC	ISI	Max ISI[b]	BUI	FWI
Jasper Warden													
21	30.8	27	4.0	13.4	64°	0	94.3	124	595	9.7	15.4	163	37
22	31.1	22	6.1	9.0	356°	0	94.7	130	605	11.2	13.1	169	41
23[c]	18.9	30	12.6	12.6	260°	3.5	78.6	87	598	1.9	1.9	128	10
24[c]	23.7	33	6.6	12.2	35°	0	88.7	91	606	4.9	6.6	133	21.8
Ranger Creek													
21	33.3	15	12.1	14.6	128°	0	96.3	115	507	19.0	21.6	147	55
22	30.0	23	6.7	21.2	306°	0	95.9	121	516	13.7	28.4	153	45
23	23.4	20	6.9	9.8	295°	2.0	87.7	105	524	4.4	5.0	140	20
24	27.2	15	6.0	13.9	173°	0	94.7	111	532	11.3	16.7	146	39
Dorothy													
21	30.0	28	7.2	10.6	140°	0	93.1	120	508	9.6	11.3	151	36
22	29.0	24	6.9	19.5	316°	0.5	93.9	126	517	10.5	19.9	156	38
23	18.9	30	12.6	12.6	260°	2.0	84.1	107	524	3.5	3.5	142	17
24	21.8	23	10.1	12.2	270°	0	91.4	111	532	8.8	9.7	146	33

Abbreviations: BUI, Buildup Index; DC, Drought Code; DMC, Duff Moisture Code; FFMC, Fine Fuel Moisture Code; FWI, Fire Weather Index; ISI, Initial Spread Index; Max ISI, maximum hourly ISI; RH, relative humidity; Temp, temperature; WD, wind direction; WS, wind speed.

[a] For details about FWI, see Section 3.1, **Box 3**.

[b] Max ISI was calculated using the maximum hourly wind speed (Max WS) with the standard daily FFMC value (FFMC), an acceptable practice [57]. This was done in order to avoid the effects of rapidly changing moisture conditions at the weather station, which may not have affected fuel moisture near the fire.

[c] Due to a data gap, July 23, 2024, observations for Jasper Warden Station are taken from Dorothy Station. A rain gauge at the nearby Jasper National Park Operations Compound recorded 3.5 mm of rain on the morning of July 23. The resulting FWI component values for July 23 and 24 should be considered estimates, especially the FFMC and ISI values.

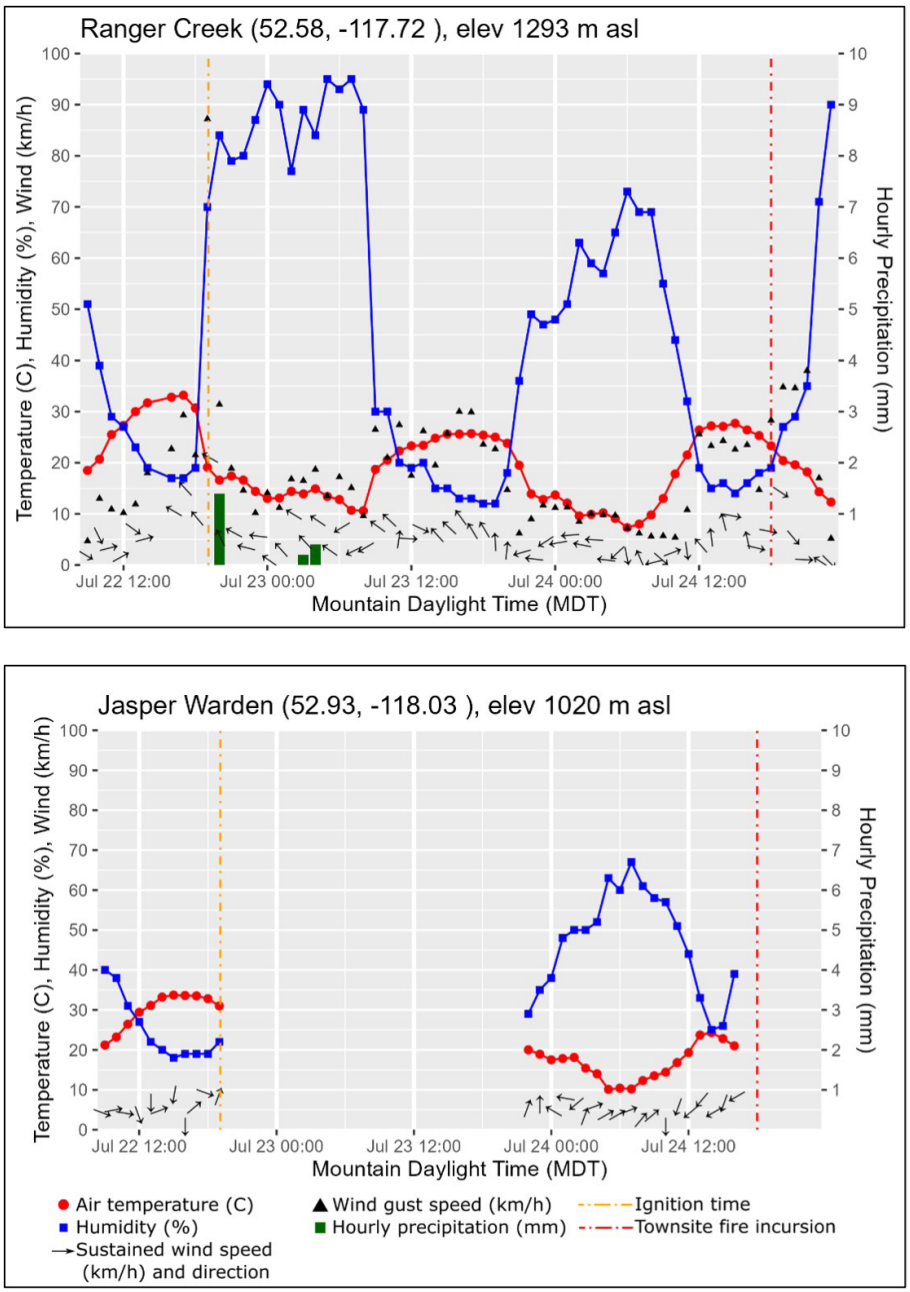

Figure 7. Surface hourly weather observations at the Ranger Creek (top) and Jasper Warden (bottom) weather stations, July 22–24, 2024. Data gaps in the Jasper Warden Station records were apparently caused by power failures; see Footnote 2 for details.

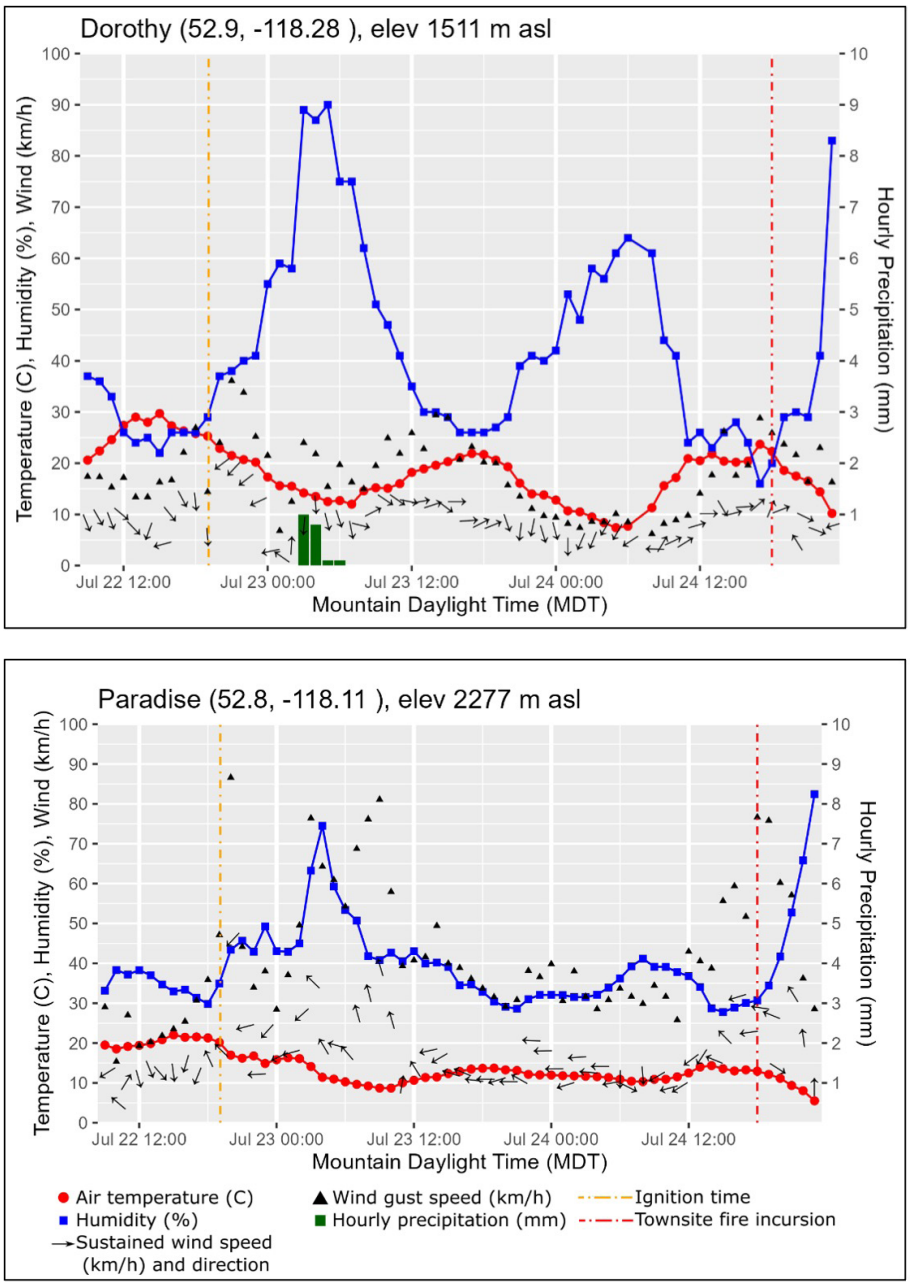

Figure 8. Surface hourly weather observations at the Dorothy and Paradise (Marmot Basin) weather stations on July 22–24, 2024.

To complement the weather station observations, high-resolution (1 km) weather from an experimental version of Environment and Climate Change Canada's High-Resolution DeterministicPrediction System (HRDPS) model [18] was also analyzed. The modelled CAPE (Appendix B3) suggests that although the ridge breakdown led to instability in the region in the days leading up to the fire, the instability in and around Jasper was low during most of the fire progression.

Figure 9 provides modelled HRDPS wind profiles taken from grid points close to the head fire during the burn period. Both the upper-level winds and the surface winds were highest during the morning of July 23, a period that also saw relatively high southeasterly directional wind shear and surface winds. During the other periods, winds were generally from the southerly quadrant throughout the atmospheric column. Maps of modelled surface wind speed and direction across the region are shown in Figure S-7 (Appendix B4) for several periods during the burn period. The persistent wind flow from the southerly quadrant in the Athabasca valley is also seen here. As would be expected, wind direction at the Jasper townsite, located at the junction of several valleys, was more variable, with local areas of converging and diverging wind speeds. In general, modelled surface wind speeds near the head of the fire were 5 to 15 km/h. These modelled winds provide a general sense of the external wind fields affecting the fire; actual wind fields in and around the fire were significantly altered by the fire itself, which was not included in the model. In addition, small-scale convective storm activity, such as the event that led to the ignitions and the localized downburst observed at Ranger Creek Station (Section 4.1), would also not be resolved by the model.

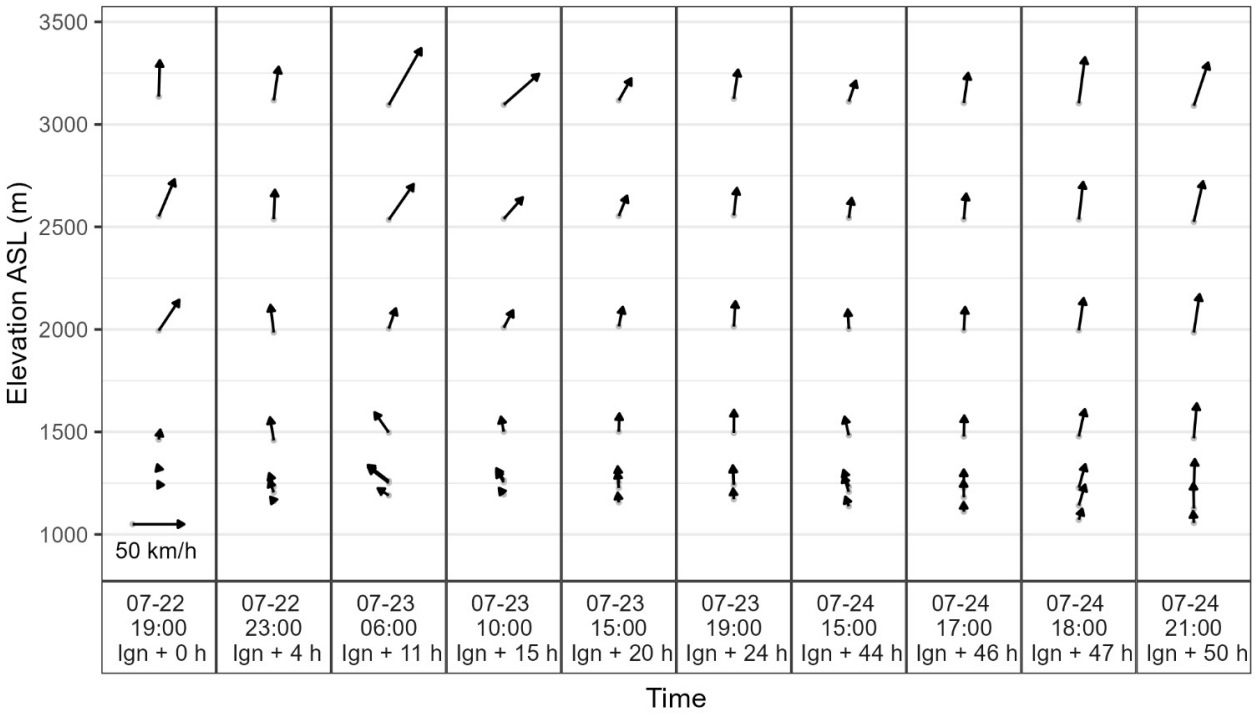

Figure 9. HRDPS-modelled wind profiles near the head of the Jasper Complex Wildfire. ASL indicates above sea level; HRDPS, High-Resolution Deterministic Prediction System; Ign, ignition. Arrows represent wind vectors (direction and speed) indicating influence on fire spread. A reference vector of 50 km/h is provided (bottom left).

4. Fire growth chronology

This section provides a detailed description of the evolving fire weather and growth across 5 half-day intervals over the 52 hours between ignition at about 19:00 on July 22, 2024, and fire growth stalling at Roche Bonhomme at 23:00, during a rain shower (**Table 3**). Particular focus is given to the afternoon and evening of July 24 when the South Fire reached the Jasper townsite. The fire progression was mapped using a combination of satellite and aerial imaging. This imaging included active fire "hotspot" products, satellites detecting high infrared intensity that indicate a heat source, which were obtained for 11 scenes from the Moderate Resolution Imaging Spectroradiometer (MODIS) and Visible Infrared Imaging Radiometer Suit (VIIRS) sensors flown on National Aeronautics and Space Administration (NASA) and National Oceanic and Atmospheric Administration (NOAA) Earth observation satellites; raw mid-wave infrared imagery from the VIIRS instrument (Appendix B6); and 13 oblique aerial photographs from fire personnel that were registered to a Digital Elevation Model (Appendix A2). Additional observations of fire behaviour or weather events (e.g. smoke, wind, embers) have been reported based on interviews with fire suppression personnel. For the location of landscape features mentioned in this section, see **Figures 11**, **13**, **16**, **19–20**, and **22**.

4.1 Fire ignition: July 22, 19:05

On July 22 at the Ranger Creek Station (1293 m), approximately 10 km south of the ignition location, the hottest and driest conditions occurred at 17:00. Fuel conditions indicated a probability of sustained ignition greater than 90% in lodgepole pine forests [61] and the potential for continuous crown fire behaviour even under light wind conditions [5]. The breakdown of the high-pressure ridge that had persisted for several days brought unstable atmospheric conditions that afternoon, including thunderstorms, across a vast region stretching from Crowsnest Pass in southwestern Alberta to Prince George, British Columbia (Figure S-5 in Appendix B3). Environment and Climate Change Canada's radar at Silver Star Mountain near Vernon, British Columbia, tracked a thunderstorm cell moving northward from Mica Dam at Kinbasket Lake (~90 km SSW of Jasper) at 17:30.

Lightning activity began near the southern, eastern, and northern boundaries of Jasper National Park around 17:50. The Canadian Lightning Detection Network recorded 3 lightning strikes 6 km apart on the east and west sides of the Athabasca River from 1210 to 1260 m elevation (Appendix B2). The first strike occurred at 19:05, approximately 2 km southeast of Athabasca Falls, near the base of Mount Kerkeslin. The second and third strikes followed at 19:06 and 19:08, about 4 km north-northwest of Athabasca Falls near Highway 93, north and northeast of Leach Lake (**Figure 1**). Winds at Ranger Creek increased to 21 km/h with gusts to 87 km/h at 19:00 coincident with the lightning strikes and thunder cell passage. Estimates from the HRDPS for 19:00 at the ignition site were as follows: temperature, 29 °C; RH, 27%; windspeed, 2 km/h southeasterly. Winds were modelled at 36 km/h south-southwesterly at approximately 800 m above ground level. Thunderstorms delivered 1.4 mm of rain at the Ranger Creek Station, where RH rose sharply by 20:00.

The North Fire also appears to have ignited the evening of July 22, with the first fire report received by 18:45 near the Jasper Transfer Station. The cause of the North Fire remains under investigation as of July 2025, and no cloud-to-ground lightning strikes were detected by the Canadian Lightning Detection Network at that time within the final North Fire perimeter (Appendix B2).

4.2 Interval 1: July 22 19:05 to July 23 06:00 (0–11 h)

Hourly weather and FWI values recorded at Ranger Creek Station just before and during this interval are provided in **Table 4**. The Ranger Creek Station at 19:00 recorded an hourly ISI of 22.1, though the effective ISI at the fireline was estimated to be 28.4..[3] The FBP System C-2 fuel type, a reasonable fit for representing subalpine spruce-balsam conifer stands, predicts continuous crown fire behaviour with head fire intensity (HFI; see Section 5.3) of 78,000 kW/m in such conditions. Light southeasterly winds were recorded at Ranger Creek Station immediately south of the fire and at higher elevations (Paradise and Tangle Ridge Stations).

Video footage captured by southbound motorists on Highway 93 appears to show rapid acceleration and active crown fire development of the Mount Kerkeslin (southernmost) ignition point from 19:07 through 19:09, along with strong winds and rain showers; witnesses reported very strong wind gusts and broken tree branches striking their vehicle.[4]

[3] Calculated using a daily FFMC of 95.9 and maximum hourly winds (recorded at 19:00) of 21.2, assuming no effects from scattered showers or rising humidity. See Table 2.

[4] Based on a conversation with D. Mo and E. Leisure on 26 May, 2025. Raw mobile phone video footage is available (uncensored video; discretion advised): https://zenodo.org/records/17009070 [Accessed 02 Sept. 2025].

Table 3. Summary of the Jasper South Fire progression intervals during July 22–24, 2024

Time Start–End[a]	Elapsed Time (h)	Area (ha)	RGR (%)	Narrative[b]
Interval 1				
19:00–06:00 July 22–23	4	3,094	143	At 19:05, 3 ignitions began within 6 km, one on the E side of the Athabasca River, S of Athabasca Falls, and two 2 km W of the Athabasca River N and NE of Leach Lake; the fires crowned within <5 min; rapid fire growth occurred over 3–5 h; the fires merged into 1 fire, which spread N over a 12-km distance, reaching 2.5 km N of the mouth of Whirlpool River (E of Highway 93) and entering inside the Jasper municipal boundary
	11	3,548	2	
Interval 2				
06:00–14:00 July 23	15	5,027	9	Light-to-moderate southwesterly winds; fire spread occurred mostly E of the Athabasca River up the slopes of Mount Hardisty, in Hardisty Creek drainage, up Curator Mountain, and to the base of Amber Mountain
	17	5,321	3	
	18	5,950	11	
	19	8,571	36	
Interval 3				
14:00–06:00 July 23–24	20	9,701	12	Light valley bottom winds with low RH; E of the Athabasca River, the fire reached Fifth Lake; W of Athabasca River, the fire reached Edith Cavell Road
	21	10,231	5	
	24	11,115	3	
	25	11,203	1	
Interval 4				
06:00–14:00 July 24	43	13,720	1	Strong morning inversion until 13:00 restricted fire growth; the fire front spanned from Wabasso Campground to Wabasso Lake
Interval 5				
14:00–23:00 July 24	43	15,348	29	At 14:10, the fire developed 2 fronts W and E of the Athabasca River; at 17:30, the first embers were seen in Jasper townsite; at 17:36, the NW fire front reached the top of The Whistlers; at 17:45, the NW convection column collapsed, bringing strong winds and surface smoke into Jasper; at 18:00, spot fires and structure ignitions were being actioned in Jasper townsite; at 18:48, the NE fire front spread from Old Fort Point and Signal Mountain to Jasper Park Lodge; at 20:48, the fire spread 6 km from Jasper Park Lodge to Roche Bonhomme; at 22:00, the fire spread up steep slopes on Roche Bonhomme to the treeline; precipitation arrested fire growth shortly after 22:00.
	44	17,060	21	
	46	20,725	10	
	47	24,735	18	
	50	29,145	5	

Abbreviations: RGR, relative growth rate (% ln(ha)/h); RH, relative humidity.

[a]Time zone is mountain daylight time.

[b]For the location of noted landscape features, see **Figures 11**, **13**, **16**, **19**, **20**, and **22**.

Table 4. Hourly weather and FWI System[a] values from the Ranger Creek Station during Interval 1, July 22–23, 2024

Day	Time	Temp (°C)	RH (%)	WS (km/h)	Wind Gust (km/h)	WD (deg)	Precipitation (mm)	Hourly FFMC	Hourly ISI	Hourly FWI
22	17:00	33.2	17	15.3	29.3	137	0	95.9	21.2	59.3
	18:00	30.7	19	9.6	21.5	140	0	96.0	16.0	49.8
	19:00	19.1	70	21.2	87.2	119	0	94.1	22.2	61.1
	20:00	16.6	84	5.8	31.4	153	1.4	63.8	0.7	4.2
	21:00	17.4	79	6.6	18.9	118	0	64.9	0.7	4.6
	22:00	16.6	80	3.6	14.6	104	0	65.8	0.7	4.1
	23:00	14.4	87	5.7	10.2	97	0	66.3	0.7	4.4
23	00:00	13.0	94	1.2	14.1	125	0	66.5	0.6	3.7
	01:00	13.1	90	3.4	11.2	138	0	66.9	0.7	4.2
	02:00	14.4	77	10.2	16.8	121	0	67.9	1.0	6.2
	03:00	13.9	89	4.9	16.5	137	0.2	64.8	0.7	4.2
	04:00	14.9	84	9.0	18.7	124	0.4	59.4	0.6	3.9
	05:00	13.4	95	3.2	13.5	125	0	59.7	0.5	2.8
	06:00	12.8	93	7.1	17.2	59	0	60.1	0.6	3.7

Abbreviations: FFMC, Fine Fuel Moisture Code; FWI, Fire Weather Index; ISI, Initial Spread Index; RH, relative humidity; Temp, temperature; WD, wind direction; WS, wind speed.

[a]For details about FWI, see Section 3.1, **Box 3**.

Photographs captured at 19:11, 6 minutes after the southernmost lightning strike (at 19:05), show a fully involved crown fire with a large, dark, and well-organized smoke column (**Figure 10A**). Given their proximity, it is likely that the 2 northern ignitions had similar fire behaviour. Initial fire reports in radio dispatch records from Jasper National Park at 19:36 recorded 2 or 3 distinct smoke columns of similar size.

Cameras at Marmot Basin recorded a significant decrease in visibility from 8 km to 2 km at 20:00 as the South Fire smoke column reached Marmot Basin. A shift to more southwesterly winds (Paradise Station) at 20:20 improved visibility, and 2 large smoke columns are visible in photographs that are strongly tilted by southerly winds. Given the proximity of the Leach Lake ignitions, it is likely the fires had already merged by 20:20. The merging of high-intensity fires can cause rapid short-term fire acceleration, with up to 10-fold short-term increases in spread rate [62]. Flames are visible in the Marmot Basin camera images at a location approximately 1 km southeast of the Whirlpool Group Campground and the bridge over the Whirlpool River on Highway 93A at 21:50. Extreme fire behaviour at the fire front was seen near the junction between highways 93 and 93A at 20:38 (**Figure 10B**).

Photographs at 22:12 at the south end of the fire show intense crown fire activity continuing at least until sunset.

At 23:00 on July 22 near the fireline, the HRDPS-modelled surface temperature was 22 °C, RH was 36%, surface winds were 5 km/h southeasterly, and winds aloft (~800 m above ground) were 27 km/h southerly.

Georeferenced photos from shortly after ignition locate at least of one of the fires as being in the vicinity of 52.64 N, 117.87 W and is likely the southernmost of the multiple ignitions. A MODIS *Terra* fire detection at 22:59 on July 22 shows a continuous band of fire approximately 12 km north-south and as much as 4 to 5 km wide, or an area of approximately 3,100 ha. A length-to-breadth ratio of 2.4 to 3.0 would be consistent with a 17 to 22 km/h wind speed [5]. *NOAA-20* VIIRS hotspot detections at 04:53 on July 23 show no more than 1 to 2 km of further growth compared with the 22:59 fire detections. This fire growth was focused along the east side of Highway 93 as the fire moved north reaching about 2.5 km north of the mouth of the Whirlpool River and into the Jasper Municipality. The fire perimeter at the end of this interval (July 23, 06:00) is shown in **Figure 11**.

Figure 10. Fire behaviour during Interval 1 of the Jasper Wildfire Complex, July 22. **A**, Intense fire behaviour at 19:11, 6 minutes after the first lightning strike. The fire is approximately 1 km from the photographer's position. The tall column of dark smoke and the visible glow from the flames indicate very intense initial fire behaviour with crown involvement. Wind effects are visible on trees in the right foreground, suggesting easterly surface winds ≥30 km/h associated with the passing convective cell. Light rain is visible in front of the truck headlights, also associated with convection. Identifying information has been masked for privacy purposes. **B**, Head fire behaviour at 20:38, July 22, 93 minutes after ignition. Fire front approximately 5.5 km northwest of the southern junction between highways 93 and 93A. The camera is facing south.

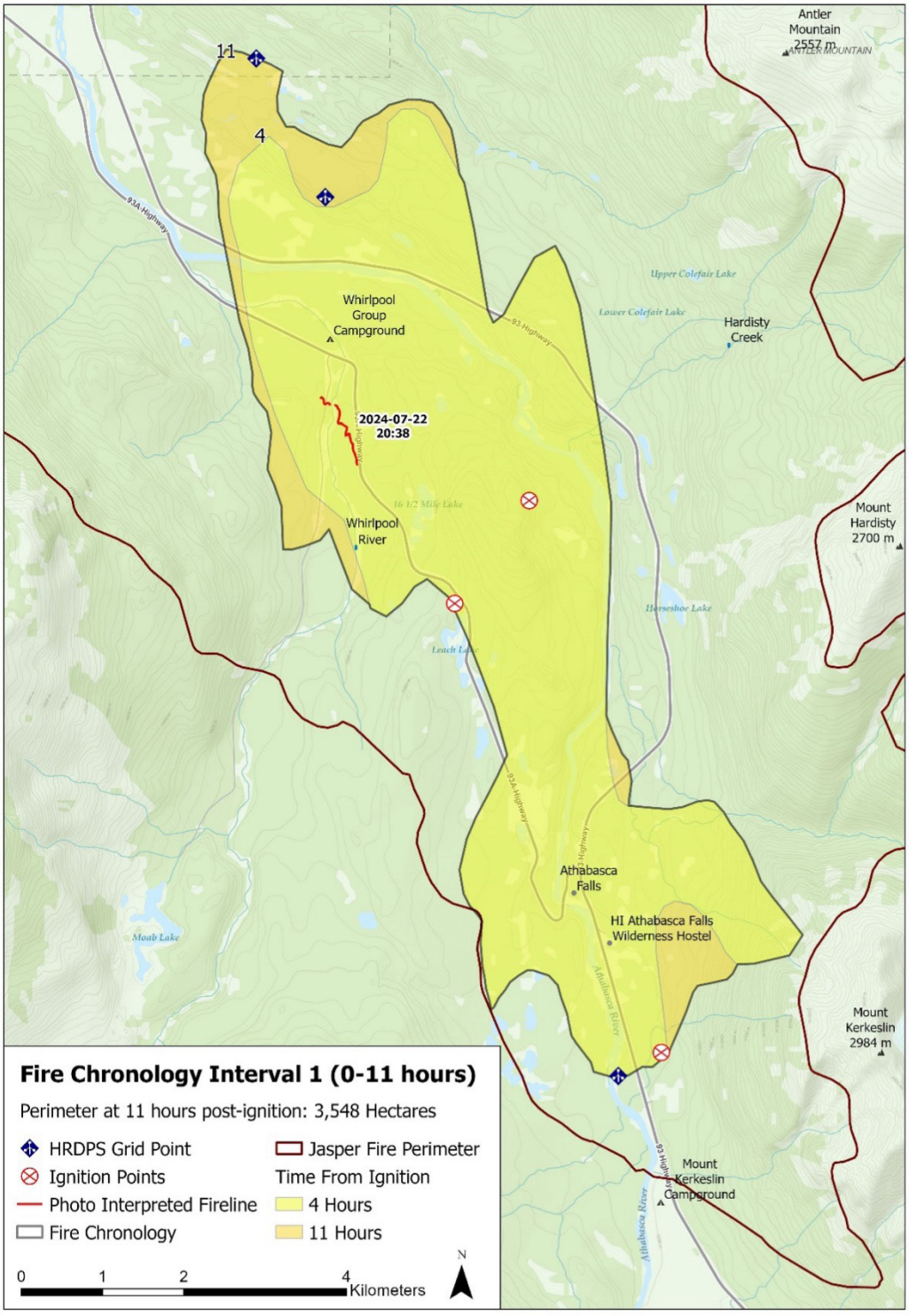

Figure 11. Jasper Wildfire Complex fire progression map from 19:05 on July 22 through 06:00 on July 23 (Interval 1). Area burned was approximately 3,550 ha by the end of Interval 1. Fire progression polygons were mapped using a combination of VIIRS and MODIS hotspot data interpolation along with photogrammetric analysis of aerial photographs (accuracy, <5 m). Perimeter mapping from photogrammetry at 20:38 on July 22 based on the image shown in **Figure 10B**.

4.3 Interval 2: July 23, 06:00–14:00 (11–19 h)

Most surface stations recorded good overnight RH recovery (>80%) by 06:00, but all stations showed a rapid decrease in RH during daytime hours. Early afternoon RH values were between 10% and 30% in the valley bottom. During this interval average winds at Ranger Creek Station remained below 10 km/h, while gusts were up to 30 km/h. Wind direction at Ranger Creek Station was variable. However, winds at higher elevations (Paradise Station) ranged between 10 and 40 km/h, with gusts up to 80 km/h. Winds at the Dorothy Station showed consistent flow from the west into the Athabasca valley. At 10:00 on July 23 near the fireline, HRDPS-modelled surface temperature was 19 °C, RH was 40%, surface winds were 8 km/h southeasterly, and winds aloft (~800 m above ground) were 19 km/h south-southwesterly. The HRPDS model suggested that instability within the region decreased substantially within the region during this period (Figure S-6 in Appendix B3).

The South Fire was assessed by aircraft at 09:57 on July 23, with only the southwest portion (back of the fire) along Highway 93 visible; low smoke due to moderate southwesterly winds obscured the head fire (north) and eastern flank (**Figure 12A**). Fire behaviour on the west and south sides of the fire was visible in photographs as a surface fire (estimated Intensity Class 3 [63]) at first assessment, but by 10:34 portions of the flanks of the fire were already beginning to crown (**Figure 12B**). The head fire was only briefly visible as it ascended steep slopes on Mount Hardisty, showing very intense crown fire behaviour associated with the alignment of slope and winds.

Photos by Air Attack Officers at 12:25 show a strong capping inversion with poor smoke ventilation topping out at c. 4,000 m above sea level; a smoke plume rising above approximately 5,000 m or higher was observed at that time primarily over the east side of the fire suggesting very high–intensity fire lofting smoke into strong southwesterly winds aloft had already developed before noon. Air Attack Officers actioning the South Fire noted strong turbulence at 3,000 to 4,000 m above sea level (at this time, the Tangle Station measured winds at 40 km/h, gusting up to 70 km/h) and extreme fire behaviour. Estimated fire progression in the late morning and early afternoon was focused on areas east of the Athabasca River, with the 12:28 MODIS *Terra* satellite detections showing approximately 2 km of growth east and uphill to the treeline and steep slopes of Mount Hardisty. Northward growth of 1 to 2 km toward Wabasso Lake on the east side of the Athabasca River was observed in this satellite perimeter estimate in comparison with the 04:53 satellite observation. The NOAA constellation of satellites all with the VIIRS sensor onboard passed over the South Fire in close succession at 13:02 (*NOAA-20*), 13:53 (*NOAA-21*), and 14:17 (*S-NPP*) (Appendix B6) and provide a more precise fire location than obtained from the MODIS observations, as VIIRS has a finer spatial resolution (pixel size: VIIRS, 375 m; MODIS, 1 km). Compared with the 04:53 morning VIIRS overpass, the South Fire had moved approximately 4 km up the Hardisty Creek Drainage, 3 to 4 km up the treeline at Curator Mountain, and approximately 5 km north to the base of Amber Mountain to an elevation of 1900 m. Fire progression on the west side of the fire and the Athabasca River during Interval 2 was very limited due to the southwesterly winds. A map of the fire perimeter at the end of Interval 2 (July 23, 14:00) is shown in **Figure 13**.

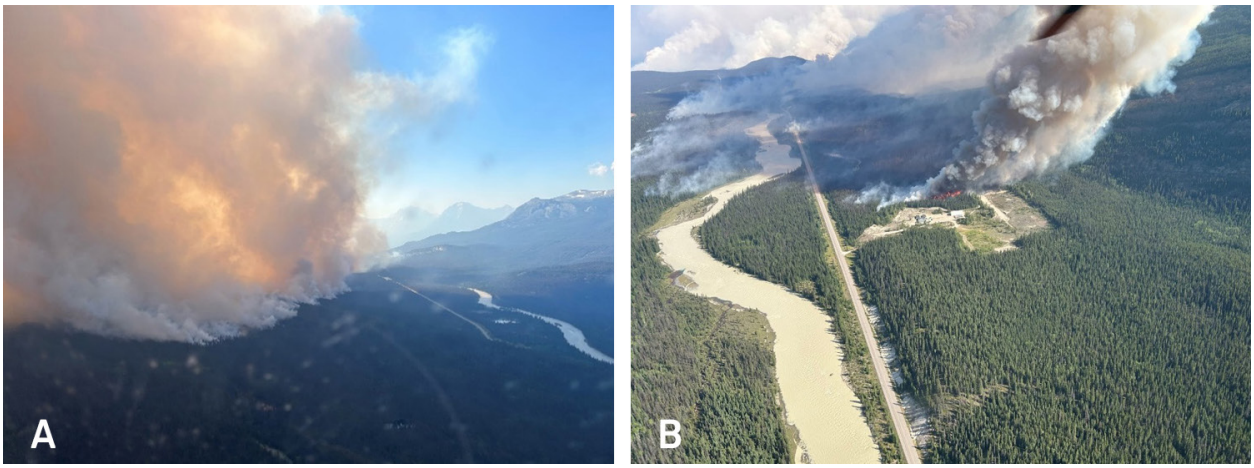

Figure 12. Fire behaviour during Interval 2 of the Jasper Wildfire Complex, July 23, 2024. **A**, Surface fire behaviour at 09:57. The fireline is approximately 1.4 km east of the Wabasso Campground. The camera is facing south-southeast. **B**, Fire behaviour at 10:34. The camera is facing north toward the back of the fire at the base of Mount Kerkeslin. The 3 lightning ignitions have joined to create a continuous fire perimeter bridging Highway 93 and the Athabasca River. Visible fire behaviour includes intermittent to continuous crown fire at the head, with multiple distinct smoke columns developing. The back and flanks of the fire show moderate surface fire behaviour. Smoke from the Jasper North Fire is visible in the top left of the image.

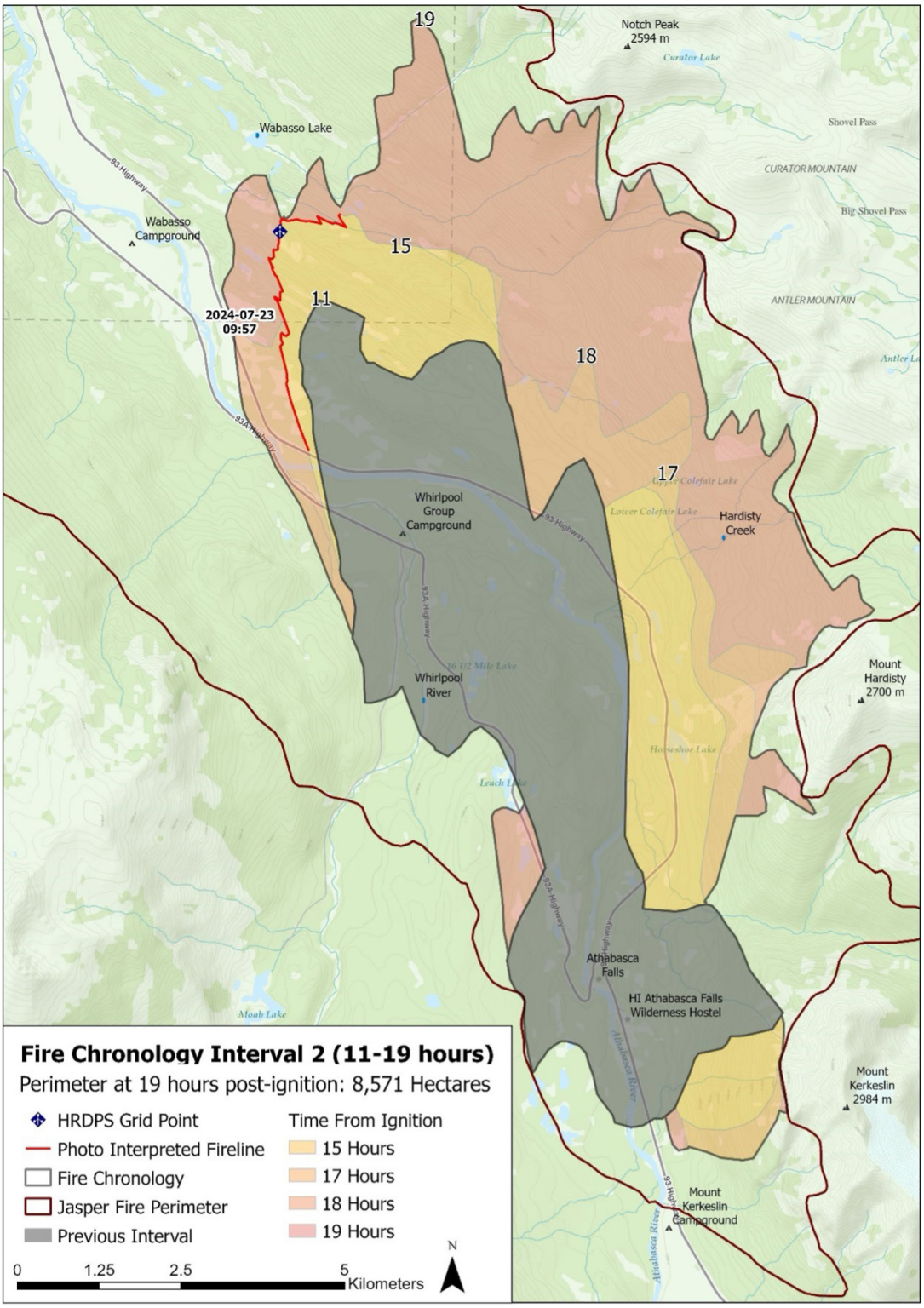

Figure 13. Jasper Wildfire Complex fire progression from July 23, 06:00 through July 23, 14:00. The fire perimeter was estimated at approximately 8,600 ha at 19 hours post-ignition. Perimeter mapping from photogrammetry at 09:57 on July 23 based on the image shown in **Figure 12A**.

4.4 Interval 3: July 23 14:00 to July 24 06:00 (19–35 h)

Valley bottom winds generally decreased to light winds through this period. Wind direction at Ranger Creek Station remained variable, while winds at Dorothy Station shifted from westerly to northerly. Mid-slope winds at Paradise Station remained easterly between 10 to 20 km/h, with gusts up to 40 km/h. On the evening of July 23, there was a significant increase in RH value in the valley bottom, especially at Ranger Creek Station; by the early morning of July 24, RH values ranged between 60% and 75%. At 19:00 on July 23 near the fireline, HRDPS-modelled surface temperature was 25 °C, RH was 20%, wind speed was 10 km/h southerly, and winds aloft (~800 m above ground) were 25 km/h southerly. Modelled atmospheric instability remained low during this period (Figure S-6 in Appendix B3).

Photos of fire behaviour during Interval 3 are shown in **Figure 14**. Both the North and South Fires were well developed as fully engaged crown fires by 14:00. A map of the fire perimeter at the end of Interval 3 (July 24, 06:00) is shown in **Figure 16**. The South Fire showed more intense fire behaviour, with flame heights greater than 30 m observed by 15:12. Intense fire activity was influenced by the sustained southwesterly upper winds that pushed the fire up to the tree line toward Amber Mountain, Curator Mountain, and Shovel Pass. The very dry air (minimum RH of 12% at Ranger Creek Station) allowed for Intensity Class 5 fire activity to be observed on both the North and South Fires until at least 21:30 and 23:00, respectively. Despite the significant smoke plume height and fire intensity, embers were not lofted overtop of Amber Mountain to the forest on the other side, a distance of 3 to 4 km. Sustained southerly to southwesterly ridge-top winds at Tangle Station (elevation, 3,000 m above sea level) were recorded at 30 to 40 km/h, with gusts of 50 to 70 km/h. Modest humidity recovery and low winds associated with an inversion were observed by 06:00 July 24.

The *NOAA-21* VIIRS detection at 15:33 showed the first significant fire growth west of Highway 93A. By 20:00, the fire was detected within 2 km of the junction between Highway 93A and Edith Cavell Road. MODIS *Terra* detections at 22:02 locate the northern extent of the fire within 1 to 3 km due south of the summit of Mount Tekarra and the vicinity of Fifth Lake. Over the 6.5-hour interval between the 15:33 satellite observations and the 22:02 observations near Fifth Lake, the fire moved approximately 4 km to the northwest toward the Jasper townsite.

Westward and upslope fire spread (flanking) began on July 24 at about 05:30, with an estimated spread rate of one-half to one-quarter the speed of the fire's northward advance. Significant fire spread of 3 to 4 km toward the west and northwest, near the base of Edith Cavell Road, was detected by the *NOAA-20* VIIRS overpass at 02:54 (July 24). However, this likely captured residual heat from fire spread the previous evening. Large flames remained visible south of the Jasper townsite well after sunset at 23:00. However, even with near-zero wind conditions, the FFMC of approximately 90 suggests that a fire spread rate of 5 m/min (0.3 km/h) would be possible on level terrain, using the C-2 fuel type in the Canadian FBP System to represent subalpine spruce-balsam stands or grey attack stage, dead pine stands.

Overnight, the fire advanced from the Athabasca River near the Cavell Ranger Station along Highway 93A to the ridgetop north of Cavell Meadows, covering a distance of 3.5 km. The FBP System suggests that the 30% slope would have accelerated fire progression to 11.7 m/min (0.7 km/h) as a crown fire. Ridgetop southwesterly winds, observed at the Tangle Station through the night and into the morning of July 24, combined with the level terrain, likely prevented further westward or downslope fire spread toward the Edith Cavell Hostel and Astoria River.

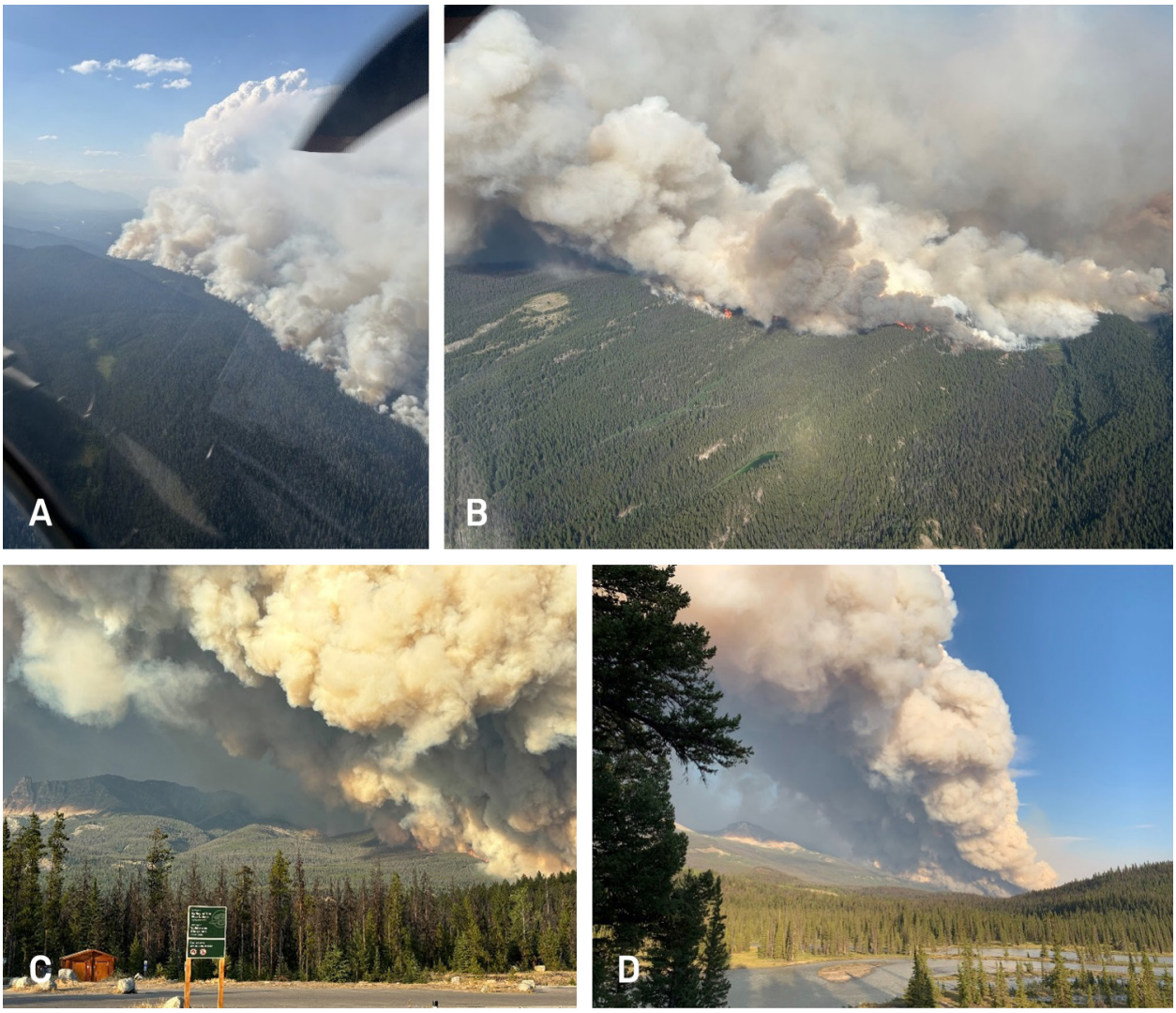

Figure 14. Fire behaviour during Interval 3 of the Jasper Wildfire Complex on July 23. **A**, Vigorous surface fire with intermittent crowning at the flank of the fire at 19:14. Photo location is east of the Edith Cavell range, approximately 3 km southwest of the Whirlpool Campground, looking northwest. **B**, Continuous crown fire at the head fire at 19:18. Fireline and photo locations are approximately 2 km southeast and 1.1 km southwest of Fifth Lake in the Valley of Five Lakes, respectively. Portions of the head are obscured by the smoke column. **C**, Plume-driven fire coupled with strong southeasterly winds at 20:32. The fire was pushed to the Valley of the Five Lakes and up the slopes of Mount Tekarra (peak visible on the left). Photo was taken from the Miette River bridge on Highway 93A (Athabasca Road) facing southeast. **D**, Continuous crown fire with a well-developed smoke column at the head fire at 20:30. Fireline location was perpendicular to Highway 93, approximately 1.5 km southeast of Tekarra Creek. Photo location was at the Valley of Five Lakes facing east.

4.5 Interval 4: July 24, 06:00–14:00 (35–43 h)

The morning and early afternoon of July 24 saw similar valley-bottom temperatures and RH values compared with the previous day (July 23), although the afternoon RH at Ranger Creek Station had increased slightly. Winds at Ranger Creek Station increased throughout Interval 4 but remained below 10 km/h, with gusts up to 25 km/h in the afternoon. Mid-slope winds at the Paradise Station remained similar to Interval 3 but began to trend upwards in the afternoon period. At 15:00 on July 24, the HRDPS-modelled surface temperature near the fireline was 26 °C, RH was 16%, surface winds speeds were 10 km/h south-southeasterly, and winds aloft (~800 m above ground) were 19 km/h southerly. Modelled atmospheric instability remained low during this period (Figure S-6 in Appendix B3).

A strong inversion was observed by Jasper National Park staff at both the South Fire and North Fire, with fire activity in the morning of July 24 limited to extensive but low-intensity surface fires that burned under the inversion, creating low visibility and hazardous flying conditions. The Tangle Station, at 3,000-m elevation, showed no evidence of an inversion. Instead, it recorded sustained south-southwesterly winds of 30 to 40 km/h, with gusts to >70 km/h and low RH continuing from the previous overnight period and through the morning of July 24. By 12:50, the valley inversion had started to lift, with smoke columns at the Edith Cavell Road above the switchbacks showing influence from southwesterly winds aloft.

Photos of fire behaviour during Interval 4 are shown in **Figure 15**. The MODIS *Terra* satellite overpasses at 10:32 and 12:08 were partially obscured by thick smoke and cloud. Though significant fire activity on the evening of July 23 was observed at the eastern edge of the fire, the thick smoke and southwesterly winds obscured the eastern edge of the fire during this interval. Satellite fire observations at 12:08 revealed intense fire activity west of Highway 93A and upslope to the ridge separating the Astoria River and the main Athabasca valley. The same satellite images identified the fire front location as stretching from adjacent to the Wabasso campground to as far north as Wabasso Lake. These 12:08 observations by the MODIS *Terra* satellite are limited to 2-km resolution at the edge of the satellite overpass. Incident photography from rotary wing aircraft corroborates the satellite assessment. Thick smoke also prevented aircraft from flying safely on the eastern edge of the fire near the base of the Amber and Tekarra Mountains.

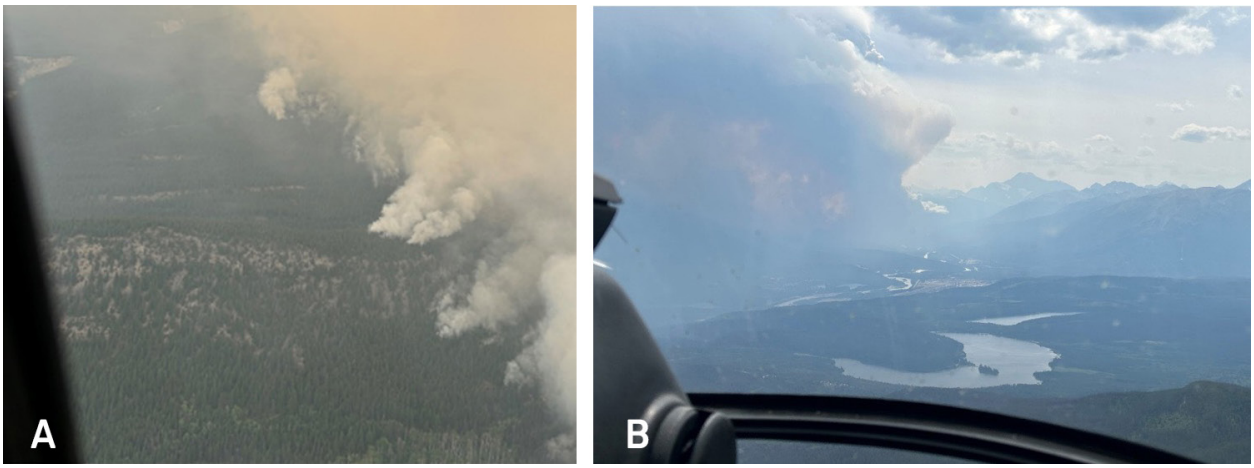

Figure 15. Fire behaviour during Interval 4 of the Jasper Wildfire Complex, July 24. **A**, The northernmost extent of the fire at 12:54. The camera is facing northeast from the Valley of the Five Lakes trail approximately 750 m south of Fifth Lake, toward the face of Mount Tekarra. **B**, A well-developed smoke column is present across the entire Athabasca valley at 13:41. The influence of the southwesterly winds aloft pushing the smoke eastward (left in the image) is evident. The thin upper clouds that obscured the satellite images in Interval 4 are also visible. The camera is facing south toward the Jasper townsite and Mount Edith Cavell and the Athabasca valley from the base of Pyramid Mountain.

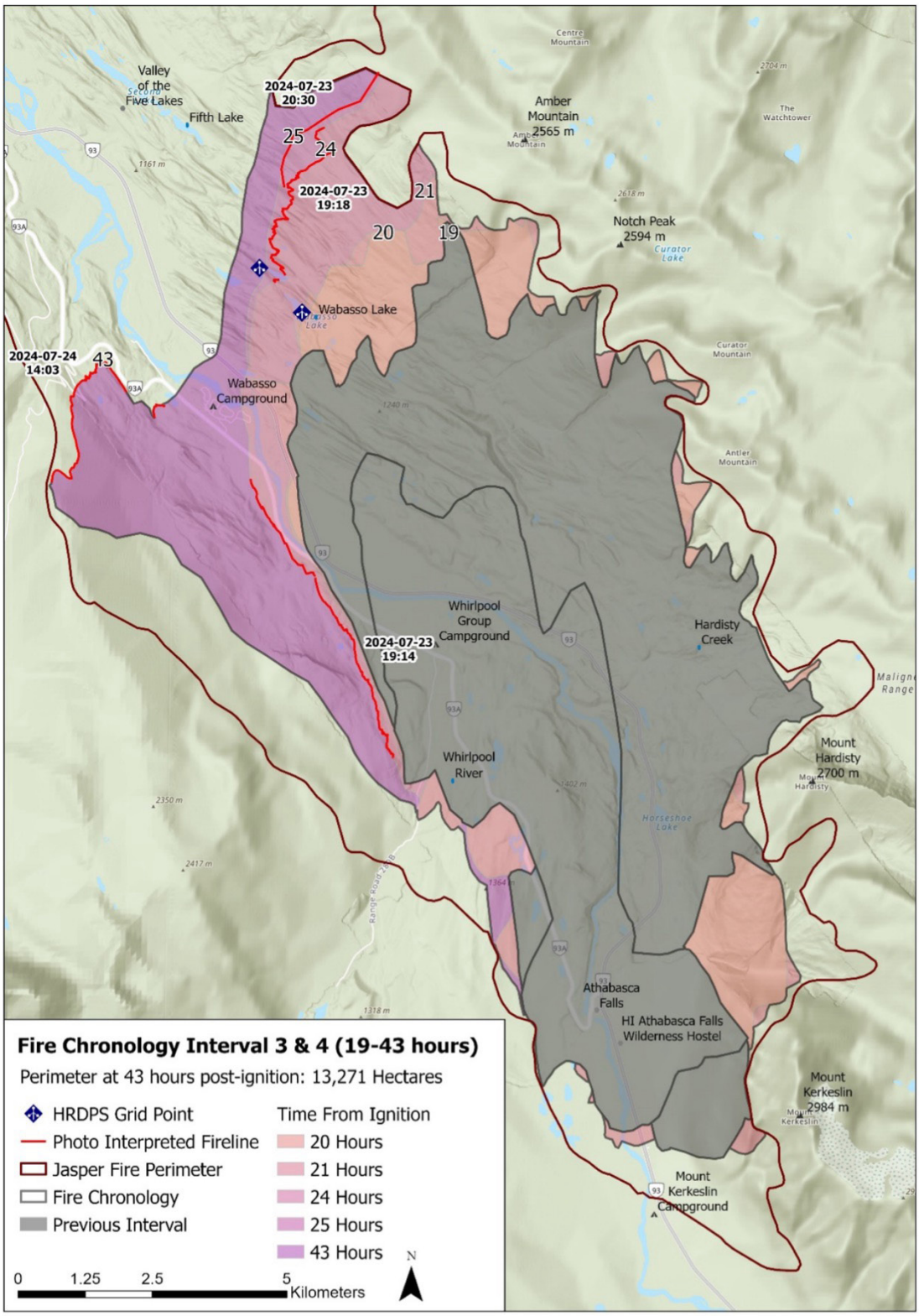

Figure 16. Fire progression during Intervals 3 and 4, July 23, 14:00 through July 24, 14:00. Area burned is estimated at 13,271 ha at 43 hours post-ignition. Perimeter mapping is from VIIRS and MODIS imagery, as well as photographs at 19:14 (**Figure 14A**) 19:18 (**Figure 14B**), 20:23 (**Figure 15C**) on July 23 and 14:03 on July 24 (**Figure 17A**).

4.6 Interval 5: July 24, 14:00–23:00 (43–52 h)

This interval had increased winds throughout the region and featured the fastest-spreading and most intense fire activity that was observed directly by aerial and ground observers. Wind direction remained variable at Ranger Creek Station, while winds at the Dorothy Station remained westerly, blowing into the Athabasca valley. Treeline wind speeds at the Paradise Station increased, with gusts up to around 80 km/h. By the end of July 24, RH increased to >80% with the arrival of widespread showers. At 17:00 on July 24, HRDPS-modelled surface temperature near the fireline was 25 °C, RH was 18%, winds were 9 km/h southerly, and winds aloft (~800 m above ground) were 23 km/h southerly (**Figure 19**). Modelled atmospheric instability remained low during Interval 5 (Appendix B3).

As the fire approached and began to impinge the Jasper townsite, the remaining wildland fire personnel were evacuated and all air operations ceased. Clouds obscured some of the afternoon and evening satellite imagery (Appendix B6) as moist air arrived prior to the late evening precipitation event. Consequently, fewer photos and images of the fire exist during this episode (Intervals 5.2 and 5.3) and the timing and nature of fire spread mechanisms are somewhat speculative.

4.6.1 Interval 5.1: Astoria River to Wapiti Campground 14:00–17:00

Photos of fire behaviour for Interval 5.1 are shown in **Figure 17** and **Figure 18**. Perimeter mapping from photogrammetry was based on images captured at 14:47 (**Figure 17C**), 14:57 (**Figure 17D**), 16:55 (**Figure 18B**), and 17:02 (**Figure 18C**). The perimeter at the end of Interval 5.1 is shown in **Figure 19**. Three fire spread observations during this interval were mapped using a combination of photogrammetric methods and hotspot mapping (Appendix A2), producing 3 very high ROS and fire intensity observations, described in Section 5.3 and Section 5.4. The fastest ROS (5-6 km/h; Section 5.4) was associated with cross-slope spread of the western head of the fire (approx. 1200-1300 m elevation ASL), between 14:03 and 14:30.

During Interval 5.1, the fire was still observed as a single continuous front stretching across the entire valley from the confluence of the Astoria and Athabasca Rivers to Mount Tekarra. At 14:03, the smoke column at the bottom of the Edith Cavell Road was observed to be rotating in a clockwise manner, potentially influenced by southwesterly winds aligned with and flowing out of the Astoria River valley. Rotating smoke columns are indicative of plume-driven fire behaviour, when convective forces overwhelm the influences of ambient winds [10]. Typical attributes of plume-driven fires include light ambient surface winds, high fuel loading, and strong winds aloft above 3,000 m [64]; all these features were present in the upper Athabasca valley during this time (Section 5.3). Strong wind effects were observed both inside and outside the burned area at Wabasso Campground (Appendix B10), consistent with prior observations of fire-induced winds and debris movement associated with such events [64]. Plume-induced winds led to extensive high-severity blowdown (100% windthrow rate) during this interval (**Figure 18D**). In the absence of fire, blowdown is more typically associated with gusts from short-duration convective thunderstorms in boreal forests with winds of 140 km/h or more [65]. Wind-induced ground scouring and impacting of 3 mm gravel particles in tree trunks as well as widespread scouring and bark stripping of burned tree bark are damage patterns similar to tornados rating 4 to 5 on the Enhanced Fujita (EF) Scale [66]. Tornados of this magnitude feature wind speeds of 260 km/h or more [66]. This type of damage pattern was also observed over parts of the 2023 Grouse Complex Wildfire in West Kelowna. That incident also featured extreme fire intensity and Douglas-fir- and lodgepole pine-dominated fuels, though with a more extreme drought condition and less evidence of MPB effects [67].

Intense fire activity was also observed on the slopes of Mount Tekarra to the northeast and downwind of the rotating smoke column. The eastern portion of the fire did not have a documented rotating smoke column, possibly due to lower fire intensity caused by downwind movement of the dense smoke, which can cast shade [68] and increase the moisture content of fine fuels [69]. Smoke also prevented any aircraft operations and aerial photography at this time.

Stands of leafed-out deciduous species (e.g. aspen) are normally associated with much slower fire spread than conifer forests [70]. However, an approximately 25 ha patch of largely continuous aspen forest burned during this interval, due to the combination of the severe drought and the intensity of the surrounding fire. Evidence of intense surface fire behaviour with flame heights and bole charring of 2 to 3 m in height suggest Intensity Class 4 [63] fire behaviour (**Figure 31**, Section 5.3). Previous removal of beetle-killed trees (Section 2.4) significantly reduced fuel loads and fire intensity across the Wapiti and Whistlers Campgrounds (Section 5.2).

At 17:02, observations from Wapiti Campground suggested that the fire front had split into 2 distinct heads: one moving to the northwest along the base of The Whistlers toward the Jasper townsite, and another along the base of Signal Mountain, heading toward Jasper Park Lodge. The following sections (Intervals 5.2 and 5.3) will detail the fire progression and observed behaviour of the northwestern and northeastern fire fronts.

Figure 17. Plume-driven fire behaviour during Interval 5.1 of the Jasper Wildfire Complex, July 24. **A**, Crown fire behaviour is apparent at 14:03 with column rotation, south of the intersection between Mount Edith Cavell Road and Highway 93A. The camera is facing south-southeast. **B**, The smoke column is visibly dark at 14:39, while clear sky conditions allow for the view of Mount Edith Cavell; southwesterly winds in the lower atmosphere have tilted the smoke column to the northeast toward Hinton. The camera is facing south from the Parks Canada operations compound. **C**, There was continuous crown fire with a well-developed column at the head fire at 14:47. The head fire is perpendicular to the intersection between Marmot Road and Highway 93A, south of Portal Creek. The photo was taken from Jasper SkyTram's upper station facing southeast. **D**, The fireline extended across the valley by 14:57. The fireline is in a *U*-like shape from the west (north of Portal Creek) crossing Highway 93A. The deep flame front and easterly indraft to the main fire convection column are indicative of plume-driven fire behaviour. The extreme convective force likely contributed to the extensive fire blowdown observed in the vicinity afterwards (**Figure 18D**). Looking south from near First Lake toward the Highway 93 bridge across the Athabasca River. **E**, At 14:32, crown fire behaviour and a well-developed smoke column were observed on valley bottom and lower subalpine slopes. The photo was taken from the Highway 93 access gates, looking south.

Figure 18. Fire behaviour and effects during Interval 5.1 of the Jasper Wildfire Complex, July 24 (continued). **A**, At 14:57, intermittent crown fire behaviour with a well-developed plume was observed at the head fire south and east of Wapiti and Whistlers Campgrounds. The camera is facing northwest. **B**, Continuous crown fire behaviour at the head fire at 16:55. The head fire is located south of Wapiti Campground along Highway 93 and east across the Athabasca River near the Valley of Five Lakes. The camera is facing southeast. **C**, Intermittent crown fire with a well-developed plume is seen at the head fire at 17:02. The head fire is south and east of Wapiti and Whistlers Campgrounds. The camera is facing west. D, Aftermath of rotational plume-driven fire and extreme fire-induced winds, photographed on August 3. There is near-100% tree breakage and bark stripping near Wabasso Campground. The camera is facing west.

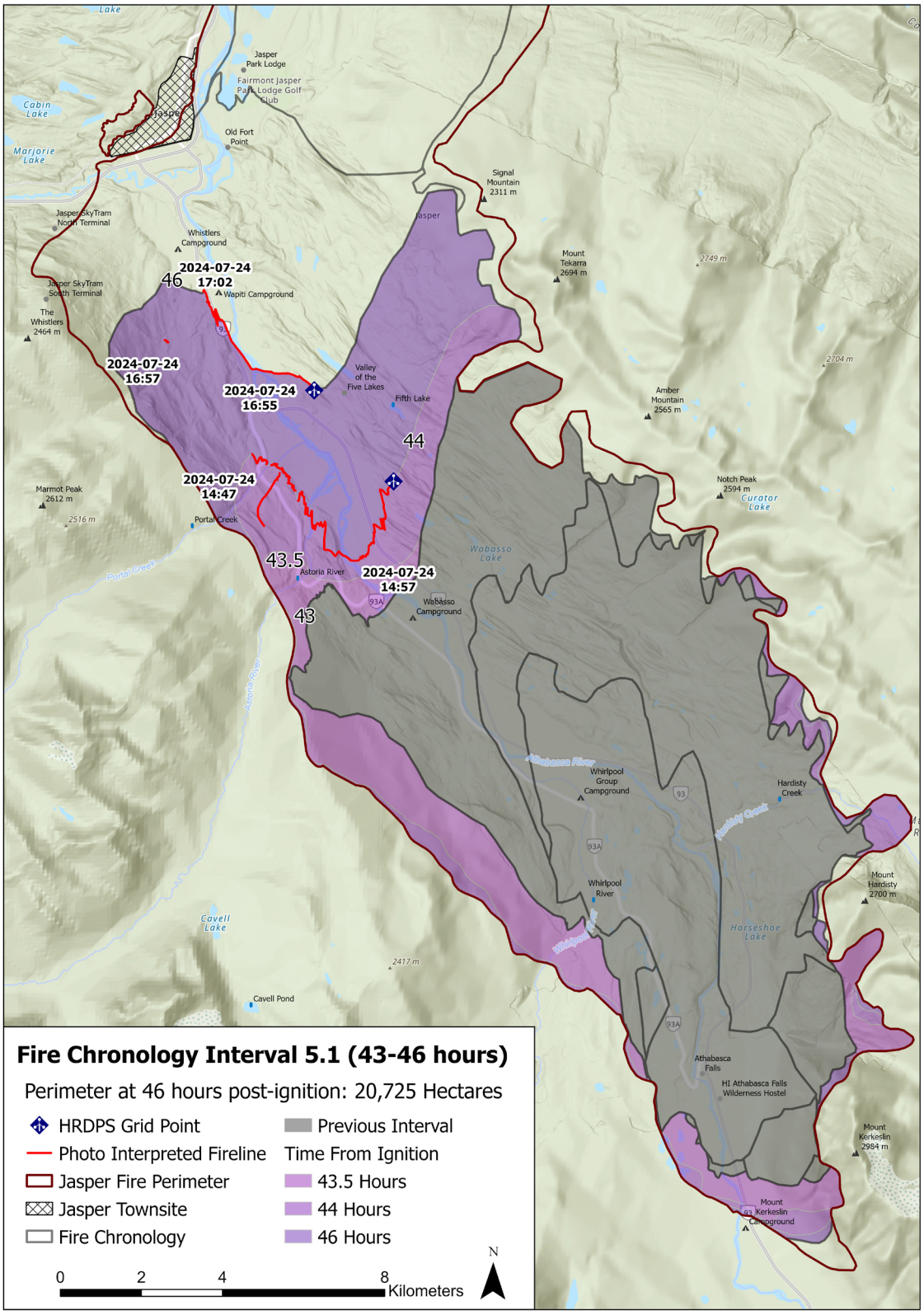

Figure 19. Fire progression map during Interval 5.1 on July 24. Fireline mapping from photogrammetry is based on **Figure 17C** (14:47), **Figure 17D** (14:57), **Figure 18A** (16:57), **Figure 18B** (16:55), and **Figure 18C** (17:02).

4.6.2 Interval 5.2: Northwest spread to Jasper townsite 17:00–19:00

Aerial ignition operations were conducted using a helicopter-deployed plastic sphere dispenser [71] from 16:40 to 17:10 to draw the fire up The Whistlers away from the Jasper townsite (Appendix B7). By 17:09, the northwestern head fire was observed to be spreading up the slopes of The Whistlers, following the 27% slope and northeast aspect. The fire perimeter at the end of Interval 5.2 is shown in **Figure 20**. Applying the FBP System slope-wind vectoring model [5], the interaction between the light southerly cross-slope winds of about 15 km/h and the steep slope likely steered the fire to the northwest (310°) toward the Jasper SkyTram, rather than due north toward the Jasper townsite.

Fire personnel in the Jasper townsite observed the arrival of ground-level smoke and the first burning embers at 17:30. As the fire neared the tramway base at 17:36, it was influenced by westerly winds from the Yellowhead Pass, slowing fire spread west; intense fire activity was observed from the base of The Whistlers at 1150 m to the end of continuous fuels at the treeline at 1900 m.

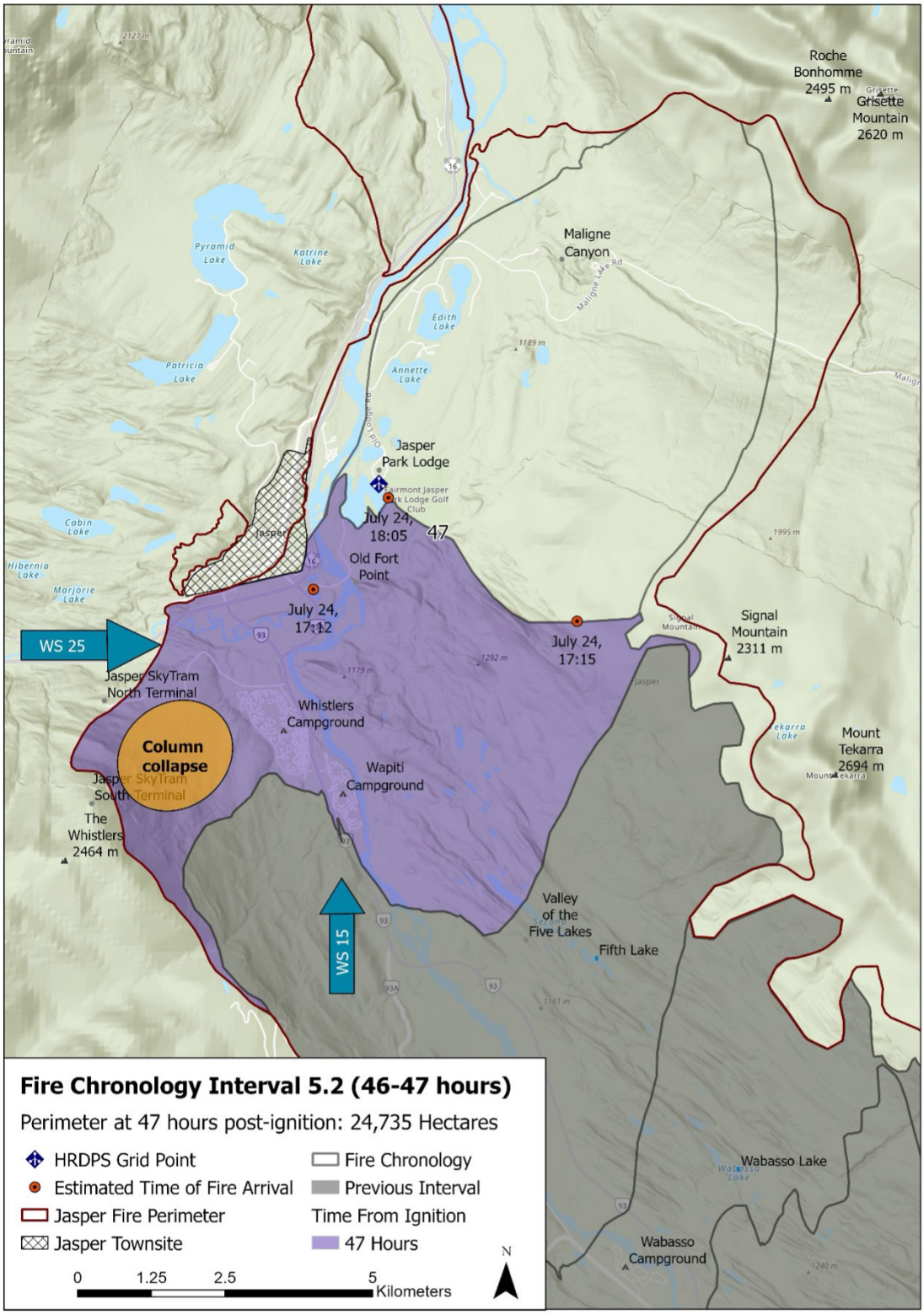

Figure 20. Fire progression map during Interval 5.2 on July 24. Estimated time of arrival points based on observations discussed in Section 4.6.3.

The convection column at the northwest head of the fire collapsed at about 17:40 to 17:45 (**Figure 21A**). Several factors are believed to have contributed, including (1) converging valley winds (southerly from the Athabasca valley and westerly from Yellowhead Pass), (2) uphill pull contributed by steep slopes, and (3) the end of continuous fuels above the treeline on The Whistlers. The column collapse produced thick, continuous ground-level smoke and strong, but short-lived, southwest winds over the Jasper townsite starting around 17:45. Visibility dropped to less than 100 m, causing streetlights to be triggered by the sudden darkness (**Figure 21B**). This event likely also accelerated the pulse of embers into the Jasper townsite, but precise timing and location are unknown. Visibility dropped to less than 100 m, causing streetlights to be triggered by the sudden darkness. Strong winds broke branches off large broadleaf trees, suggesting gusts up to 110 km/h. Downed but unburned mature spruce trees located in residential areas indicated stronger winds in parts of the townsite. Windthrown trees were consistently aligned, suggesting a straight-line wind pattern rather than the rotational pattern observed at 14:00 near Wabasso Campground. The origin of these intense winds alongside ground-level smoke is unclear, given that smoke is otherwise lofted from intense fire convection. The first spot fires and structure ignitions were both documented within the Jasper townsite at 18:00, with ignitions observed to have initiated on rooftops. The winds subsided by 18:05, although dense smoke lingered until approximately 18:45 (**Figure 21A**).

Brief, intense wind events from convection column collapse have been documented on fires under light wind conditions [72]. These phenomena occur when heavier-than-air smoke parcels descend due to sudden decreases in fire intensity [73]. Although typically associated with ember transport, such events are poorly represented in firebrand transport models, which assume steady convection [74]. Fluid dynamics simulations of similar wildfires suggest that column collapse events can generate horizontal wind speeds up to 72 km/h, even 2 to 3 km from the fire edge [75]. This aligns with observations of broken branches and spot fires near the Jasper National Park Administrative Building, 2.5 km from the active fire perimeter at Whistlers Campground. Wind damage was also noted at Pyramid Lake Road and Forest Park Hotel, despite these areas experiencing no direct fire impacts.

By 18:15, surface winds from the Yellowhead Pass decreased, as observed west of Jasper along Highway 16. With diminished westerly winds, the fire likely advanced northward from Whistlers Campground, crossing the Miette River, Highway 16, and the Canadian National Railway tracks. Recent fuel treatments at the townsite boundary, between Highway 16 and the rail tracks, likely reduced fire intensity, transitioning the fire from an Intensity Class 6 active crown fire to a vigorous, Intensity Class 4 surface fire [63]. This transition is evident from the lower crown involvement in the treated areas as well as lower fuel consumption and overall severity in treated fuel consumption plots (Section 2.4 and Section 5). Surface fires, although less destructive than crown fires, can still produce flame lengths of 2 to 4 m, release embers, and cause structure ignition. However, the firebrand production and travel distance in surface fires [76] are significantly lower than those in crown fires [77], reducing the exposure risk to distant structures.

Neighborhoods north of the Jasper Information Centre and hospital may have been spared by proximity to the Canadian National Railway yard to the east and the steep Pyramid Bench slopes, which both limited fire spread due to the southwesterly winds. By 19:02, Intensity Class 4 to 5 fire behaviour [63] was observed on the Pyramid Bench hillside near Bonhomme Street and Miette Avenue. Given the intense structure fires nearby, the Pyramid Bench ignitions were likely caused by a combination of long-distance (>1 km) ember transport and embers produced from nearby burning structures, a process that has been documented numerous times in fires of similar intensity [78], [79].

4.6.3 Interval 5.3: Northeast spread toward Maligne Canyon 17:00–23:00

Photos of fire behaviour for this interval are shown in **Figure 21**. A map of the fire progression at the end of this interval (July 24, 23:00) is shown in **Figure 22**. By 17:12, the fire's northeastern head extended in a line from Old Fort Point upslope due east to the treeline near the old fire tower on Signal Mountain. Compared with the fire front's earlier position near Fifth Lake at 12:54, this represents a northward spread of 7 km over a 4.25-hour period—a rate of spread of 1.6 km/h (27 m/min). Intensity Class 6 fire behaviour [63] was observed throughout this period.

Aerial ignition operations were carried out at the base of Signal Mountain to work with westerly winds from the Yellowhead Pass to steer the fire's main head north-northeast, with the goal of preventing direct head fire contact with Jasper Park Lodge (Appendix B7). As the fire advanced northeast from Old Fort Point, it encountered extensive areas of less flammable fuels, including aspen stands and sparsely vegetated south-facing slopes in the valley bottoms east of Old Fort Point. These fuel types likely reduced fire spread rate and intensity compared with MPB-affected lodgepole pine or other conifer forest types. However, despite lower flame lengths and spread rates in aspen and fuel-treated stands, neither fuel type fully halted fire spread. Fuel reduction treatments around Beauvert Lake, near the Henry House historic site, reduced crown fuel load and fire intensity.

At 18:05, the fire reached Jasper Park Lodge, approximately 1.6 km from Old Fort Point, with a rate of spread of 1.6 km/h

(27 m/min), similar that observed since 13:00. The impact of the wind event observed at the Jasper townsite from 17:45 to 18:00 on spread in this sector of the fire is unknown. At Jasper Park Lodge, the golf course fairways and extensive thinning in stands around the course likely contributed to the reduced crown fraction burn observed in treated areas compared with unmanaged forest farther from town and tourism infrastructure.

The head of the fire continued to spread north-northeast toward the Skyline Trail trailhead and Maligne Canyon. Less-intense flanking fire behaviour of Intensity Class 4 to 5 [63] was observed in the Jasper Park Lodge to Edith Lake corridor. Intensity Class 4 to 5 fire with intermittent crowning [63] was also observed at 20:45 at Moberly Bridge over the Athabasca River north of Edith Lake, indicating continued north-northeast spread as the southerly winds from the Athabasca valley (the Tangle Station reported south-southwesterly winds of 14 km/h, gusting up to 27 km/h at 20:00) mixed with westerly winds coming through the Yellowhead Pass from British Columbia.

By 20:48, the fire had spread 6 km toward the base of Roche Bonhomme and Grisette Mountain, north of Maligne Canyon at Sixth Bridge, a spread rate of 2.2 km/h (36 m/min). Slopes of 20° (32%) would be expected to double the fire's spread rate as it moved from the Maligne Canyon Hostel upslope to the treeline ahead of a rapid increase in humidity and rainfall between 22:00 and 23:00 on July 24 that halted further fire spread that day.

Figure 21. Fire behaviour during Intervals 5.2 and 5.3 of the Jasper Wildfire Complex, July 24. **A**, The convection column collapse and downburst, observed from Highway 16 west of Jasper townsite at 17:41. The camera is facing east. **B**, Thick smoke and poor visibility conditions occurred during and after the convection column collapse event, photographed in the Jasper townsite at 18:20. **C**, Intermittent to continuous crown fire with a well-developed plume was observed at 20:45 at the flank of the fire located between Edith Lake and Annette Lake. The camera is facing east. **D**, Continuous crown fire was observed at 20:48 at the flank of the fire located approximately 2 km northeast of Lake Edith. The camera is facing southeast.

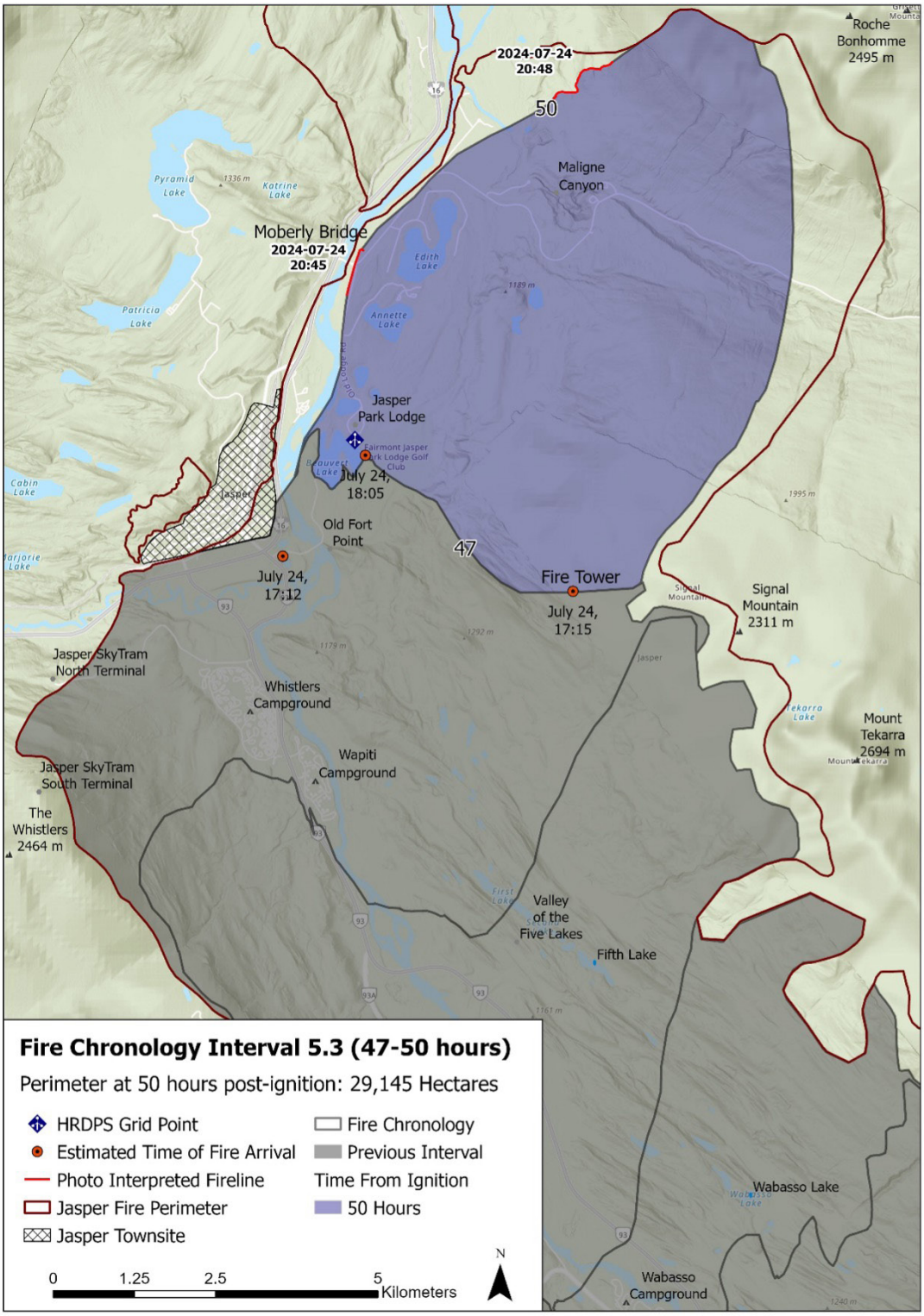

Figure 22. Fire progression map during Intervals 5.2 and 5.3 (17:00–23:00) on July 24. This shows the northeast spread of the fire front. Estimated time of fire arrival points are based on observations discussed in Section 4.6.3. Perimeter mapping from VIIRS and MODIS instruments and monoplotting using photographs taken at 20:45 (**Figure 21**) and 20:48 (**Figure 21D**).

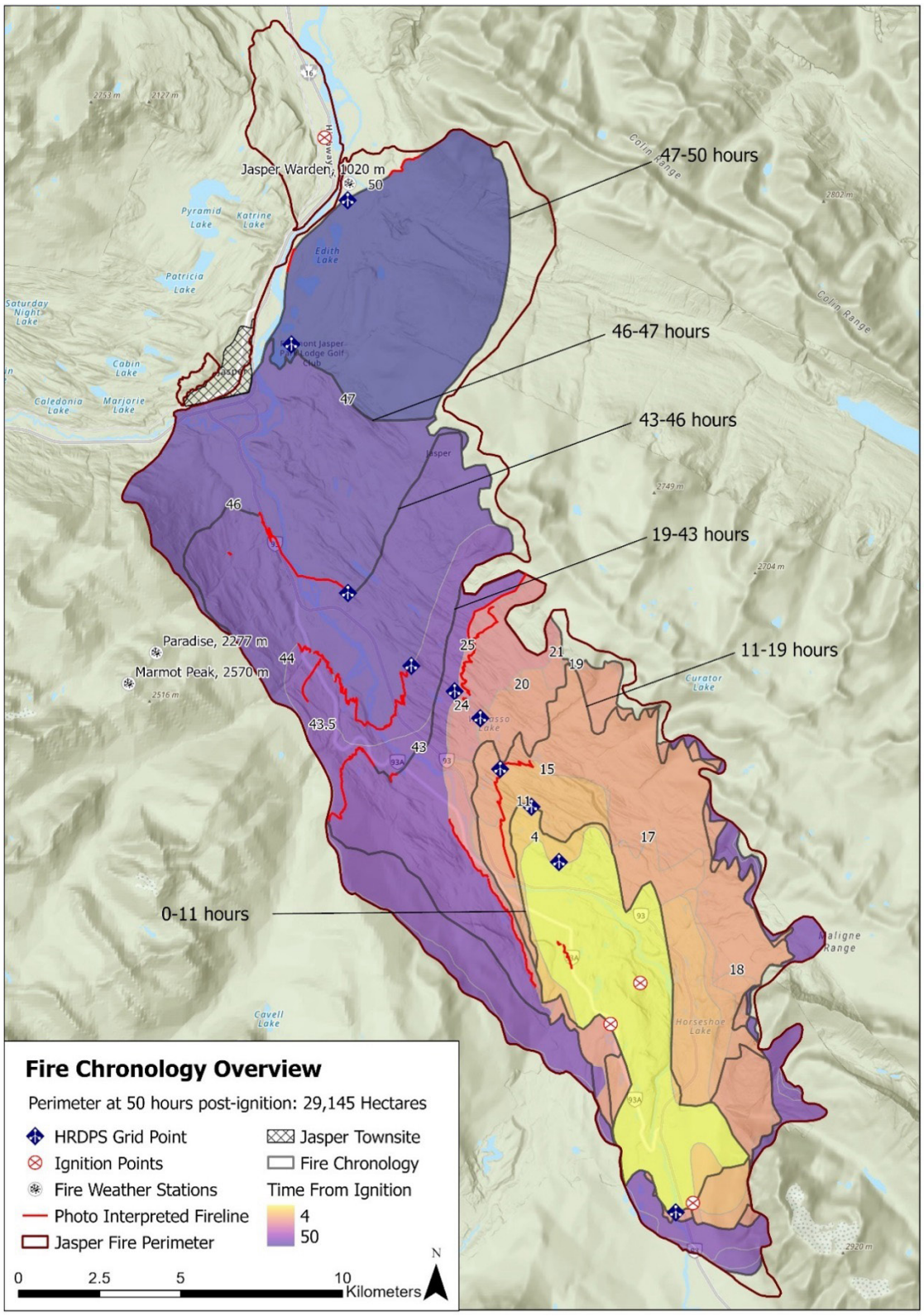

Figure 23. Full fire progression map during Intervals 1–5 of the Jasper Wildfire Complex, July 22–24, 2024. The area within the South Fire perimeter was estimated at approximately 29,145 ha at 50 hours post-ignition, late in the evening on July 24.

5. Fire severity and behaviour analyses

5.1 Fire severity

Fire severity is an important wildland fire attribute that quantifies fire impacts on vegetation and soil, which can vary greatly depending on fire behaviour and ecological characteristics [9]. In practice, fire severity is often measured as the degree of change to biomass and land cover based on measurements before and after a fire event. In addition to biomass consumption, these changes include the scorching of foliage and the immediate mortality of woody stems and branches [80]. Wall-to-wall measurement of fire severity across large wildland fires requires the use of Earth observation satellites with moderate (10–30 m) resolution, such as from the *Landsat* series or *Sentinel-2* missions. Previous research showed that satellite-based methods based on the differenced normalized burn ratio (dNBR) were effective for assessing fire severity measures in the Canadian Rockies, including Jasper National Park [81]. Analysis of immediate post-fire severity on the Jasper South Fire was conducted using *Sentinel-2* imagery. Detailed methods are described in Appendix A3.

Most of the fire area was classed as extreme (52%) and high (27%) severity, indicating extensive canopy mortality and loss of cover. Unburned and low-severity fire area classes, which indicate lower levels of biomass consumption, can provide refugia for vegetation and wildlife and accounted for approximately 12% of the fire area (**Figure 24**). Recent analysis of fire severity patterns for forests in the Montane Cordillera in British Columbia from 1985 to 2021 suggest that the severity of the Jasper Wildfire Complex was consistent with other extremely large fires (i.e. largest 5% of fires, those over 7,500 ha) in montane regions of western Canada (L. Collins, unpublished data). However, we note that differences in satellite imagery (i.e. *Landsat* series vs *Sentinel-2*), fire severity mapping approaches (i.e. year before-year after fire differencing vs. year before-year of fire differencing), and geographic extent (i.e. British Columbia vs Alberta) limit direct comparisons. Furthermore, large areas of forest affected by the MPB outbreak prior to the fire may have been incorrectly classified, as dNBR-based methods do not differentiate fire severity well in stands affected by prior disturbance [82].

Examination of fire severity patterns within the chronology intervals (Section 4) showed that extreme fire severity was widespread during the first 50 hours of fire development (i.e. Intervals 1 to 5), accounting for more than 45% of area burnt during each interval examined (**Table 5**). Extreme fire severity was the most prevalent severity class during Intervals 2 and 5, accounting for 54% to 60% of fire area. Areas that burnt in the following days (i.e. after Interval 5) displayed more heterogeneous burn patterns, with areas experiencing extreme (32%) and high (16%) fire severity, and approximately 40% experiencing low fire severity with minimal impact to the tree canopy (**Table 5**).

Fire severity is also discussed in the context of hazard reduction treatments in Section 5.2.2.

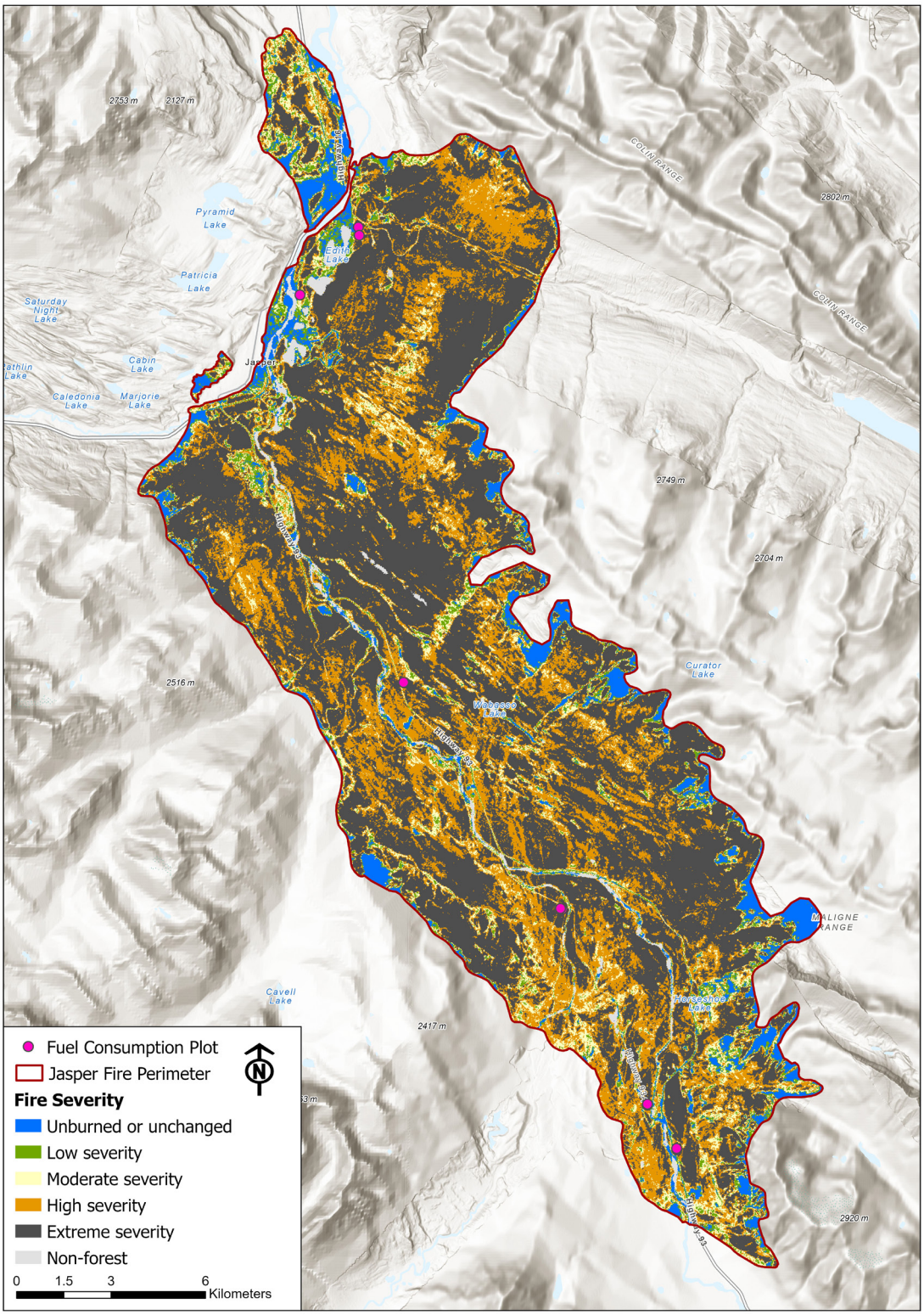

Figure 24. Fire severity mapping for the Jasper Wildfire Complex with fuel consumption plot locations. Fire severity maps were derived using *Sentinel-2* imagery (20-m resolution).

Table 5. Fire severity class distribution by chronological interval within the mapped fire perimeter for the Jasper Wildfire Complex, 2024

	Intervals[a]						After Interval 5	Full Extent
	1	2	3 and 4	5.1	5.2[b]	5.3[b]		
Affected area (ha)	3,548	5,023	5,149	7,005	4,010	4,410	3,136	32,281
Fire severity class								
Unburned or unchanged	2.1	4.0	6.5	7.7	4.7	2.6	26.2	7.0
Low	3.2	4.3	4.8	4.4	5.0	3.8	13.6	5.2
Moderate	7.9	6.9	9.4	8.1	7.4	6.2	12.5	8.1
High	35.9	27.3	33.4	25.8	22.5	28.5	16.1	27.3
Extreme	50.9	57.4	45.9	54.0	60.3	58.8	31.6	52.4

[a]Intervals are outlined in Section 4. Intervals 3 and 4 are grouped due to low affected area in Interval 4.

[b]Lower confidence in timing of fire arrival and area affected.

5.2 Fire behaviour field analysis

5.2.1 Rapid assessment plots and fuel treatment effectiveness

During the early August 2024 field campaign, 247 rapid assessment plots were assessed within the fire perimeter (**Figure 25A**). In rapid assessment plots, fire investigation techniques were used to identify fire spread direction, while estimates were made of overall crown fuel involvement and char height.[5] These investigative techniques followed the internationally recognized methods for determining fire spread direction using 1 or more of the 11 fire pattern indicators (protection, grass stem, foliage freeze, angle of char, spalling, curling, sooting, staining, ash deposits, cupping, and *V* pattern) [84]. Precise plot locations were selected from a 100 × 100 m grid and established 50 m or more from roadways. The rapid assessment plots were widely established across the fire perimeter, including oversampling within hazard reduction treatments (Section 2.4). Where possible, paired plots were established within and outside of fuel-treated areas to evaluate any influence of fuel treatments on fire behaviour.

Hazard reduction treatments were previously described in Section 2.4. **Figure 25B** shows the hazard reduction treatments overlaid on the fire severity categories near the Jasper townsite. Visual inspection suggests that severity levels were lower within most treatment polygons compared with untreated areas, although some older treatment areas still supported high and extreme severity levels.

5.2.2 Estimated crown fuel involvement

In the FBP System, crown fraction burned (CFB) is defined as the predicted proportion of the canopy involved and consumed in a fire [5]. The CFB proportion defines the fire type as either surface (0%–9% CFB), intermittent crown (10%–89% CFB), or continuous crown fire (≥90% CFB) [5]. CFB is a useful indicator of fire behaviour and severity, as it describes a gradient of crown fuel consumption and crown fuel contribution to fire intensity. In the context of evaluating fuel treatment effectiveness, a lower CFB value indicates reduced crown involvement, reduced crown fuel consumption, and reduced fire intensity; thus, a lower CFB indicates higher fuel treatment success in mitigating wildfire behaviour.

Char height is a secondary factor in determining fuel treatment effectiveness because it provides insights into fireline intensity, flame height, and tree survival following surface fire exposure. Bole char height is defined as the height above ground of visible blackening of bark and consumption of vegetation tissues, including needles or leaves in the canopy of conifer forests; it is lower than lethal scorch height [85]. When assessing fuel treatment effectiveness, lower bole char and crown scorch heights indicate lower fire intensity levels, flame lengths, and tree mortality and reflect the success of fuel treatments in reducing both vertical and horizontal fuel connectivity.

[5] Note that char height refers to visible blackening on trunks and branches and is most representative of flame height in surface fires; crown consumption refers to actual crown biomass combustion, in real or relative units. For details, see [83].

Because CFB and bole char height were only visually estimated (an ocular estimate was made by 2 trained observers), the accuracy values of these measurements is expected to be at best modest. The purpose of these assessments was to rapidly evaluate a large proportion of the fire area. In contrast, the fire severity (described above) and fuel consumption (described below, Section 5.2.3) assessments were more objective, but were either much more time-consuming and dependent on a few pre-fire plots (fuel consumption) or more difficult to interpret in the absence of ground data (fire severity).

The CFB was compared among stands from 3 treatment status groups (N=247) across all rapid assessment plots (**Figure 26**). Treatment groups consisted of the recent group (treatment years, 2017–2022; n=58), old group (treatment years, 2003–2011; n=48), and untreated group (n=141). The median CFB values for the stands in the recent group were 22%; old group, 60%; and untreated group, 90%. Differences between treatments were tested using a Kruskal-Wallis test followed by Dunn pairwise comparison test. The untreated group had significantly higher CFB values than the recent and old groups, regardless of treatment age ($P<0.001$). Differences were marginally significant ($P=0.08$) between recent and old groups, with high variability evident in the CFB in all groups. Additionally, bole char heights were compared among treatment groups (N=188) (**Figure 27**). The median char height in the recent group (n=49) was 3 m; old group (n=41), 5 m; and untreated group (n=98), 9 m. Char heights were tested between treatment groups (analysis of variance and Tukey tests); the untreated group had significantly higher bole char heights than the treated group, regardless of treatment age (recent group: $P<0.001$; old group: $P=0.03$). Differences were not significant between the recent and old groups ($P=0.54$).

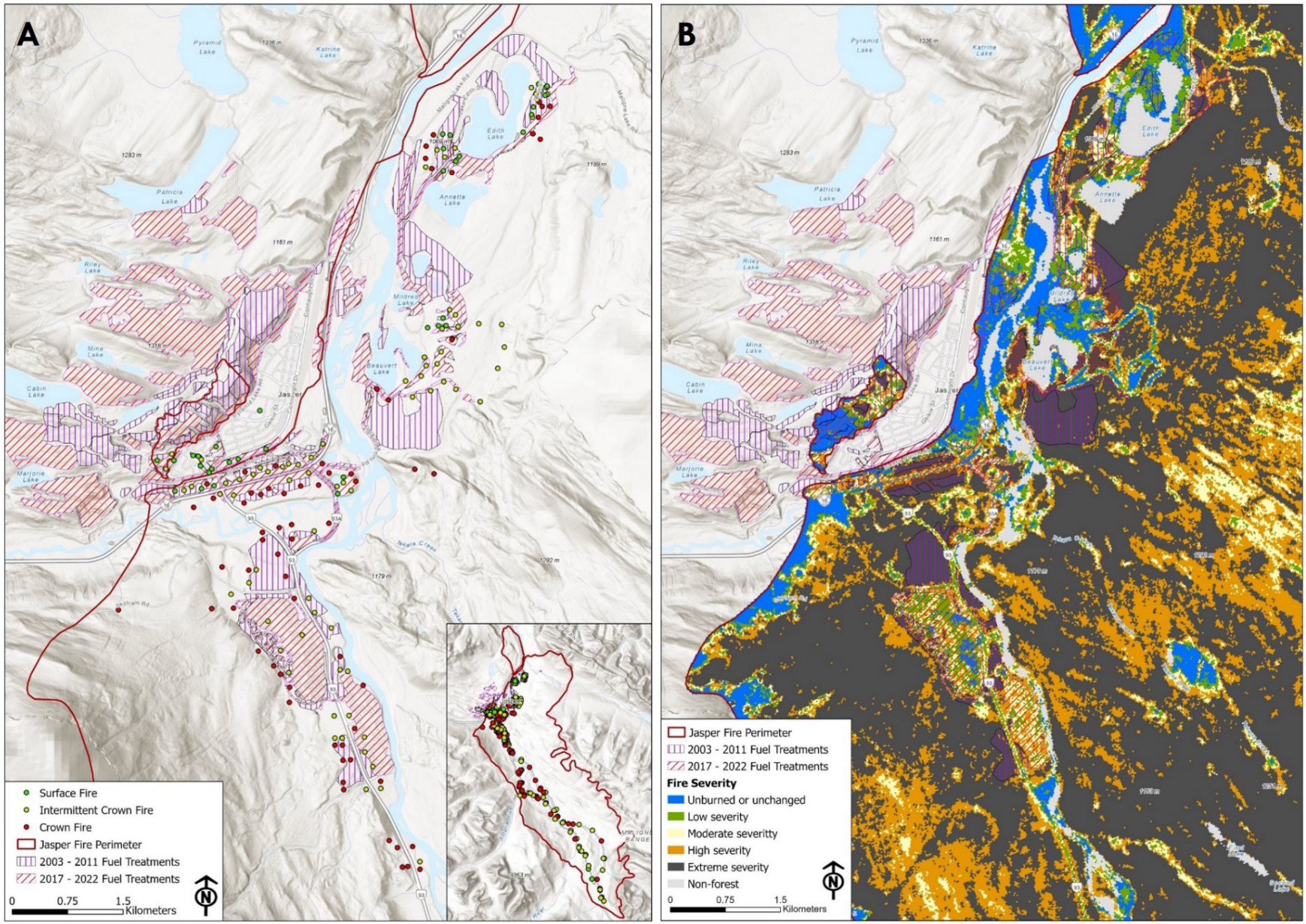

Figure 25. Hazard reduction treatments and rapid assessment plots within the Jasper Wildfire Complex perimeter during the early August field campaign. **A**, Fire type as a function of crown fraction burned from rapid assessment plots within the Jasper Wildfire Complex perimeter and wildland urban interface. **B**, Fire severity overlaid with fuel treatments near the Jasper townsite. The 2 treatment groups were old (treatment years, 2003–2011) and recent (treatment years, 2017–2022).

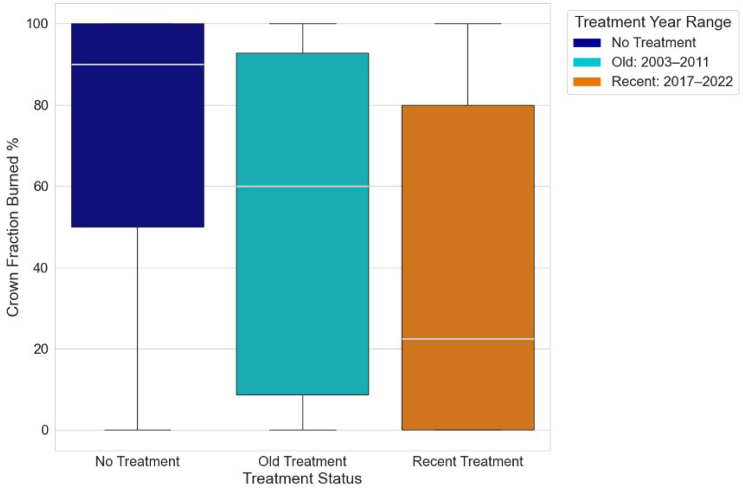

Figure 26. Distribution of crown fraction burned (%) across treatment types in the Jasper townsite wildland urban interface. The white lines indicate the treatment medians, the boxes indicate the interquartile range, and the whiskers indicate the 95% confidence interval. Differences between the untreated group and the treated groups (recent and old) were significant (α=0.05).

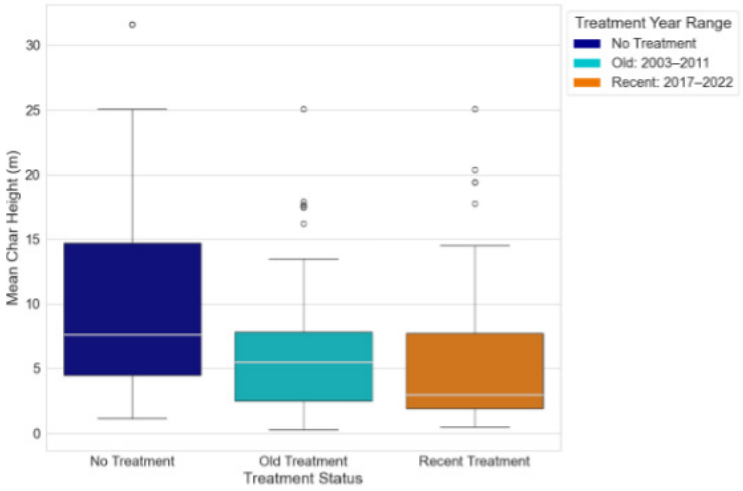

Figure 27. Distribution of mean bole char height across treatment types in the Jasper townsite wildland-urban interface. The white lines indicate the treatment means, the boxes indicate the interquartile range, the whiskers indicate the 95% confidence interval, and the circles indicate outliers.

5.2.3 Fuel consumption

In a project completed before the fire, vegetation plots were measured from 2021 through 2023 to quantify vegetation and fuel structure across the upper Athabasca valley [86]. These plots focussed specifically on the MPB effects (Section 2.2) and hazard reduction treatments (Section 2.4) surrounding the Jasper townsite. By happenstance, 18 pre-fire plots were burned in the Jasper South Fire; 11 of these were remeasured in August 2024 to quantify the consumption of various elements of the fuel bed.[6]

Detailed field methods and calculations are described in Appendix A4. We repeated the previously-used sampling and measurement approach [86] to match post-fire measurements as accurately as possible to pre-fire data. Briefly, fuel remeasurement involved assessing surface fuels at each plot using line intersect and forest floor depth measurements. Canopy fuels were assessed by first sampling overstorey trees using distance measurements. Crown fire activity was estimated by visually estimating crown consumption and char height.

[6] As noted in Section 2, pre-burn plots were collected by T. Skretting, E. Jones, L. Chasmer, and their field assistants at the University of Lethbridge, Dept. of Geography. The Documentation team is grateful for their generous sharing of data and assistance to assist our remeasurements.

Figure 28. Example plot photo showing extreme fuel consumption from the Jasper Wildfire Complex (Plot JP11). Snags (trees dead before the fire) frequently exhibited complete loss of branch structure and deep bole charring. Density reductions of approximately 40–80% indicated that many dead trees were consumed nearly completely, whether while standing or after toppling. Coordinates and bearing information are provided by the Theodolite application.[7]

Surface fuel consumption was calculated as the difference between pre-fire and post-fire forest floor and woody fuel loading. Canopy fuel consumption was complicated by the significant losses of overstorey density following the fire, where many dead trees fell and were partly or fully consumed. Although it is unknown whether dead trees fell prior to being consumed due to fire-induced winds (Appendix B10), or if they were consumed while standing, the result is the same in terms of total fuel consumption (TFC) and calculated head fire intensity (Section 5.3). Loss of branch structure and deep bole charring were frequently observed in standing dead trees, as previously reported from fires in central British Columbia [87]. Trees that were alive before the fire lost foliage and fine branch wood but had no similar deep charring (**Figure 28**).

Mean pre-fire forest floor fuel loading (litter and duff) in the 11 plots was 4.8 kg/m^2, but was highly variable, ranging from 2.7 kg/m^2 to 7.1 kg/m^2.[8] The mean value was roughly similar to values from experimental burns in boreal forests, where jack pine and black spruce stands had mean forest floor fuel loading values of 3.3 kg/m^2 and 8.3 kg/m^2, respectively [88]. Total surface fuel loading including all woody debris (mean: excluding fuel treatments, 9.0 kg/m^2; fuel treatments, 5.2 kg/m^2) was slightly lower than reported values for plots in nearby Banff National Park ([89]; mean: untreated, 11.5 kg/m^2; treated, 8.2 kg/m^2).

Fuel consumption and snag losses are summarized in **Table 6**, along with overall fire behaviour and severity classification. Classes were assigned based on fuel consumption (classified based on natural groupings), CFB and type of fire [5], and density reduction (absolute stems/ha and %). There was wide variation in the TFC, as well as in related measures such as CFB and density reductions. The mean TFC among the untreated group was 8.6 kg/m^2, which included 6.2 kg/m^2 of surface fuel consumption (SFC) and 2.4 kg/m^2 of estimated canopy and standing woody fuel consumption. In the 3 hazard reduction treatment plots, mean SFC, canopy fuel consumption (including standing woody consumption), and TFC values were all lower than untreated forest values, at 3.3 kg/m^2, 1.4 kg/m^2 and 4.7 kg/m^2, respectively. However, these means mask the variation between the 3 hazard reduction treatment plots. Based on the fuel consumption and estimated overall fire behaviour, 2 fuel treatment plots (JP21 and JP23) had much lower consumption measures and appeared largely successful at reducing crown fire activity; in contrast, 1 plot (JP20), the oldest treatment (completed in 2003), experienced extreme fuel consumption (9.6 kg/m^2) and crown fire, with 100% CFB estimated from the sampled trees and 39% reduction in overstorey density due to consumption of standing snags.

[7] See https://theodolite.app. Copyright Hunter Research and Technology LLC.

[8] Calculated from data provided by T. Skretting, E. Jones, and L. Chasmer, University of Lethbridge.

Table 6. Fuel consumption, density reduction, and overall type of fire behaviour and severity class from 11 detailed fuel plots. Hazard reduction treatment plot names include the treatment year (FTYYYY).

	FFFC	Fine WFC	Coarse WFC	Standing WFC	CFC	TFC	CFB	Type of Fire	Density Loss (/ha)	Density Loss (%)	Overall Severity[a]
Main plots											
JP1	1.46	0.68	1.16	0.60	0.06	3.95	13	Int. Crown (<50)	189	42	Medium
JP2	4.69	0.69	1.42	1.98	0	8.80	0	Surface	710	65	High
JP7	6.63	0.10	2.78	2.31	0.72	12.55	98	Cont. Crown	269	83	Extreme
JP8	7.03	0.06	0	0	0.38	7.47	88	Int. Crown (>50)	0	0	Medium
JP11	3.71	0.10	3.84	5.68	1.05	14.40	100	Cont. Crown	590	60	Extreme
JP12[b]	3.91	0.15	1.38	2.79	1.41	9.64	100	Cont. Crown	542	52	Extreme
JP13	3.16	1.57	0.60	0.24	0.66	6.23	100	Cont. Crown	114	9	High
JP14	1.11	1.02	2.51	1.29	0.03	5.96	4	Surface	494	51	Medium
Overall mean	3.96	0.55	1.71	1.86	0.54	8.62	62.9	NA	363.4	45.1	High
Treatment plots											
JP20.FT2003	4.60	0.35	0.84	2.31	1.53	9.62	100	Cont. Crown	262	39	High
JP23.FT2009	1.54	0.32	0	0	0.27	2.14	33	Int. Crown (<50)	0	0	Low
JP21.FT2022	1.84	0.33	0	0	0.04	2.21	2	Surface	0	0	Low
Overall mean	2.66	0.33	0.28	0.77	0.61	4.66	44.9	NA	87.3	12.9	NA

Abbreviations: CFB, crown fraction burned; CFC, crown fuel consumption; Cont., continuous; FFFC, forest floor fuel consumption; Int., intermittent; NA, not applicable; TFC, total fuel consumption; WFC, woody fuel consumption.

[a]See table below for details on severity classes.

[b]Estimated coarse WFC value; measured value was negative due to newly fallen logs from standing dead trees.

Severity	Type of Fire	Fuel Consumption	Density Loss
Low	Surface	<3	<50/ha or <5%
Medium	Intermittent crown <50% CFB	3–7	50–200/ha or 5–25%
High	Intermittent crown >50% CFB	7–10	200–400/ha or 25%-50%
Extreme	Continuous Crown	>10	400/ha or >50%

Fuel consumption plots were overlaid on the fire severity map (Section 5.1) to identify correlations between fuel consumption-based severity measures and remotely sensed severity categories. Although there was insufficient data for hypothesis testing, as **Figure 29** shows, there was moderately strong correlation between satellite-derived fire severity and detailed fuel consumption values, with high and extreme severity plots coincident with high and extreme severity pixels, and low fuel consumption class plots (fuel treatments JP21 and JP23) coincident with low to moderate severity classes. The relationship is not perfect due to some apparent inconsistencies: for example, plots JP2 and JP14 were classified as surface fire behaviour and low severity based on estimated CFB values of 0% to 4%, but had 50% to 65% reduction of standing tree density, suggesting extreme fire behaviour and severity; and some plots in moderate and high consumption and fire type classes landed in extreme severity pixels. The overall results suggest that fire severity mapping accurately reflects actual changes to the fuel and vegetation complex due to the behaviour of the Jasper South Fire.

The estimated HFI calculations used the final mean fuel consumption of 8.6 kg/m^2 and the maximum fuel consumption of 14.4 kg/m^2 (Section 5.3). Although the maximum value is extreme, the few consumption plots do not necessarily reflect the most severe fire impacts, where fuel consumption may even have been higher (e.g. **Figure 18D**). **Figure 30** shows additional examples of varying fire severity and consumption levels observed inside fuel treatments.

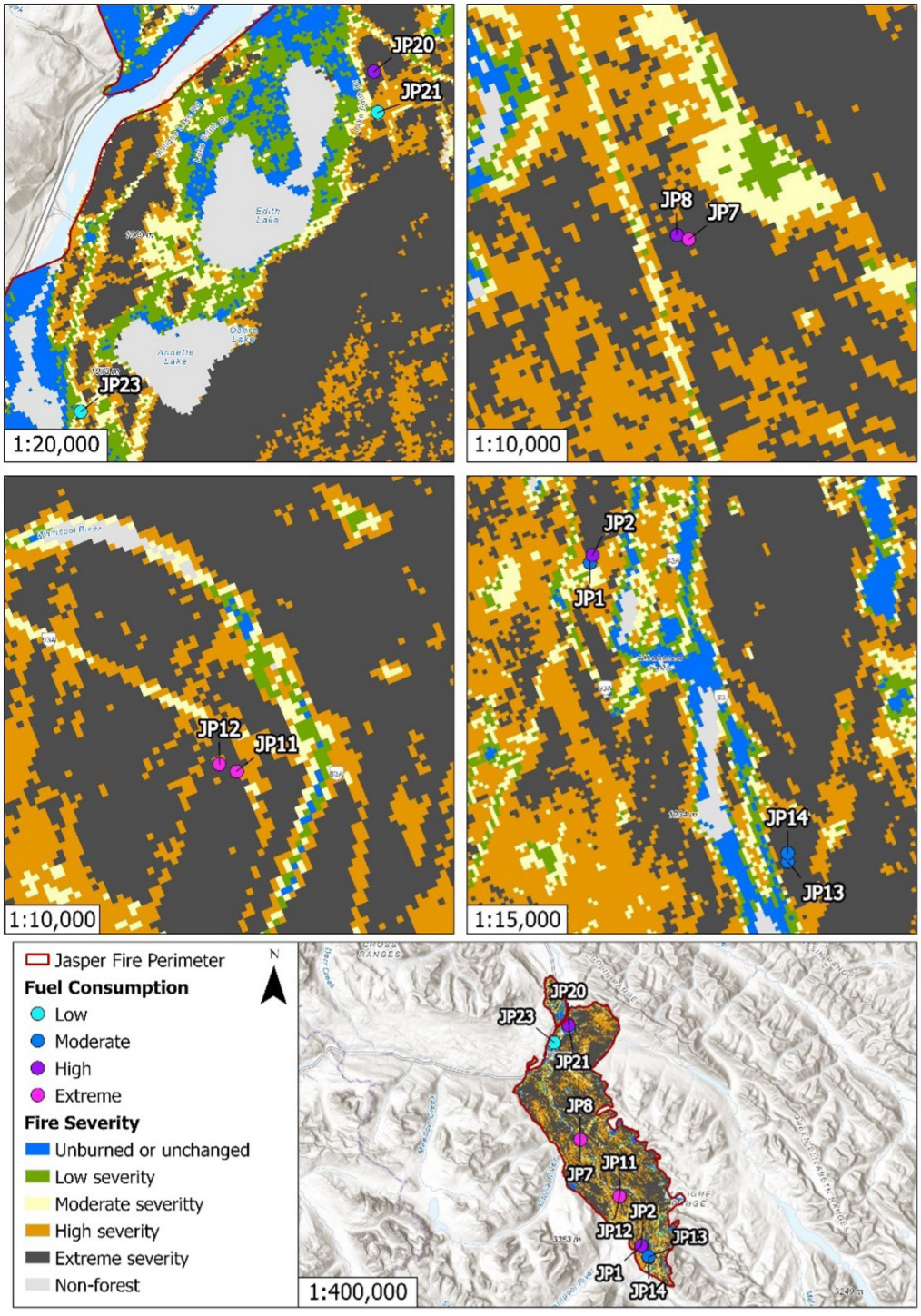

Figure 29. Fine-scale maps of fuel consumption plots overlaid with the fire severity map within the Jasper Wildfire Complex perimeter.

Figure 30. Examples of burned fuel treated stands illustrating a gradient of fire severity and tree mortality. **A**, Moderate severity with partial crown scorch and low mortality at the Jasper Park Lodge. **B–D**, High severity with almost complete crown consumption and extensive mortality at south of the hostel and lumber yard (**B**), the Wapiti Campground (**C**); and Whistlers Campground (**D**).

5.3 Head fire intensity

The intensity of the flaming front is a fire behaviour characteristic that expresses the heat release rate from the most active portion of a wildland fire (**Box 4**) [90]. In the Canadian FBP System, this measure is termed head fire intensity (HFI)[9] and is expressed in kW per metre of fireline (kW/m). HFI is correlated with operational measures of fire suppression effectiveness [91], [92] and is a key forecast variable for wildfire management.

Although fire intensity and HFI represent continuous physical variables with no upper or lower limit, wildfire personnel typically describe fire intensity using head fire intensity classes (IC), as follows (values represent kW/m): Class 1, <10 kW/m; Class 2, 10–500 kW/m; Class 3, 500–2,000 kW/m; Class 4, 2,000–4,000 kW/m; Class 5, 4,000–10,000 kW/m; Class 6, >10,000 kW/m (**Figure 31**) [63].

Table 7 shows estimated HFI values for the most intense spread episodes on July 24 (Section 4.6), estimated using measured ROS values, the mean TFC value from field plots (Section 5.2) and using the FBP System assumptions (**Box 4**). Where the highest ROS estimate (91.9 m/min) overlapped with the highest fuel consumption values (e.g. 14 kg/m^2; **Table 6** and **Figure 28**), HFI would be as high as 386,000 kW/m. As noted in **Box 4**, these extremely high values are not necessarily indicative of extreme flame lengths but rather reflect long residence times and high fuel consumption caused by the strong rotating fire plume.

Box 4. Calculating fire intensity

Fire intensity is an important measure used to compare fire behaviour within similar fuel types. It is intended to reflect the energy release rate from flaming combustion, calculated as the product of the heat content of the burning biomass , the rate of spread (ROS) of a fireline, and total fuel consumption (TFC) [80]. In the Canadian Fire Behaviour Prediction (FBP) System it is simplified as HFI = 300 × ROS × TFC for values of HFI in kW/m, ROS in m/min, and TFC in kg/m^2 [5]. For practical purposes, fire intensity is often linked to flame length, a quantity easily observed by fire suppression personnel. However, forest fire flames are transient phenomena and visual estimates of flame lengths can be imprecise. Measuring TFC during active flaming combustion in the field is challenging. Thus, it is often determined as the difference between pre- and post-burn fuel load measures days or weeks later, as in this study. However, because post-burn measurements also include fuel consumed during smoldering combustion—slow, flameless burning—their use overestimates fireline intensity. A key factor affecting HFI is the flame residence time, which is the duration of active flaming in a fuel bed. For wind-driven crown fires in boreal forests, residence time typically ranges from 30 to 60 seconds. However, in extreme fire events—such as rotating fire plumes or mass fires— residence time can extend to several minutes, leading to much higher TFC values. The elevated HFI values in such cases are not due to faster heat release or longer flames but rather prolonged flaming combustion due to efficient ventilation and abundant fuel.

[9] Earlier Canadian documents and studies used the term *frontal fire intensity*, but since the FBP System technical description was published, HFI has become standard.

Table 7. Estimated head fire intensity (HFI) of the Jasper Wildfire Complex during the afternoon of July 24[a]

Time (MDT)	Distance (m)	ROS (m/min)	ROS (km/h)	HFI (kW/m)	Est. Flame Length (m)[b]
14:03–14:30 [c]	1,520	56.3	3.4	145,244	48.4
14:30–14:57 [c]	2,480	91.9	5.5	236,978	67.0
14:03–14:57 [c]	4,000	74.1	4.4	191,111	58.1
14:57–16:55 [d]	4,790	40.6	2.4	104,731	38.9

[a] Based on a mean total fuel consumption of 8.6 kg/m^2 from field measurements (Section 5.2.3).

[b] Estimated flame length is a broad estimate of the flame size based on HFI [83], [93].

[c] Fireline position at 14:30 was mapped from satellite hotspots (Appendix A2, Appendix B6) and may be less accurate than other mapped fire positions. The combined ROS observation from 14:03–14:57 encompasses the two shorter spread distances, with fireline mapped solely from photogrammetry, and is therefore likely more accurate.

[d] Includes portions of fireline affected by ignition operations starting at 16:40 (Section 4.6.2).

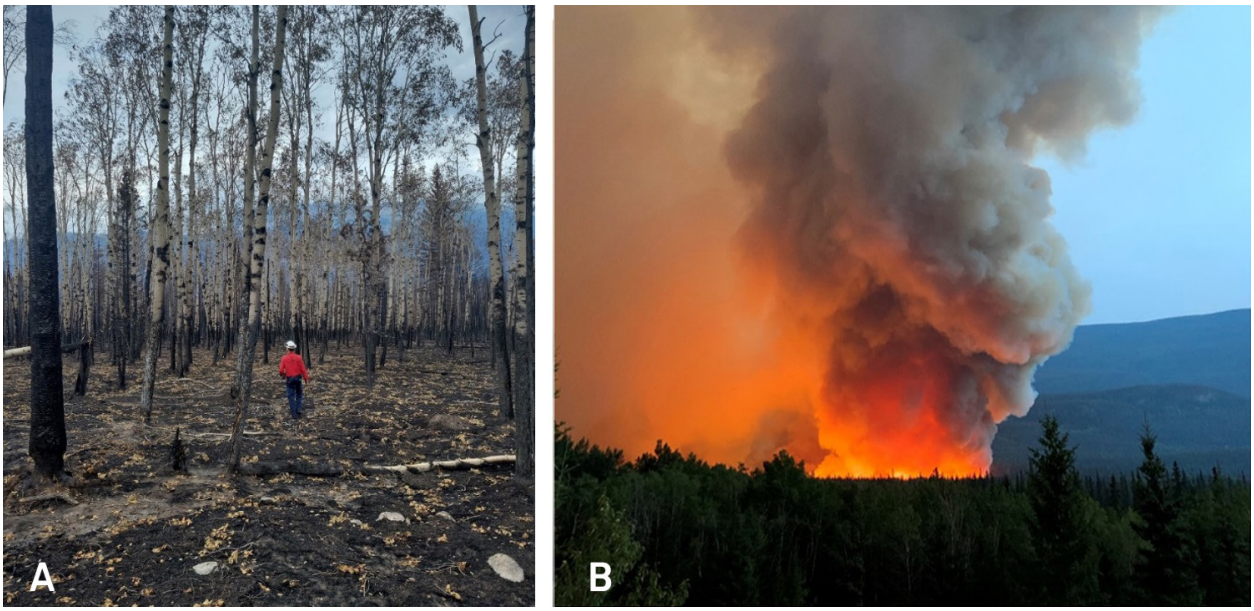

Figure 31. Additional fire behaviour examples. **A**, Example of the aftermath of high-intensity surface fire behaviour in a continuous aspen stand near Whistlers Creek. The actual fire ROS is unknown, but char heights >3 m on aspen trunks suggest a fire of at least Intensity Class 4 or higher, exceeding typical fire intensity values for leaf-out aspen forest. **B**, Intensity Class 5 fire behaviour as observed at 22:10 on the North Fire on July 23, showing evidence of intense burning conditions and an extended burning period. Note the vertical smoke column typical of fire activity under lower wind conditions.

5.4 Rate of spread comparison

Three fire spread observations from Interval 5.1 (Table 7) are shown in **Figure 32** and compared with existing rate of spread (ROS) models in the format of the FBP System (Section 2). ROS is presented as a function of the ISI (Section 3.1), which blends experimentally observed effects of fuel moisture and wind speed [5], [56]. ISI is typically calculated using the best available FFMC and wind speed observations. The mean FFMC used in this case (93.8) was the mean daily value between 2 valley bottom stations, Ranger Creek Station (94.7) and Jasper Warden Station (92.8, when rainfall is excluded), since the head of the fire was located between them. Hourly wind speeds were from Ranger Creek Station, similar to the surface wind speed values predicted by the HRDPS model.

It is apparent that the July 24 ROS observations are well above the FBP System predictions using the C-2 (boreal spruce) and C-3 (mature jack or lodgepole pine) fuel types typically used to predict fire behaviour in this region. Rate of spread models representing red attack stage MPB-affected pine [94], and an unpublished grey attack stage MPB-affected lodgepole pine model based on wildland fire observations in British Columbia also underpredicted spread rates. Instead, observations from Jasper were closer to the FBP model predictions using 2 fuel complexes representing higher fire spread rates: the M-3 model representing dead balsam fir-dominated mixedwood defoliated by the spruce budworm (shown for the 100% dead fir condition: M-3/100%DF), and the boreal pine-spruce forests measured during the International Crown Fire Modelling Experiment (ICFME).

The ICFME fuel complex from the Northwest Territories was noted for its high vertical fuel continuity and ease of crown fire development [95], [96]. Based on the described fuel characteristics (Section 2), at least some stands contained characteristics of both the M-3/100%DF and ICFME fuel complexes: a mostly dead, insect-killed, conifer overstorey as well as a vertically-continuous structure, with abundant ladder fuels in the form of spruce or subalpine fir saplings [41]. There has been some suggestion, amidst varying opinions regarding the impacts of MPB on fire activity (Section 2.2), that pre-fire stands with intermediate proportions of dead pine (together with live conifer) result in the highest fire severity levels, and possibly the most volatile fire behaviour compared with low or extremely high dead pine proportions [87]. The reasoning follows that the live canopy fuels (overstorey, ladder, or midstorey components) maintain horizontal and vertical fuel continuity and connectivity, whereas dead pines provide significant additional intensity via available (dry) coarse woody fuel.

It is important to note that the observations plotted in **Figure 32** reflect observed open wind speed values recorded by the valley bottom Ranger Creek Station (3–10 km/h from 14:00 through 17:00 on July 24), and are very low considering the extreme fire activity that was described. Higher winds speeds were modelled (**Figure 9**) and observed at higher elevations. For instance, sustained wind speeds on the afternoon of July 24 varied between 16 km/h and 31 km/h at the 2200 m level, represented by the Paradise Station, with gusts more than 75 km/h (**Figure 8**). Extreme fire activity in the presence of light ground-level winds is often the result of strong buoyancy and rising air in the fire occurring in a well-developed fire convection column [64]. As air rises in the convection column, fire-induced, turbulent, near-ground winds bring oxygen-rich fresh air downward and inward to replace rising heated air. Intense convective plumes can also interact with stronger and drier winds aloft, which can mix downward toward the ground, further increasing fire activity. This type of complex fire-weather interaction is not well-represented by operational fire behaviour models, which tend to assume simple surface wind–driven fire behaviour as detected by open ground-level (10 m) wind readings [5], [97]. Thus, another reason for the underprediction of operational models (Figure 32) is simply that they are not meant to represent plume-driven fire spread. Extreme ROS observations may also reflect rapid propagation via medium-range spotting (e.g., approx. 200 m–2 km [74]), where embers start new ignitions well ahead of the existing fireline and the disconnected fires are later joined.

Physics-based models attempt to capture these more complex interactions; however, computational resource limits and the need for detailed 3-dimensional fuels and atmospheric information precludes their utility for near-real time predictions of fire behaviour. Instead, they have been used to reconstruct alternative management scenarios to reveal fire environment factors that may have contributed to observed behaviour [98], [99], [100], [101]. Efforts are underway to conduct a detailed fire reconstruction on the Jasper South Fire using 3-dimensional coupled fire-atmosphere models [102], [103].

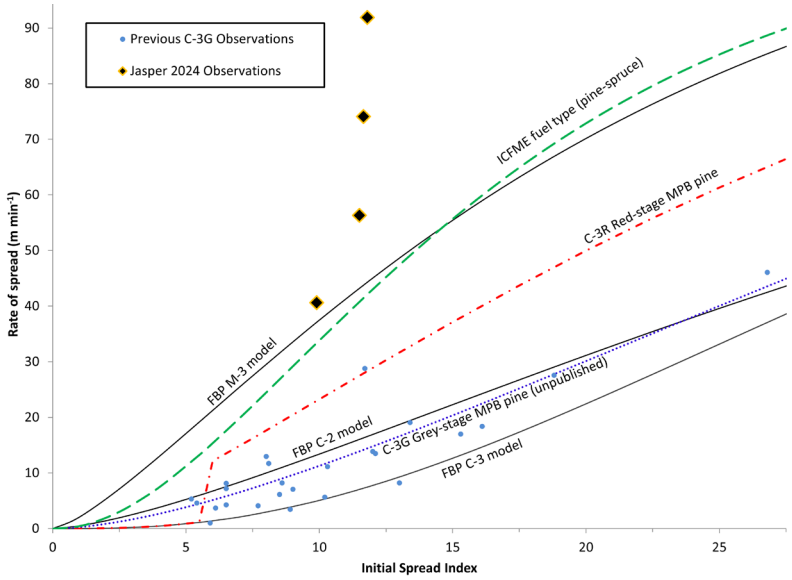

Figure 32. Observed rates of spread (ROS) on July 24 (Jasper 2024 Observations) compared with standard FBP System [11] and other ROS models, excluding the BUI effect. C-2 indicates boreal spruce FBP System fuel type; C-3, mature jack or lodgepole pine FBP System fuel type; C-3G, grey attack stage MPB-affected lodgepole pine from previous wildland fires and experimental fires (fitted model; DDB Perrakis, unpublished data); C-3R, red attack stage MPB-affected lodgepole pine fuel type [94]; FBP, Fire Behaviour Prediction; ICFME, dense pine-spruce stands of the Boreal Plains [96]; M-3, dead balsam fir mixedwood–leafless, 100% dead fir condition FBP System fuel type. 'Jasper 2024 observations are the same as in Table 7, with ISI values calculated using hourly wind speeds from Ranger Creek Station and daily FFMC as the average from the Ranger Creek and Jasper Warden stations (93.8). The point at ISI 11.7/ROS 74.1 represents the combined ROS from 14:03–14:57.

.

6. Summary and conclusions

6.1 Key factors contributing to observed fire activity

1. Drought:

Prolonged dry conditions prior to ignition significantly increased the amount of fuel available for combustion. FWI System data from nearby stations at the end of the July heat wave showed FFMC values as high as 96 and BUI values exceeding 160, representing some of the highest BUI values ever recorded in the upper Athabasca valley. This level of drying rendered nearly all surface fuels available for combustion, including litter, duff layers, and woody debris, even in healthy conifer stands.

2. Fuel connectivity:

The presence of continuous flammable vegetation is a precondition for fire growth, as fire spread follows available fuel. The source area of the fire, the upper Athabasca River valley, contained continuous mature conifer forest extending over approximately 25 km. This provided a nearly unbroken corridor for fire spread (excepting the river and highways) that was also aligned to enable wind flow channeling down the valley. The extensive fuel continuity enabled unchecked fire growth during the 50-hour window of favorable fire weather following ignition (July 22 to 24, 2024).

3. Mountain pine beetle impact:

Extensive areas of approximately 7-year-old, moderately to severely impacted, dead, grey attack stands resulting from the MPB outbreak that peaked in 2017 provided little canopy cover. This accelerated fuel drying due to increased solar exposure and wind penetration increasing surface fuel availability. MPB-induced tree mortality also turned live, moist trees into dry standing and downed woody fuel. Fuel consumption (7–14 kg/m^2) and associated fire intensities (100,000–300,000 kW/m on July 24) were 2 to 3 times higher than in unaffected green forests. The abundance of dry fuel likely led to longer daily burning periods, whereas the extreme fire intensities likely contributed to strong convective activity and plume development during some burning periods. Pre-fire sampling plots established by university researchers enabled precise fuel consumption measurements.

4. Initial ignition and rapid acceleration:

A convective storm cell moving north from British Columbia passed over the upper Athabasca valley on the evening of July 22, triggering at least 3 lightning-ignited fires near Athabasca Falls at 19:05. Within 10 minutes, intense fire behaviour was observed due to sustained 21 km/h winds and extreme gusts recorded at the closest weather station. By 23:00, the fire had exceeded 3,500 ha, well beyond initial attack or rapid containment resources.

5. Sustained fire intensity and growth:

The fire progressed from the ignition locations 23 km north to the Jasper townsite over about 48 hours, then northeast for another 8 km prior to the arrival of widespread rain showers. There was rapid fire growth when the RH was less than 30% on the night of July 22, late morning and early afternoon of July 23, and the afternoon and evening of July 24. The fire growth rate was lower in the early morning of July 23 and especially the night and morning of July 24 due to higher RH, exacerbated by prolonged atmospheric inversions in the valley bottom. However, intense fire activity was observed or calculated for several overnight and morning periods. This deviated significantly from the textbook pattern of peak fire activity in the late afternoon with minimal activity overnight due to typical diurnal trends in temperature and RH. Increased overnight burning has been linked with severe drought and climate change [104] and may have been further enabled by abundant MPB-affected fuels.

6. Plume-driven fire behaviour and fire-generated winds:

Aerial imagery indicates plume-driven fire behaviour, with deep flame in-drafting and pyrocumulus cloud formation, particularly on the afternoon of July 24. Drought conditions, high fuel consumption, moderate winds, and rapid fire spread on steep slopes contributed to intense plume formation [10]. Fire-induced winds likely exceeded 200 km/h near the main smoke column on July 24, knocking down trees over an extensive area. Amplification of fire intensity led to flame heights exceeding 50 m during periods of intense convection. Ambient valley bottom winds outside the active fire area remained light to moderate. Fire spread rates were much higher than predicted with present operational systems during this time interval.

7. Column collapse, ember transport, and downdrafts into Jasper:

Ember production and transport is a major cause of structure damage in wildland-urban interface fire disasters. Strong convection and plume development were maintained as the northwest head fire spread rapidly up The Whistlers in the late afternoon of July 24. However, the convection column collapsed at about 17:40 to 17:45, likely due to complex interactions between (1) converging valley winds (southerly from the Athabasca valley and westerly from the Yellowhead Pass), (2) the fire's uphill pull on steep slopes, and (3) the end of continuous fuels above the treeline.

The column collapse produced thick, continuous ground-level smoke and strong but short-lived southwesterly winds over the Jasper townsite from around 17:45 to 18:05. Visibility dropped suddenly and strong winds broke branches off large broadleaf trees, suggesting localized gusts up to 110 km/h. This event likely caused long distance (>1 km) transport of embers into the Jasper townsite and the initial structure ignitions. However, the dynamics of column collapse remains poorly quantified.

8. Fuel treatments:

Hazard reduction treatments implemented around the Jasper townsite since 2003 moderated fire behaviour. In treated areas, fire severity, fuel consumption, and crown fire behaviour were lower compared with untreated areas, reducing the extent of sustained crown fire and consequently reducing the ROS. Instead, intense surface fire with torching dominated in treated areas. These treatments also likely limited ember production and transport. There is some evidence that recent treatments (<10 years) were more effective than older treatments at mitigating extreme fire behaviour.

9. Uncertain wind speed and wind profile:

Wind speed is the most influential factor affecting wildland fire ROS, crown fire initiation, and ember transport [74], [105], [106] and many previous wildland-urban fire disasters have been associated with strong sustained wind speeds (>30 km/h). Surface wind data for the Jasper townsite and upper Athabasca valley were compiled from up to 8 weather stations and from the high-resolution HRDPS numerical weather model. Although sustained winds exceeding 30 km/h were intermittently recorded at higher-elevation stations (>2,200 m at Paradise and >3,000 m at Tangle), valley bottom stations (e.g. Ranger Creek, Jasper Warden, Dorothy) and high-resolution weather model output (from the HRDPS) all suggested lower speeds, except for gusts around ignition time. Observations from fire personnel on the ground or in aircraft suggested localized higher wind speed episodes, but these are difficult to reconcile with automated weather station instrument measurements. High fire ROS values despite low surface wind speeds suggest unmeasured atmospheric influences and complex atmospheric-topographic interactions that may have been influential.

6.2 Interpretations and implications for managers

Wildfire case studies

This report presents a comprehensive analysis of the ignition and spread of the Jasper South Fire. By examining fuel conditions, fire weather, and fire growth, as well as post-fire assessments of impacts and severity, a detailed, evidence-based chronology of fire behaviour was developed that accounts for how the fire progressed from ignition to impacting values in Jasper over a critical 50-hour period. Each wildfire disaster has certain unique characteristics: case studies serve to highlight these elements and reveal complex real-world challenges requiring further examination. Notably, high-profile, high-impact wildfire events that attract public attention provide opportunities to increase awareness and understanding of fire dynamics.

Increasing hazard

The probability of a large wildfire impacting a community is determined by the potential occurrence of a fire igniting and escaping initial attack with weather conditions favorable for rapid spread, and the fuel characteristics within the fireshed, or the landscape area from which a fire can spread to the community. The fuels within the Jasper South Fire perimeter primarily consisted of interconnected mature conifer forest stands extending over 25 km from the upper Athabasca valley to the Jasper townsite. Before 1900, the valley featured a more heterogeneous mix of open vegetation and closed forest, particularly in the valley bottom and lower slopes. However, over a century of fire exclusion led to a denser, more uniform forest structure. High canopy fuel connectivity created conditions favorable for sustained crown fire spread and large wildfires, as well as stands more susceptible to MPB (Section 2). This situation is not unique—mature forest cover has increased throughout the Canadian Cordillera, and previous large fires in montane and subalpine forests, including Jasper National Park (Appendix B8), demonstrate the increasing potential for significant wildfire events.

Rapid growth can exceed response capacity and trigger disaster

The lightning ignitions on July 22 occurred following a severe drying period, in line with recent studies identifying fuel aridity as a major factor contributing to increasing burned area and fire severity in western Canada [2], [107], [108]. The South Fire rapidly accelerated upon ignition and crowned under the influence of thunderstorm-driven winds. Direct suppression tactics became ineffective within scant minutes after ignition and remained unfeasible until Jasper was breached due to the fire's sustained intensity and rapid growth. Although most full response wildland fires in Canada are successfully contained within the first day after detection [109], containment depends on early detection and rapid resource deployment before the perimeter length or intensity exceed the capabilities of ground crews and aerial support [110], [111], [112]. Successful containment typically requires a moderation in wind speed or increased fuel moisture (and so reduced intensity and fire growth), as well as a rate of fireline construction surpassing the fire perimeter increase; natural barriers or fuel breaks are also frequently important. The Jasper Wildfire Complex exhibited an extremely rapid and sustained growth chronology compared with other recent cordilleran wildfires (Appendix B8). This exemplifies how a small percentage of ignitions that occur under extreme conditions are uncontrollable as long as those conditions persist. Early recognition of extreme fire potential by both Parks Canada and the Jasper townsite residents was crucial to the safe and effective evacuation of residents and visitors.

Many past wildland fire disasters can be attributed to the rapid evolution of events—a rapidly spreading wildland fire advances and impinges on a community within hours or days, outpacing the deployment of protection measures and firefighting resources [113]. The tempo of such disasters is often linked with strong to extreme winds (e.g. [67]). However, during the 50 hours of active spread of the Jasper South Fire, surface winds remained moderate, highlighting knowledge gaps in mountain meteorology and the influence of atmospheric profiles on fire behaviour.

Extreme fire intensity and plume development

The severe MPB outbreak heightened the flammability of montane and subalpine forest fuels. Combined with significant drought conditions, abundant dry fuels extended burning periods, most notably the 13 hours of sustained crown fire (10:00 to 23:00) on July 23. High fuel consumption and a favorable wind profile produced strong convective energy, leading to plume-driven fire spread.

The downburst event that affected Jasper on the afternoon of July 24 occurred under complex meteorological conditions, involving converging valley winds and the collapse of a powerful convection column. Determining the relative impact to the ember event of column collapse, wind characteristics, and more distant subalpine crown fire versus intense surface fire near the townsite remains a challenge and is beyond the capacity of current prediction models.

Community resilience

Fuel management around communities is designed to mitigate direct fire impacts and limit ember transport over short to medium distances. Jasper National Park had implemented more extensive fuel mitigation efforts around its townsite than any other Canadian community affected by a wildland fire disaster. Fuel treatments, along with natural and artificial fuel breaks (rivers, lakes, highway, railway, golf course, deciduous forest patches) likely reduced fire intensity and ember impingement in the wildland community interface, reducing the threat to safety and improving defensible positions for structural firefighters; this likely decreased structure loss in the townsite and surrounding areas.

However, wildfire disasters are the culmination of a sequence of events: (1) severe wildfire potential; (2) extreme burning conditions; (3) multiple ignitions or flammable structures; and (4) overwhelmed suppression resources [114]. An emerging consensus suggests that enhancing community resilience to wildland fires requires a multifaceted, integrated approach [115], [116]. This involves strategies including landscape risk assessment; landscape and wildland-urban interface fuel management to reduce fire severity; fire-resistant structure design, construction and maintenance; and community and pre-suppression planning and preparedness to maximize evacuation and emergency response, tailored to each community's socioecological context [117]. Early findings from the present report, particularly regarding ember transport from distant sources, as well as the successful evacuation and structure protection efforts, support this approach.

Recent wildfires impacting communities share common characteristics—particularly preceding drought conditions and extreme fire behaviour that are often beyond local experience and risk perception, challenging fire management strategies. By thoroughly documenting and analyzing fire environments and behaviour during high-profile events, we can enhance our understanding of wildland fire spread under extreme conditions and its effects on communities. Learning from these events is essential for adapting to Canada's evolving fire landscape.

7. References

[1] MNP LLP, "A Review of the 2016 Horse River Wildfire: Alberta Agriculture and Forestry Preparedness and Response," Edmonton, 2017. [Online]. Available: https://open.alberta.ca/publications/a-review-of-the-2016-horse-river-wildfire-alberta-agriculture-and-forestry-preparedness-and-response

[2] P. Jain *et al.*, "Drivers and Impacts of the Record-Breaking 2023 Wildfire Season in Canada," *Nat. Commun.*, vol. 15, no. 1, p. 6764, Aug. 2024, doi: 10.1038/s41467-024-51154-7.

[3] B. J. Stocks *et al.*, "The Canadian Forest Fire Danger Rating System: An Overview," *For. Chron.*, vol. 65, no. 6, pp. 450–457, Dec. 1989, doi: 10.5558/tfc65450-6.

[4] S. W. Taylor and M. E. Alexander, "Science, technology, and human factors in fire danger rating: the Canadian experience.," *Int. J. Wildland Fire*, vol. 15, no. 1, pp. 121–135, Mar. 2006, doi: 10.1071/WF05021.

[5] Forestry Canada Fire Danger Rating Group, *Development and structure of the Canadian Forest Fire Behavior Prediction System*, vol. ST-X-3. Ottawa, Canada: Forestry Canada, 1992. Accessed: Oct. 28, 2019. [Online]. Available: https://cfs.nrcan.gc.ca/publications?id=10068

[6] K. G. Hirsch, *Canadian Forest Fire Behavior Prediction (FBP) System: user's guide*, vol. 7. Edmonton: Canadian Forestry Service, 1996. Accessed: Jun. 23, 2020. [Online]. Available: https://ostrnrcan-dostrncan.canada.ca/handle/1845/234077

[7] M. A. Finney, S. S. McAllister, J. M. Forthofer, and T. P. Grumstrup, *Wildland Fire Behaviour: Dynamics, Principles and Processes*. Csiro Publishing, 2021. [Online]. Available: https://ebooks.publish.csiro.au/content/wildland-fire-behaviour

[8] M. G. Cruz, M. E. Alexander, and P. M. Fernandes, "Evidence for lack of a fuel effect on forest and shrubland fire rates of spread under elevated fire danger conditions: implications for modelling and management," *Int. J. Wildland Fire*, vol. 31, no. 5, pp. 471–479, Apr. 2022, doi: 10.1071/WF21171.

[9] K. C. Ryan, "Dynamic interactions between forest structure and fire behavior in boreal ecosystems," *Silva Fenn.*, vol. 36, no. 1, Dec. 2002, Accessed: Feb. 07, 2025. [Online]. Available: https://www.silvafennica.fi/article/548

[10] P. A. Werth *et al.*, "Synthesis of knowledge of extreme fire behavior: volume 2 for fire behavior specialists, researchers, and meteorologists," *Gen Tech Rep PNW-GTR-891 Portland US Dep. Agric. For. Serv. Pac. Northwest Res. Stn. 258 P*, vol. 891, 2016, doi: 10.2737/PNW-GTR-891.

[11] T. Banerjee, W. Heilman, S. Goodrick, J. K. Hiers, and R. Linn, "Effects of canopy midstory management and fuel moisture on wildfire behavior," *Sci. Rep.*, vol. 10, no. 1, p. 17312, Oct. 2020, doi: 10.1038/s41598-020-74338-9.

[12] J. L. Coen, M. Cameron, J. Michalakes, E. G. Patton, P. J. Riggan, and K. M. Yedinak, "WRF-Fire: Coupled Weather–Wildland Fire Modeling with the Weather Research and Forecasting Model," *J. Appl. Meteorol. Climatol.*, vol. 52, pp. 16–38, Jan. 2013, doi: 10.1175/JAMC-D-12-023.1.

[13] A. Bakhshaii and E. A. Johnson, "A review of a new generation of wildfire–atmosphere modeling," *Can. J. For. Res.*, vol. 49, no. 6, pp. 565–574, Jun. 2019, doi: 10.1139/cjfr-2018-0138.

[14] M. E. Alexander and M. G. Cruz, "Are the applications of wildland fire behaviour models getting ahead of their evaluation again?," *Environ. Model. Softw.*, vol. 41, pp. 65–71, Mar. 2013, doi: 10.1016/j.envsoft.2012.11.001.

[15] S. W. Taylor, D. G. Woolford, C. B. Dean, and D. L. Martell, "Wildfire Prediction to Inform Fire Management: Statistical Science Challenges," *Stat. Sci.*, vol. 28, no. 4, pp. 586–615, Nov. 2013, doi: 10.1214/13-STS451.

[16] J. J. Sharples, "An overview of mountain meteorological effects relevant to fire behaviour and bushfire risk," *Int. J. Wildland Fire*, vol. 18, no. 7, pp. 737–754, Oct. 2009, doi: 10.1071/WF08041.

[17] M. J. Schroeder and Buck, *Fire weather: a guide for application of meteorological information to forest fire control operations*. in Agriculture Handbook, no. 360. Washington, D.C.: USDA Forest Service, 1970. Accessed: Jul. 02, 2025. [Online]. Available: https://www.frames.gov/catalog/30294

[18] J. A. Milbrandt, S. Bélair, M. Faucher, M. Vallée, M. L. Carrera, and A. Glazer, "The Pan-Canadian High Resolution (2.5 km) Deterministic Prediction System," *Weather Forecast.*, vol. 31, no. 6, pp. 1791–1816, Dec. 2016, doi: 10.1175/WAF-D-16-0035.1.

[19] R. E. Keane, *Wildland Fuel Fundamentals and Applications*. Springer International Publishing, 2015. doi: 10.1007/978-3-319-09015-3.

[20] Ecological Stratification Working Group, "A National Ecological Framework for Canada," Agriculture and Agri-Food Canada and Environment Canada, Ottawa, 1996. [Online]. Available: https://sis.agr.gc.ca/cansis/publications/manuals/1996/index.html

[21] C. E. Van Wagner, M. A. Finney, and M. Heathcott, "Historical Fire Cycles in the Canadian Rocky Mountain Parks," *For. Sci.*, vol. 52, no. 6, pp. 704–717, Dec. 2006, doi: 10.1093/forestscience/52.6.704.

[22] R. D. Chavardès, L. D. Daniels, Z. Gedalof, and D. W. Andison, "Human influences superseded climate to disrupt the 20th century fire regime in Jasper National Park, Canada," *Dendrochronologia*, vol. 48, pp. 10–19, Apr. 2018, doi: 10.1016/j.dendro.2018.01.002.

[23] E. L. Davis, C. J. C. Mustaphi, A. Gall, M. F. J. Pisaric, J. C. Vermaire, and K. A. Moser, "Determinants of fire activity during the last 3500 yr at a wildland—urban interface, Alberta, Canada," *Quat. Res.*, vol. 86, no. 3, pp. 247–259, Nov. 2016, doi: 10.1016/j.yqres.2016.08.006.

[24] R. D. Chavardès and L. D. Daniels, "Altered mixed-severity fire regime has homogenised montane forests of Jasper National Park," *Int. J. Wildland Fire*, vol. 25, no. 4, pp. 433–444, Feb. 2016, doi: 10.1071/WF15048.

[25] G. F. Tande, "Fire history and vegetation pattern of coniferous forests in Jasper National Park, Alberta," *Can. J. Bot.*, vol. 57, no. 18, pp. 1912–1931, Sep. 1979, doi: 10.1139/b79-241.

[26] C. A. Stockdale, S. E. Macdonald, and E. Higgs, "Forest closure and encroachment at the grassland interface: a century-scale analysis using oblique repeat photography," *Ecosphere*, vol. 10, no. 6, p. e02774, 2019, doi: https://doi.org/10.1002/ecs2.2774.

[27] R. E. Keane, K. C. Ryan, T. T. Veblen, C. D. Allen, J. Logan, and B. Hawkes, "Cascading effects of fire exclusion in the Rocky Mountain ecosystems: a literature review," Fort Collins, CO, General Technical Report RMRS-GTR-91, 2002. Accessed: Feb. 07, 2025. [Online]. Available: https://doi.org/10.2737/RMRS-GTR-91

[28] W. Brookes, L. D. Daniels, K. Copes-Gerbitz, J. N. Baron, and A. L. Carroll, "A Disrupted Historical Fire Regime in Central British Columbia," *Front. Ecol. Evol.*, vol. 9, 2021, Accessed: May 04, 2022. [Online]. Available: https://www.frontiersin.org/article/10.3389/fevo.2021.676961

[29] J. M. Rhemtulla, R. J. Hall, E. S. Higgs, and S. E. Macdonald, "Eighty years of change: vegetation in the montane ecoregion of Jasper National Park, Alberta, Canada," *Can. J. For. Res.*, vol. 32, no. 11, pp. 2010–2021, Nov. 2002, doi: 10.1139/x02-112.

[30] C. White and E. J. Hart, *The Lens of Time: A Repeat Photography of Landscape Change in the Canadian Rockies*. University of Calgary Press, 2007.

[31] Canadian Parks Service, "Keepers of the Flame," Canadian Parks Service, Natural Resources Branch, Ottawa, 1989.

[32] A. Dhar, L. Parrott, and S. Heckbert, "Consequences of mountain pine beetle outbreak on forest ecosystem services in western Canada," *Can. J. For. Res.*, vol. 46, no. 8, pp. 987–999, Aug. 2016, doi: 10.1139/cjfr-2016-0137.

[33] B. J. Cooke and A. L. Carroll, "Predicting the risk of mountain pine beetle spread to eastern pine forests: Considering uncertainty in uncertain times," *For. Ecol. Manag.*, vol. 396, pp. 11–25, Jul. 2017, doi: 10.1016/j.foreco.2017.04.008.

[34] D. C. Romualdi, S. L. Wilkinson, and P. M. A. James, "On the limited consensus of mountain pine beetle impacts on wildfire," *Landsc. Ecol.*, vol. 38, no. 9, pp. 2159–2178, Sep. 2023, doi: 10.1007/s10980-023-01720-z.

[35] G. Abbott and M. Chapman, "2017 Freshet and Wildfires Provincial After Action Review," Emergency Management BC, Victoria, BC, 2018. [Online]. Available: https://www2.gov.bc.ca/assets/gov/public-safety-and-emergency-services/emergency-preparedness-response-recovery/provincial-emergency-planning/embc_after_action_review_report_2017.pdf

[36] H. Woo, C. Bone, K. Nadeem, and S. W. Taylor, "Influence of mountain pine beetle outbreaks on large fires in British Columbia," *Ecosphere*, vol. 15, no. 1, p. e4722, 2024, doi: 10.1002/ecs2.4722.

[37] M. A. Wulder, C. C. Dymond, J. C. White, and B. Erickson, "Detection, mapping, and monitoring of the mountain pine beetle," in *The mountain pine beetle : a synthesis of biology, management, and impacts on lodgepole pine*, Victoria, British Columbia: Canadian Forest Service, Pacific Forestry Centre, 2006. Accessed: Feb. 07, 2025. [Online]. Available: https://publications.gc.ca/site/eng/287218/publication.html

[38] W. G. Page, M. E. Alexander, and M. J. Jenkins, "Wildfire's resistance to control in mountain pine beetle-attacked lodgepole pine forests," *For. Chron.*, vol. 89, no. 06, pp. 783–794, Dec. 2013, doi: 10.5558/tfc2013-141.

[39] R. Brett, "Forest Insect and Disease Surveys of Jasper National Park, 2010-2020 (unpublished)," Canadian Forest Service, Northern Forestry Centre, Edmonton, 2020.

[40] B. C. Bright, A. T. Hudak, A. J. H. Meddens, T. J. Hawbaker, J. S. Briggs, and R. E. Kennedy, "Prediction of Forest Canopy and Surface Fuels from Lidar and Satellite Time Series Data in a Bark Beetle-Affected Forest," *Forests*, vol. 8, no. 9, Art. no. 9, Sep. 2017, doi: 10.3390/f8090322.

[41] T. Skretting, L. Chasmer, C. J. Watson, P. M. A. James, I. Townshend, and D. D. B. Perrakis, "Forest fuel structure and loading along a gradient of gray-phase mountain pine beetle severity in Jasper National Park, Alberta, Canada," *Can. J. For. Res.*, vol. 55, pp. 1–14, Jan. 2025, doi: 10.1139/cjfr-2024-0319.

[42] M. J. Jenkins, J. B. Runyon, C. J. Fettig, W. G. Page, and B. J. Bentz, "Interactions among the Mountain Pine Beetle, Fires, and Fuels," *For. Sci.*, vol. 60, no. 3, pp. 489–501, Jun. 2014, doi: 10.5849/forsci.13-017.

[43] J. A. Hicke, M. C. Johnson, J. L. Hayes, and H. K. Preisler, "Effects of bark beetle-caused tree mortality on wildfire," *For. Ecol. Manag.*, vol. 271, pp. 81–90, May 2012, doi: 10.1016/j.foreco.2012.02.005.

[44] J. Ren *et al.*, "Bark beetle effects on fire regimes depend on underlying fuel modifications in semiarid systems," Earth and Space Science Open Archive. Accessed: Mar. 28, 2022. [Online]. Available: http://www.essoar.org/doi/10.1002/essoar.10510802.1

[45] S. L. Stephens, A. A. Bernal, B. M. Collins, M. A. Finney, C. Lautenberger, and D. Saah, "Mass fire behavior created by extensive tree mortality and high tree density not predicted by operational fire behavior models in the southern Sierra Nevada," *For. Ecol. Manag.*, vol. 518, p. 120258, Aug. 2022, doi: 10.1016/j.foreco.2022.120258.

[46] R. E. Keane, "Describing wildland surface fuel loading for fire management: a review of approaches, methods and systems," *Int. J. Wildland Fire*, vol. 22, no. 1, pp. 51–62, Aug. 2012, doi: 10.1071/WF11139.

[47] W. A. Kurz *et al.*, "Mountain pine beetle and forest carbon feedback to climate change," *Nature*, vol. 452, no. 7190, pp. 987–990, Apr. 2008, doi: 10.1038/nature06777.

[48] A. J. H. Meddens, J. A. Hicke, and C. A. Ferguson, "Spatiotemporal patterns of observed bark beetle-caused tree mortality in British Columbia and the western United States," *Ecol. Appl.*, vol. 22, no. 7, pp. 1876–1891, 2012, doi: 10.1890/11-1785.1.

[49] B. M. Wotton, M. E. Alexander, and S. W. Taylor, "Updates and revisions to the 1992 Canadian Forest Fire Behaviour Prediction System," Canadian Forest Service, Sault Ste Marie, Ontario, GLC-X-10, 2009. Accessed: Dec. 03, 2019. [Online]. Available: http://publications.gc.ca/site/eng/343100/publication.html

[50] J. K. Agee and C. N. Skinner, "Basic principles of forest fuel reduction treatments," *For. Ecol. Manag.*, vol. 211, no. 1, pp. 83–96, Jun. 2005, doi: 10.1016/j.foreco.2005.01.034.

[51] S. T. McKinney, I. Abrahamson, T. Jain, and N. Anderson, "A systematic review of empirical evidence for landscape-level fuel treatment effectiveness," *Fire Ecol.*, vol. 18, no. 1, p. 21, Sep. 2022, doi: 10.1186/s42408-022-00146-3.

[52] J. L. Beverly, S. E. R. Leverkus, H. Cameron, and D. Schroeder, "Stand-Level Fuel Reduction Treatments and Fire Behaviour in Canadian Boreal Conifer Forests," *Fire*, vol. 3, no. 3, Art. no. 3, Sep. 2020, doi: 10.3390/fire3030035.

[53] T. Banerjee, "Impacts of Forest Thinning on Wildland Fire Behavior," *Forests*, vol. 11, no. 9, Art. no. 9, Sep. 2020, doi: 10.3390/f11090918.

[54] P. E. Vézina and GY. Péch, "Solar Radiation Beneath Conifer Canopies in Relation to Crown Closure," *For. Sci.*, vol. 10, no. 4, pp. 443–451, Dec. 1964, doi: 10.1093/forestscience/10.4.443.

[55] B. E. Potter, "A dynamics based view of atmosphere–fire interactions," *Int. J. Wildland Fire*, vol. 11, no. 4, pp. 247–255, 2002, doi: 10.1071/wf02008.

[56] C. E. Van Wagner, *Development and structure of the Canadian Forest Fire Weather Index System*, vol. 35. Ottawa: Canadian Forestry Service, 1987. Accessed: Dec. 13, 2019. [Online]. Available: https://cfs.nrcan.gc.ca/publications?id=19927

[57] B. D. Lawson and O. B. Armitage, *Weather Guide for the Canadian Forest Fire Danger Rating System*. 2008. Accessed: Feb. 19, 2020. [Online]. Available: https://cfs.nrcan.gc.ca/publications?id=29152

[58] B. M. Wotton, "Interpreting and using outputs from the Canadian Forest Fire Danger Rating System in research applications," *Environ. Ecol. Stat.*, vol. 16, no. 2, pp. 107–131, Jun. 2009, doi: 10.1007/s10651-007-0084-2.

[59] B. S. Lee, M. E. Alexander, B. C. Hawkes, T. J. Lynham, B. J. Stocks, and P. Englefield, "Information systems in support of wildland fire management decision making in Canada," *Comput. Electron. Agric.*, vol. 37, no. 1, pp. 185–198, Dec. 2002, doi: 10.1016/S0168-1699(02)00120-5.

[60] Canadian Forest Service Fire Danger Group (CFSFDG), *An overview of the next generation of the Canadian Forest Fire Danger Rating System*. in Information Report, no. GLC-X-26. Sault Ste Marie, Ontario: Canadian Forest Service, 2021. Accessed: Nov. 04, 2021. [Online]. Available: http://cfs.nrcan.gc.ca/publications?id=40474

[61] B. D. Lawson and G. N. Dalrymple, "Probabilities of sustained flaming ignition: lodgepole pine, interior douglas-fir and white spruce-subalpine fir forests. Supplement to Field guide to Canadian forest fire behavior prediction (FBP) system," Canadian Forest Service, Pacific Forestry Centre, Victoria, British Columbia, FRDA Handbook 012 supplement, 1998.

[62] D. J. McRae, B. J. Stocks, and C. J. Ogilvie, "Fire acceleration on large-scale convection burns," 1989, Accessed: Dec. 18, 2024. [Online]. Available: https://ostrnrcan-dostrncan.canada.ca/handle/1845/234362

[63] S. W. Taylor and M. E. Alexander, *Field guide to the Canadian Forest Fire Behavior Prediction (FBP) System*, 3rd ed. in Special Report, no. 11. Edmonton, Canada: Natural Resources Canada, Canadian Forest Service, 2018. Accessed: Apr. 03, 2020. [Online]. Available: https://cfs.nrcan.gc.ca/publications?id=39516

[64] D. J. McRae and M. D. Flannigan, "Development of large vortices on prescribed fires," *Can. J. For. Res.*, vol. 20, no. 12, pp. 1878–1887, Dec. 1990, doi: 10.1139/x90-252.

[65] K. A. Anyomi, S. J. Mitchell, and J.-C. Ruel, "Windthrow modelling in old-growth and multi-layered boreal forests," *Ecol. Model.*, vol. 327, pp. 105–114, May 2016, doi: 10.1016/j.ecolmodel.2016.02.003.

[66] D. Burgess *et al.*, "20 May 2013 Moore, Oklahoma, Tornado: Damage Survey and Analysis," *Weather Forecast.*, vol. 29, no. 5, pp. 1229–1237, Oct. 2014, doi: 10.1175/WAF-D-14-00039.1.

[67] G. Baxter, M. Richards, and C. Tymstra, "A wildland-urban post-fire case study: The Grouse Complex," Institute for Catastrophic Loss Reduction, 77, 2024. Accessed: Jul. 24, 2025. [Online]. Available: https://www.iclr.org/wp-content/uploads/2024/11/Grouse-Complex-WU-Fires-N.pdf

[68] S. Treacy, "The Impact of Wildfire Smoke on Solar Photovoltaic Power Generation in Alberta, Canada," Universidade de Lisboa, Lisbon, Portugal, 2024. Accessed: Dec. 24, 2024. [Online]. Available: https://www.proquest.com/openview/dfb0900032a4a10df0653d34cde83b53/1?cbl=2026366&diss=y&pq-origsite=gscholar

[69] G. M. Byram and G. M. Jemison, "Solar radiation and forest fuel moisture," *J. Agric. Res.*, vol. 67, no. 4, pp. 149–176, 1943.

[70] M. E. Alexander, "Surface fire spread potential in trembling aspen during summer in the Boreal Forest Region of Canada," *For. Chron.*, vol. 86, no. 2, pp. 200–212, Apr. 2010, doi: 10.5558/tfc86200-2.

[71] S. M. Steber, "Ignition Devices," in *Encyclopedia of Wildfires and Wildland-Urban Interface (WUI) Fires*, Springer, Cham, 2020, pp. 1–6. doi: 10.1007/978-3-319-51727-8_202-1.

[72] D. J. McRae, "Prescribed fire aerial ignition strategies," Natural Resources Canada, Canadian Forest Service, Great Lakes Forestry Centre, Sault Ste. Marie, Ontario, NODA/NFP Technical Report TR-33, 1996. Accessed: Aug. 25, 2023. [Online]. Available: http://cfs.nrcan.gc.ca/publications?id=9557

[73] R. R. Linn, Y. Kim, S. C. Goodrick, and J. K. Hiers, "Pyrocumulus Collapse: Unpredicted Wildfire Dangers." OSTI, 2015. [Online]. Available: https://www.osti.gov/servlets/purl/1228078

[74] F. A. Albini, M. E. Alexander, and M. G. Cruz, "A mathematical model for predicting the maximum potential spotting distance from a crown fire," *Int. J. Wildland Fire*, vol. 21, no. 5, pp. 609–627, Aug. 2012, doi: 10.1071/WF11020.

[75] J. M. Canfield, "Wildfire dynamics: Understanding some behavior trends," Florida State University, 2014. Accessed: Dec. 18, 2024. [Online]. Available: https://www.proquest.com/openview/b7ab49671141ff81d3dd8c81e96ca5bd/1?cbl=18750&pq-origsite=gscholar

[76] A. Filkov *et al.*, "Investigation of firebrand production during prescribed fires conducted in a pine forest," *Proc. Combust. Inst.*, vol. 36, no. 2, pp. 3263–3270, Jan. 2017, doi: 10.1016/j.proci.2016.06.125.

[77] D. K. Thompson *et al.*, "Quantifying Firebrand Production and Transport Using the Acoustic Analysis of In-Fire Cameras," *Fire Technol.*, Feb. 2022, doi: 10.1007/s10694-021-01194-y.

[78] S. L. Manzello, S. Suzuki, M. J. Gollner, and A. C. Fernandez-Pello, "Role of firebrand combustion in large outdoor fire spread," *Prog. Energy Combust. Sci.*, vol. 76, p. 100801, Jan. 2020, doi: 10.1016/j.pecs.2019.100801.

[79] R. Wadhwani, C. Sullivan, A. Wickramasinghe, M. Kyng, N. Khan, and K. Moinuddin, "A review of firebrand studies on generation and transport," *Fire Saf. J.*, vol. 134, p. 103674, Dec. 2022, doi: 10.1016/j.firesaf.2022.103674.

[80] J. E. Keeley, "Fire intensity, fire severity and burn severity: a brief review and suggested usage," *Int. J. Wildland Fire*, vol. 18, no. 1, pp. 116–126, Mar. 2009, doi: 10.1071/WF07049.

[81] N. O. Soverel, D. D. B. Perrakis, and N. C. Coops, "Estimating burn severity from Landsat dNBR and RdNBR indices across western Canada," *Remote Sens. Environ.*, vol. 114, no. 9, pp. 1896–1909, Sep. 2010, doi: 10.1016/j.rse.2010.03.013.

[82] S. J. Saberi and B. J. Harvey, "What is the color when black is burned? Quantifying (re)burn severity using field and satellite remote sensing indices," *Fire Ecol.*, vol. 19, no. 1, p. 24, Apr. 2023, doi: 10.1186/s42408-023-00178-3.

[83] M. E. Alexander and M. G. Cruz, "Interdependencies between flame length and fireline intensity in predicting crown fire initiation and crown scorch height," *Int. J. Wildland Fire*, vol. 21, no. 2, pp. 95–113, Apr. 2012, doi: 10.1071/WF11001.

[84] C. de Ronde and J. G. Goldammer, *Wildfire Investigation: Guidelines for Practitioners*. Kessel Publishing House, 2015.

[85] M. E. Alexander, M. G. Cruz, and S. W. Taylor, "Crown Scorch Height," in *Encyclopedia of Wildfires and Wildland-Urban Interface (WUI) Fires*, S. L. Manzello, Ed., Cham: Springer International Publishing, 2018, pp. 1–7. doi: 10.1007/978-3-319-51727-8_72-1.

[86] T. N. Skretting, "Impacts of mountain pine beetle outbreak and wildland fuel reduction treatments in Jasper National Park, Alberta, Canada," Lethbridge, Alta. : University of Lethbridge, Dept. of Geography and Environment, 2024. Accessed: Dec. 09, 2024. [Online]. Available: https://hdl.handle.net/10133/6941

[87] A. C. Talucci and M. A. Krawchuk, "Dead forests burning: the influence of beetle outbreaks on fire severity and legacy structure in sub-boreal forests," *Ecosphere*, vol. 10, no. 5, p. e02744, 2019, doi: 10.1002/ecs2.2744.

[88] W. J. de Groot, J. M. Pritchard, and T. J. Lynham, "Forest floor fuel consumption and carbon emissions in Canadian boreal forest fires," *Can. J. For. Res.*, vol. 39, no. 2, pp. 367–382, Feb. 2009, doi: 10.1139/X08-192.

[89] K. G. Hirsch and I. Pengelly, "Fuel reduction in lodgepole pine stands in Banff National Park," in *Proceedings of the Joint Fire Science Conference and Workshop*, Boise, Idaho: International Association of Wildland Fire, 1999, pp. 251-257 (Vol. II). [Online]. Available: https://ostrnrcan-dostrncan.canada.ca/handle/1845/227936

[90] J. M. Johnston *et al.*, "Direct estimation of Byram's fire intensity from infrared remote sensing imagery," *Int. J. Wildland Fire*, vol. 26, no. 8, pp. 668–684, Jun. 2017, doi: 10.1071/WF16178.

[91] K. G. Hirsch, P. N. Corey, and D. L. Martell, "Using Expert Judgment to Model Initial Attack Fire Crew Effectiveness," *For. Sci.*, vol. 44, no. 4, pp. 539–549, Nov. 1998, doi: 10.1093/forestscience/44.4.539.

[92] C. McFayden *et al.*, "Reference Guide to the Drop Effectiveness of Skimmer and Rotary Wing Airtankers," Natural Resources Canada, Canadian Forest Service, Great Lakes Forestry Centre, Sault Ste. Marie, 2023. Accessed: Aug. 31, 2023. [Online]. Available: http://cfs.nrcan.gc.ca/publications?id=41009

[93] B. W. Butler, M. A. Finney, P. L. Andrews, and F. A. Albini, "A radiation-driven model for crown fire spread," *Can. J. For. Res.*, vol. 34, no. 8, pp. 1588–1599, Aug. 2004, doi: 10.1139/x04-074.

[94] D. D. B. Perrakis, R. A. Lanoville, S. W. Taylor, and D. Hicks, "Modeling Wildfire Spread in Mountain Pine Beetle-Affected Forest Stands, British Columbia, Canada," *Fire Ecol.*, vol. 10, no. 2, Art. no. 2, Aug. 2014, doi: 10.4996/fireecology.1002010.

[95] M. E. Alexander *et al.*, *Characterizing the jack pine-black spruce fuel complex of the International Crown Fire Modelling Experiment (ICFME)*. in Information Report, no. NOR-X-393. Edmonton, Canada: Canadian Forest Service, 2004. Accessed: May 21, 2020. [Online]. Available: https://cfs.nrcan.gc.ca/publications?id=24913

[96] B. J. Stocks *et al.*, "Crown fire behaviour in a northern jack pine-black spruce forest," *Can. J. For. Res.*, vol. 34, no. 8, pp. 1548–1560, Aug. 2004, doi: 10.1139/x04-054.

[97] C. Tymstra, R. W. Bryce, B. M. Wotton, S. W. Taylor, and O. B. Armitage, *Development and structure of Prometheus : the Canadian Wildland Fire Growth Simulation Model*. Edmonton: Canadian Forest Service, 2010. Accessed: Jun. 02, 2022. [Online]. Available: https://publications.gc.ca/site/eng/9.568367/publication.html

[98] M. R. Gallagher *et al.*, "Reconstruction of the Spring Hill Wildfire and Exploration of Alternate Management Scenarios Using QUIC-Fire," *Fire*, vol. 4, no. 4, Art. no. 4, Dec. 2021, doi: 10.3390/fire4040072.

[99] J. M. Reisner *et al.*, "Informed Multi-Scale Approach Applied to the British Columbia Fires of Late Summer 2017," *J. Geophys. Res. Atmospheres*, vol. 128, no. 5, p. e2022JD037238, 2023, doi: 10.1029/2022JD037238.

[100] R. Linn *et al.*, "Incorporating field wind data into FIRETEC simulations of the International Crown Fire Modeling Experiment (ICFME): preliminary lessons learned," *Can. J. For. Res.*, vol. 42, no. 5, pp. 879–898, May 2012, doi: 10.1139/x2012-038.

[101] R. R. Linn *et al.*, "Modeling Low Intensity Fires: Lessons Learned from 2012 RxCADRE," *Atmosphere*, vol. 12, no. 2, Art. no. 2, Feb. 2021, doi: 10.3390/atmos12020139.

[102] R. Linn, J. Reisner, J. J. Colman, and J. Winterkamp, "Studying wildfire behavior using FIRETEC," *Int. J. Wildland Fire*, vol. 11, no. 4, pp. 233–246, 2002, doi: 10.1071/wf02007.

[103] R. R. Linn *et al.*, "QUIC-fire: A fast-running simulation tool for prescribed fire planning," *Environ. Model. Softw.*, vol. 125, p. 104616, Mar. 2020, doi: 10.1016/j.envsoft.2019.104616.

[104] K. Luo, X. Wang, M. de Jong, and M. Flannigan, "Drought triggers and sustains overnight fires in North America," *Nature*, vol. 627, no. 8003, pp. 321–327, Mar. 2024, doi: 10.1038/s41586-024-07028-5.

[105] M. G. Cruz and M. E. Alexander, "The 10% wind speed rule of thumb for estimating a wildfire's forward rate of spread in forests and shrublands," *Ann. For. Sci.*, vol. 76, no. 2, p. 44, Apr. 2019, doi: 10.1007/s13595-019-0829-8.

[106] D. D. B. Perrakis *et al.*, "Improved logistic models of crown fire probability in Canadian conifer forests," *Int. J. Wildland Fire*, Aug. 2023, doi: 10.1071/WF23074.

[107] M. C. Kirchmeier-Young, N. P. Gillett, F. W. Zwiers, A. J. Cannon, and F. S. Anslow, "Attribution of the Influence of Human-Induced Climate Change on an Extreme Fire Season," *Earths Future*, vol. 7, no. 1, pp. 2–10, 2019, doi: 10.1029/2018EF001050.

[108] W. Wang *et al.*, "Canadian forests are more conducive to high-severity fires in recent decades," *Science*, vol. 387, no. 6729, pp. 91–97, Jan. 2025, doi: 10.1126/science.ado1006.

[109] S. G. Cumming, "Effective fire suppression in boreal forests," *Can. J. For. Res.*, vol. 35, no. 4, pp. 772–786, Apr. 2005, doi: 10.1139/x04-174.

[110] M. C. Arienti, S. G. Cumming, and S. Boutin, "Empirical models of forest fire initial attack success probabilities: the effects of fuels, anthropogenic linear features, fire weather, and management," *Can. J. For. Res.*, vol. 36, no. 12, pp. 3155–3166, Dec. 2006, doi: 10.1139/x06-188.

[111] J. Reimer, D. K. Thompson, and N. Povak, "Measuring Initial Attack Suppression Effectiveness through Burn Probability," *Fire*, vol. 2, no. 4, p. 60, Dec. 2019, doi: 10.3390/fire2040060.

[112] S. W. Taylor, "Atmospheric Cascades Shape Wildfire Activity and Fire Management Decision Spaces Across Scales – A Conceptual Framework for Fire Prediction," *Front. Environ. Sci.*, vol. 8, 2020, doi: 10.3389/fenvs.2020.527278.

[113] J. K. Balch *et al.*, "The fastest-growing and most destructive fires in the US (2001 to 2020)," *Science*, vol. 386, no. 6720, pp. 425–431, Oct. 2024, doi: 10.1126/science.adk5737.

[114] D. E. Calkin, J. D. Cohen, M. A. Finney, and M. P. Thompson, "How risk management can prevent future wildfire disasters in the wildland-urban interface," *Proc. Natl. Acad. Sci.*, vol. 111, no. 2, pp. 746–751, Jan. 2014, doi: 10.1073/pnas.1315088111.

[115] D. E. Calkin, K. Barrett, J. D. Cohen, M. A. Finney, S. J. Pyne, and S. L. Quarles, "Wildland-urban fire disasters aren't actually a wildfire problem," *Proc. Natl. Acad. Sci.*, vol. 120, no. 51, p. e2315797120, Dec. 2023, doi: 10.1073/pnas.2315797120.

[116] Canadian Council of Forest Ministers, *Canadian Dialogue on Wildland Fire and Forest Resilience - What We Heard Report, Spring 2022*. Ottawa: Natural Resources Canada, Canadian Forest Service, 2022. Accessed: Jun. 20, 2022. [Online]. Available: https://publications.gc.ca/site/eng/9.911612/publication.html

[117] S. W. Taylor, L. D. Daniels, K. Copes-Gerbitz, and K. Forbes, "Wildfires," in *Resilient pathways report : co-creating new knowledge for understanding risk and resilience in British Columbia OPEN FILE 8910 / edited by S. Safaie, S. Johnstone, and N.L. Hastings.*, Geological Survey of Canada, 2022. Accessed: Apr. 07, 2025. [Online]. Available: https://publications.gc.ca/site/eng/9.913842/publication.html

[118] D. K. Thompson, J. Studens, C. Krezek-Hanes, and B. M. Wotton, "The impact of root exclusion on duff moisture and fire danger," *Can. J. For. Res.*, vol. 45, no. 8, pp. 978–986, Mar. 2015, doi: 10.1139/cjfr-2014-0397.

[119] H. Hart, D. D. B. Perrakis, S. W. Taylor, C. Bone, and C. Bozzini, "Georeferencing Oblique Aerial Wildfire Photographs: An Untapped Source of Fire Behaviour Data," *Fire*, vol. 4, no. 4, Art. no. 4, Dec. 2021, doi: 10.3390/fire4040081.

[120] C. Bozzini, M. Conedera, and P. Krebs, "A New Monoplotting Tool to Extract Georeferenced Vector Data and Orthorectified Raster Data from Oblique Non-Metric Photographs," *Int. J. Herit. Digit. Era*, vol. 1, no. 3, pp. 499–518, Sep. 2012, doi: 10.1260/2047-4970.1.3.499.

[121] Natural Resources Canada, "High Resolution Digital Elevation Model (HRDEM) - CanElevation Series." 2024. Accessed: Feb. 09, 2025. [Online]. Available: https://open.canada.ca/data/en/dataset/957782bf-847c-4644-a757-e383c0057995

[122] N. Gorelick, M. Hancher, M. Dixon, S. Ilyushchenko, D. Thau, and R. Moore, "Google Earth Engine: Planetary-scale geospatial analysis for everyone," *Remote Sens. Environ.*, vol. 202, pp. 18–27, Dec. 2017, doi: 10.1016/j.rse.2017.06.031.

[123] C. H. Key and N. C. Benson, "Landscape Assessment (LA)," in *FIREMON: Fire effects monitoring and inventory system.*, in Gen. Tech. Rep., no. RMRS-GTR-164-CD. , Fort Collins, CO: U.S. Department of Agriculture, Forest Service, Rocky Mountain Research Station, 2006. Accessed: Oct. 04, 2021. [Online]. Available: https://www.fs.usda.gov/treesearch/pubs/24066

[124] J. Boucher *et al.*, "Sampling fuels in the context of the next-generation Canadian forest fire danger rating system," Natural Resources Canada, Canadian Forest Service, 2023. [Online]. Available: https://ca.nfis.org/fss/fss?command=retrieveByName&fileName=Field_Guide_of_NG_Protocol.pdf&fileNameSpace=docs/nfi&format=xml&promptToSave=true

[125] C. Kleinn and F. Vilčko, "A new empirical approach for estimation in *k*-tree sampling," *For. Ecol. Manag.*, vol. 237, no. 1, pp. 522–533, Dec. 2006, doi: 10.1016/j.foreco.2006.09.072.

[126] C.-H. Ung, P. Bernier, and X.-J. Guo, "Canadian national biomass equations: new parameter estimates that include British Columbia data," *Can. J. For. Res.*, Apr. 2008, doi: 10.1139/X07-224.

[127] D. B. Perrakis, G. Eade, and D. Hicks, *British Columbia Wildfire Fuel Typing and Fuel Type Layer Description*. 2018. Accessed: Nov. 05, 2019. [Online]. Available: https://cfs.nrcan.gc.ca/publications?id=39432

[128] S. Lacarte, "Canadian Forest Fire Danger Rating System (CFFDRS) Fire Behaviour Prediction (FBP) Fuel Types 2024, 30 m." Open Canada, 2024. [Online]. Available: https://open.canada.ca/data/dataset/4e66dd2f-5cd0-42fd-b82c-a430044b31de

[129] J. Wierzchowski, M. Heathcott, and M. D. Flannigan, "Lightning and lightning fire, central cordillera, Canada," *Int. J. Wildland Fire*, vol. 11, no. 1, pp. 41–51, 2002, doi: 10.1071/wf01048.

[130] E. S. Hope *et al.*, "Exploring the use of satellite Earth observation active wildland fire hotspot data via open access web platforms," *Int. J. Digit. Earth*, vol. 17, no. 1, p. 2420821, Dec. 2024, doi: 10.1080/17538947.2024.2420821.

[131] B. Ramachandran, K. Chiang, and G. Lin, "NASA Visible Infrared Imaging Radiometer Suite Level-1B Product User Guide." NASA Goddard Space Flight Center, 2021. doi: 10.5067/VIIRS/VJ103IMG.021.

[132] W. Schroeder, P. Oliva, L. Giglio, and I. A. Csiszar, "The New VIIRS 375m active fire detection data product: Algorithm description and initial assessment," *Remote Sens. Environ.*, vol. 143, pp. 85–96, Mar. 2014, doi: 10.1016/j.rse.2013.12.008.

[133] Government of Alberta, "Final documentation report Chisholm fire (LWF-063)," Alberta Sustainable Resource Development, Forest Protection Division, Edmonton, Canada, 2001. Accessed: Jan. 31, 2023. [Online]. Available: https://open.alberta.ca/publications/0778518418

Appendix A – Methodology

A1. Estimating additional forest floor drying due to MPB-driven cover loss

This report has already shown that the BUI at the time of ignition was the highest value on record for the time of year. However, the BUI index likely underpredicted just how anomalous the drying at the forest floor was relative to the historical climatology due to the recent canopy mortality from the Mountain Pine Beetle (MPB). As mentioned in Section 2.2, Jasper saw a severe MPB attack that peaked around seven years before the fire. The significant loss of foliage that occurred from this attack increased solar radiation and wind at the forest floor, both of which tend to dry fuels. However, the FWI system assumes a moderate canopy cover and cannot be easily adjusted to account for these changes to the stands. In this section we outline an approach for estimating an "enhanced BUI" that accounts for this additional drying resulting from canopy mortality.

To estimate the enhanced drying, we first used vegetation surveys of MPB-effected stands collected by [86] along with standard allometric equations to estimate canopy cover as described by the Plant Area Index (PAI). This PAI value, along with historical open weather conditions observed at the Jasper Warden weather station, was used to force a suite of models (outlined in [118]) for simulating subcanopy microclimates given open site conditions and canopy cover. These microclimatic conditions were then used to estimate Potential Evapotranspiration (PET) at the forest floor.

The vegetation surveys also identified trees that had lost their needles due to the MPB ("grey attack"). We were therefore able to model subcanopy PET for a counter-factual case where the MPB attack did not happen by adding the needle biomass back into the calculation of PAI. We then selected a stand with moderate pre-MPB canopy cover that most closely resembled the ideal pine-plantation stands utilized when developing the FWI indices. Using 62 years of open site weather data from the Jasper Warden weather station we calculated daily total subcanopy PET for both the MPB and non-MPB case and calculated and average percent increase in daily PET for the MPB case compared to the non-MPB case.

Because of the exponential relationship between the DMC and duff moisture content [9] one can assume that the log-drying rate of the DMC is linearly related to PET. Moreover, we assumed that the standard BUI reflected conditions within the moderate-canopy stand for the non-MPB case. Given these two assumptions, we applied the percent increase in daily PET calculated in the last step to the DMC log-drying rate of the non-MPB case (the standard BUI) to estimate an "enhanced BUI" that accounted for the enhanced drying potential within MPB-attacked stands.

A2. Fire progression analysis

Highly accurate fireline position delineation is possible using aerial wildfire photographs in combination with photogrammetry techniques. This monoplotting process in the context of fire behaviour reconstruction involves georeferencing oblique photographs using high resolution Digital Elevation Models (DEMs) and orthophotography; it can be used to analyze fire progression and identify fire behaviour characteristics such as rate of spread [119]. The monoplotting technique was used on the Jasper South fire using selected photographs captured by observers during reconnaissance flights or evacuation efforts, taken at various times and locations between July 22 and July 24 (**Figure 10**, **Figure 12**, **Figure 14**, **Figure 15**, **Figure 17**, and **Figure 21**). Photos with unobstructed views of the fire perimeter (head, flank or back) were analyzed (Table S-1) using the WSL Monoplotting Tool (MPT) [120], along with 1m LiDAR derived DEMs [121] and 30 cm orthophotography collected in 2020 (courtesy of Parks Canada). All firelines were mapped within a 5 m range of accuracy for mean and maximum 3D errors.

Table S-1. Fire progression information including time from ignition, date and time of individual time steps, image data used for photogrammetric analysis (photo name, time, fire location, status), source of data (source and comments) and corresponding fire chronology interval. Note: photogrammetric analysis of some images enabled the extraction of a combination of fire locations (head, flank and back).

Time From Ignition	Date	Time	Photo Name	Monoplotted Time	Fire Location	Status	Source	Comments	Fire Interval
1	2024-07-22	23:00:00	IMG_5314	20:38	Head	Calculated	MPT	Fireline from MPT	Chronology Interval 1
11	2024-07-23	6:00:00	-	-	-	-	M3	Fireline from Hotspot data only	Chronology Interval 1
15	2024-07-23	10:00:00	IMG_0194	09:57	Head	Calculated	MPT	Fireline from combination of MPT + Hotspot	Chronology Interval 2
15	2024-07-23	10:00:00	IMG_0194	09:57	Flank	Inferred	MPT	Fireline from combination of MPT + Hotspot	Chronology Interval 2
15	2024-07-23	10:00:00	-	-	-	-	M3	Fireline from Hotspot data only	Chronology Interval 2
17	2024-07-23	12:00:00	-	-	-	-	M3	Fireline from Hotspot data only	Chronology Interval 2
18	2024-07-23	13:00:00	-	-	-	-	M3	Fireline from Hotspot data only	Chronology Interval 2
19	2024-07-23	14:00:00	-	-	-	-	M3	Fireline from Hotspot data only	Chronology Interval 2
20	2024-07-23	15:00:00	-	-	-	-	M3	Fireline from Hotspot data only	Chronology Interval 3 & 4
21	2024-07-23	16:00:00	-	-	-	-	M3	Fireline from Hotspot data only	Chronology Interval 3 & 4
24	2024-07-23	19:00:00	IMG_0266	19:14	Back	Calculated	MPT	Fireline from combination of MPT + Hotspot	Chronology Interval 3 & 4
24	2024-07-23	19:00:00	IMG_0268	19:18	Flank	Calculated	MPT	Fireline from combination of MPT + Hotspot	Chronology Interval 3 & 4
24	2024-07-23	19:00:00	IMG_0268	19:18	Head	Calculated	MPT	Fireline from combination of MPT + Hotspot	Chronology Interval 3 & 4
25	2024-07-23	20:00:00	IMG_2322	20:30	Head	Inferred	KML Estimate	Fireline from combination of Hotspot + Google estimate	Chronology Interval 3 & 4
43	2024-07-24	14:00:00	IMG_0313	14:03	Head	Calculated	MPT	Fireline from combination of MPT + Hotspot	Chronology Interval 3 & 4
43	2024-07-24	14:00:00	IMG_0313	14:03	Back	Calculated	MPT	Fireline from combination of MPT + Hotspot	Chronology Interval 3 & 4
43	2024-07-24	14:00:00	IMG_0313	14:03	Flank	Inferred	MPT	Fireline from combination of MPT + Hotspot	Chronology Interval 3 & 4
43.5	2024-07-24	14:30:00	-	-	-	-	M3	Fireline from Hotspot data only	Chronology Interval 5.1
44	2024-07-24	15:00:00	IMG_2289	14:57	Head	Inferred	MPT	Fireline from combination of MPT + Hotspot	Chronology Interval 5.1
44	2024-07-24	15:00:00	IMG_0909	14:47	Head	Inferred	MPT	Fireline from combination of MPT + Hotspot	Chronology Interval 5.1
44	2024-07-24	15:00:00	IMG_0909	14:47	Head	Calculated	MPT	Fireline from combination of MPT + Hotspot	Chronology Interval 5.1
44	2024-07-24	15:00:00	IMG_2289	14:57	Head	Calculated	MPT	Fireline from combination of MPT + Hotspot	Chronology Interval 5.1
44	2024-07-24	17:00:00	IMG_2143	16:57	Head	Calculated	MPT	Fireline from combination of MPT + Hotspot	Chronology Interval 5.1
46	2024-07-24	17:00:00	IMG_2138	16:55	Head	Calculated	MPT	Fireline from combination of MPT + Hotspot	Chronology Interval 5.1
46	2024-07-24	17:00:00	IMG_2138	16:55	Head	Inferred	MPT	Fireline from combination of MPT + Hotspot	Chronology Interval 5.1
46	2024-07-24	17:00:00	IMG_2151	17:02	Head	Calculated	MPT	Fireline from combination of MPT + Hotspot	Chronology Interval 5.1
47	2024-07-24	18:00:00	-	-	-	-	Accounts and photos	Fireline estimated from accounts and photos	Chronology Interval 5.2
50	2024-07-24	21:00:00	IMG_8229	20:45	Flank	Inferred	KML Estimate	Fireline from combination of Hotspot + Google estimate	Chronology Interval 5.3
50	2024-07-24	21:00:00	IMG_8251	20:48	Flank	Calculated	MPT	Fireline from combination of MPT + Hotspot	Chronology Interval 5.3

A3. Fire severity mapping

This appendix describes the methods used to create the fire severity analysis and map in Section 5.

Fire severity mapping for the Jasper wildfire was derived using Sentinel 2 imagery in Google Earth Engine [122]. Sentinel 2 imagery was collected over two 45-day windows, beginning August 8, 2023 ("pre-fire" collection) and August 8, 2024 ("post-fire" collection). Pixels affected by cloud or snow were masked from images. The normalised burn ratio (NBR) was calculated for every image in the pre- and post-fire collections. A composite NBR was derived for every pixel by calculating the median NBR for both the pre- and post-fire collections. The differenced normalised burn ratio (dNBR) was then calculated by subtracting the post-fire NBR composite from the pre-fire NBR composite. The dNBR was categorised into five fire severity classes using thresholds suggested by [123]. Descriptions of the fire severity classes are provided in **Table S-2**. Areas of non-woody vegetation were excluded from the fire severity maps because fire severity classes lose their meaning in areas of non-woody vegetation. Woody vegetation masks were created using the Commission for Environmental Cooperation 2020 landcover layer for North America.[10]

Table S-2. Fire severity classes mapped for the Jasper wildfire. The classes have been assigned using the differenced normalised burn ratio (dNBR) thresholds suggested by Key and Benson [123].

Map value	Fire severity class	Fire type and impact
1	Unburned or unchanged	Unburned or low intensity and patchy surface fire
2	Low	Low intensity surface fire with low degree of crown scorch in the canopy layer
3	Moderate	Low intensity surface fire with moderate degree of crown scorch in the canopy layer
4	High	Fire resulting in full crown scorch or partial consumption of crown foliage in the canopy layer
5	Extreme	Fire resulting in complete or near-complete consumption of crown foliage in the canopy layer

[10] See http://www.cec.org/north-american-environmental-atlas/land-cover-30m-2020/.

A4. Fuel consumption sampling and calculations

This section describes the methods used to measure fuel consumption in the 11 field plots. As noted previously (Section 5.2.3), detailed fuel structure and loading plots were measured in 2021–2023 by researchers from the University of Lethbridge to assess fire hazard in the upper Athabasca and around Jasper; by random chance, 18 of these plots were burned in the Jasper South fire.

As per the standard for experimental fires in the Canadian Forest Fire Behavior Prediction System, fuel consumption was calculated as the difference between fuel loading before and after fire in various components of the fuel complex [5], recognizing that this likely overpredicts flaming consumption (see also Section 5.4 for discussion of fuels and fire intensity). For pre-burn sampling methods, see [86]. The methods described here refer to the plot remeasurement that occurred during the field campaign between August 4–9, 2024.

Plot locations were first located by hand-held GPS, estimated accurate within 2 m in open forests. Once the plot centre was marked, a random azimuth was selected for establishing a 40 m transect for measuring woody fuels. Standard planar intersect methods were used to survey woody fuel loading by size-class, while duff loading was estimated by measuring the duff depth at four locations along the transect [124]. Depths were converted to loading values by multiplying by the mean pre-burn duff bulk density (0.21 g/cm^3; [86]).

Tree density was estimated by measuring the distance from plot centre to the closest seven trees and calculating a circular area, as described in [125]. On the six closest trees, species and status (live/dead) were identified, height and diameter at breast height were measured and crown fraction burned (CFB) was estimated.

The mean pre-fire overstory density was 791 stems/ha excluding fuel treatment plots, with a range of 200 to 1250 stems/ha. Pre-fire density in fuel treatment plots was 675 stems/ha, 150 stems/ha and 175 stems/ha in the 2003, 2009 and 2022 treatments, respectively (data from [86]).

Total Fuel Consumption (TFC) was calculated as the sum of consumption values for individual fuel components: forest floor (litter and duff), fine woody debris (<7 cm diameter), and coarse woody debris (>7 cm diameter) as noted above, along with standing biomass (loss of whole trees), and canopy fuel. Standing biomass consumption was estimated from overstory density losses following fire. Density changes were calculated as pre–post; where density increased or decreased by less than 50/ha, measurement noise was assumed. Larger changes in density were observed to be caused by losses of dead snags; while species were not always identifiable, the overwhelming majority of snags (pre-fire) were beetle-killed lodgepole pine [86]. The mean diameter of dead pine for the plot [86] was therefore used to estimate bole, branch, and bark biomass using allometric equations for lodgepole pine [126]. To estimate canopy fuel consumption, we first estimated canopy fuel load (CFL) for each plot as the sum of (1) pre-fire individual tree estimates of foliage for live conifers or red attack stage pine (Section 2.2), and (2) branch wood estimates for snags of any species; tree values were scaled to an area basis (kg/m^2). The CFL value was multiplied by the estimated CFB value (mean of six trees) for the plot to get the final estimated CFC. Bole wood consumption on standing snags was assumed to be negligible, though deep char was frequently observed.

Appendix B – Supplemental Information

B1. Canadian Forest Fire Behavior Prediction System (FBP) fuel types

As noted in Section 2, trained fire management personnel typically assign 1 or more fuel types from the FBP System to predict the behaviour of active wildfires. To aid in these fuel type assignments, maps and data layers are often prepared ahead of time, typically based on forest inventory data or remote sensing sources. **Figure S-1** shows the most recent (pre-fire) FBP fuel type map extracted from a national FBP fuel type layer. Note that the dominant fuel type ("C-3 Mature jack or lodgepole pine") is generally applied to live pine stands [5] and this fuel type assignment does not consider the impacts of mountain pine beetle-caused overstory mortality (Section 2.2). In British Columbia, for instance, a recent fuel typing algorithm suggested that the C-2 or M-3 fuel types would be the best match for certain MPB-affected stands [127].

Figure S-1. Canadian Forest Fire Behavior Prediction (FBP) System fuel type map within the Jasper Wildfire Complex fire perimeter using the national 30m fuel type raster [128]. This classification assumes no impact from the mountain pine beetle or tree mortality in general.

B2. Lightning climatology

Cloud to ground strike information from the Canadian Lightning Data Network demonstrates the typically low lightning frequency within the Jasper National Park boundaries [129].

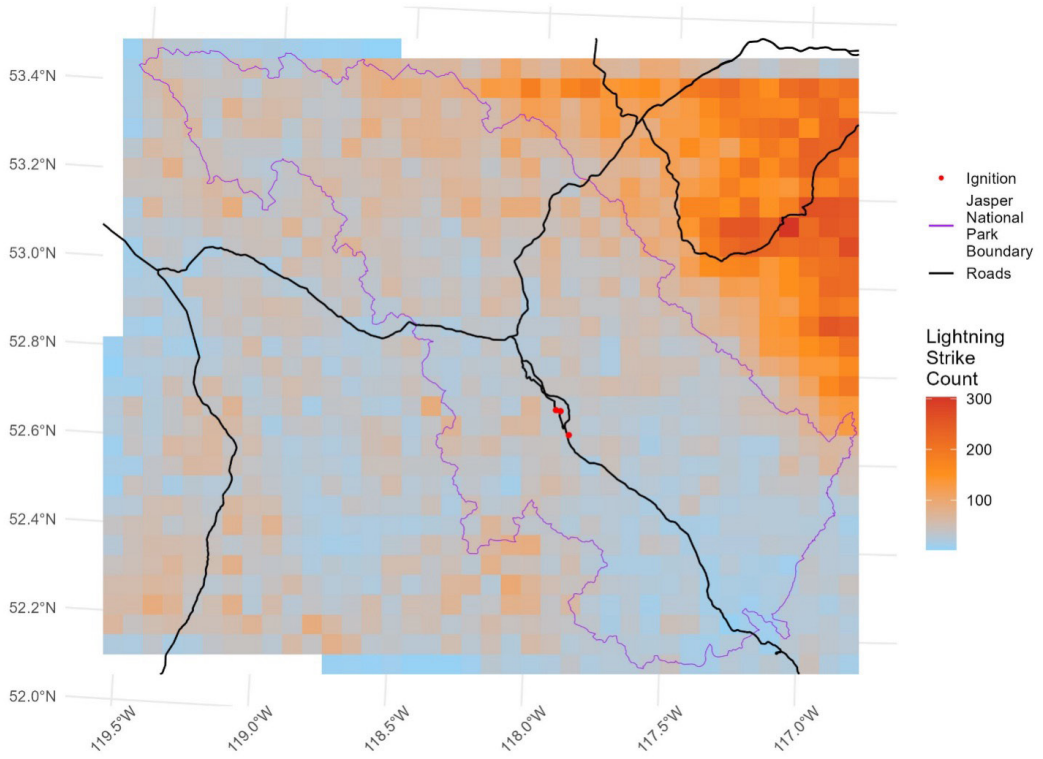

Figure S-2. Cumulative (2015-2024) count of lightning flashes per 5 km wide grid cell. Jasper National Park boundary is shown in purple, highways are shown as black lines.

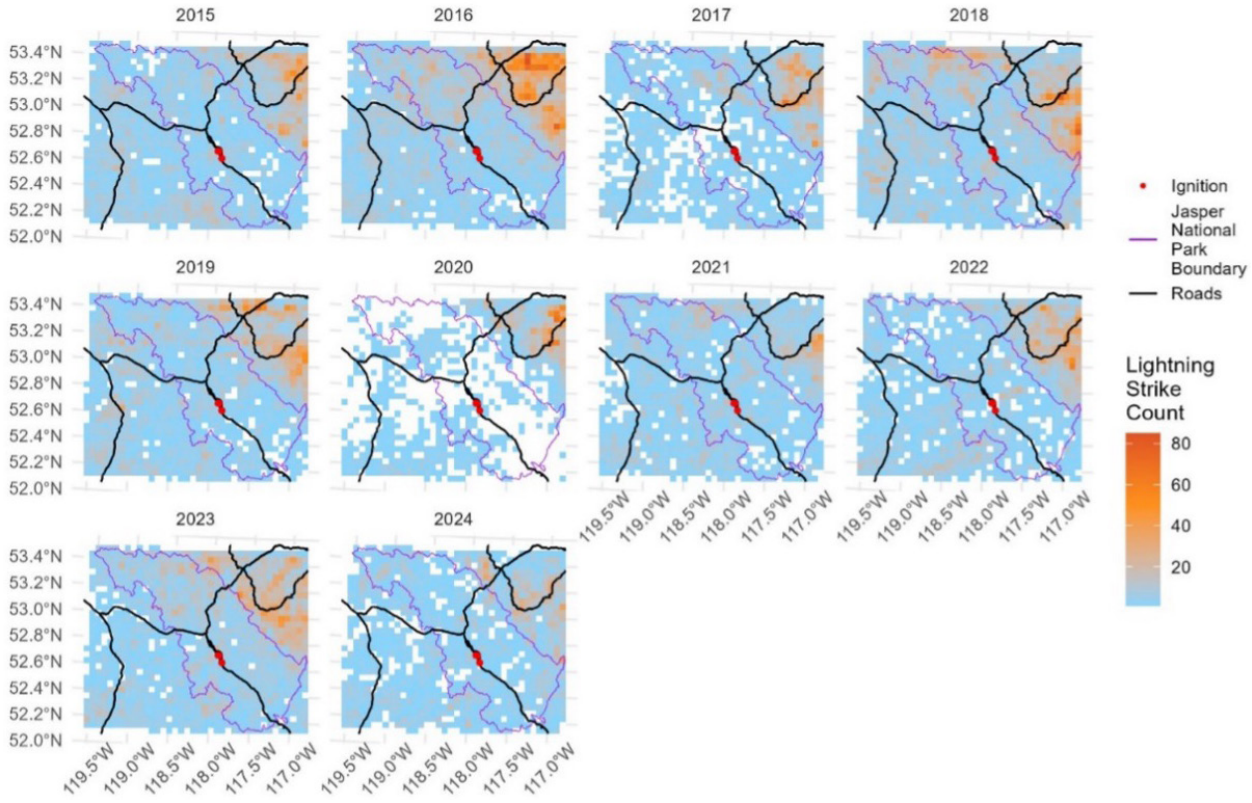

Figure S-3. Annual trends in lightning flash density in Jasper National Park (red outline) from 2015–2024. Values shown are the total count of lightning per grid cell. The white colour represents no detections in a cell for a given year.

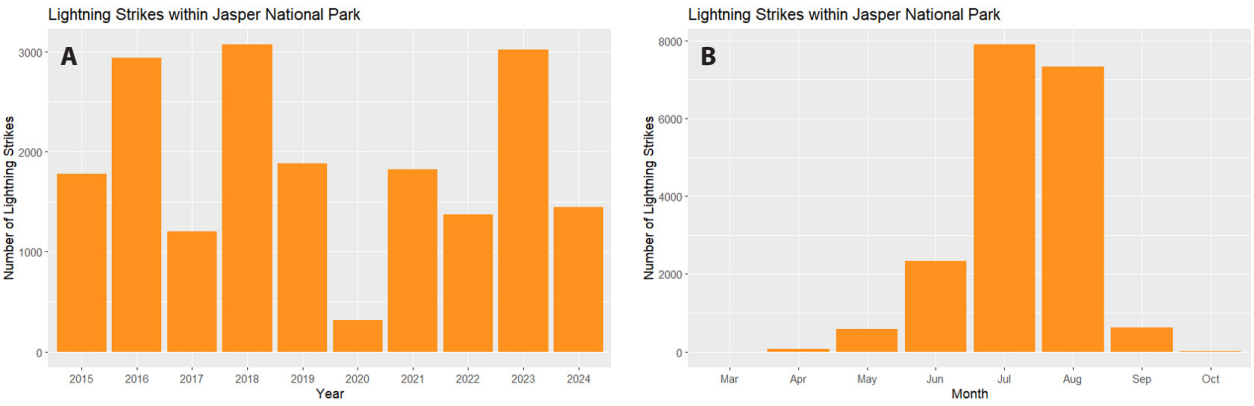

Figure S-4. Lightning strike summary for Jasper National Park. **A)** Annual cloud-to-ground lightning strike count in Jasper National Park Annual from 2015–2024. **B)** Monthly distribution in cloud-to-ground lighting strikes in JNP during the fire season.

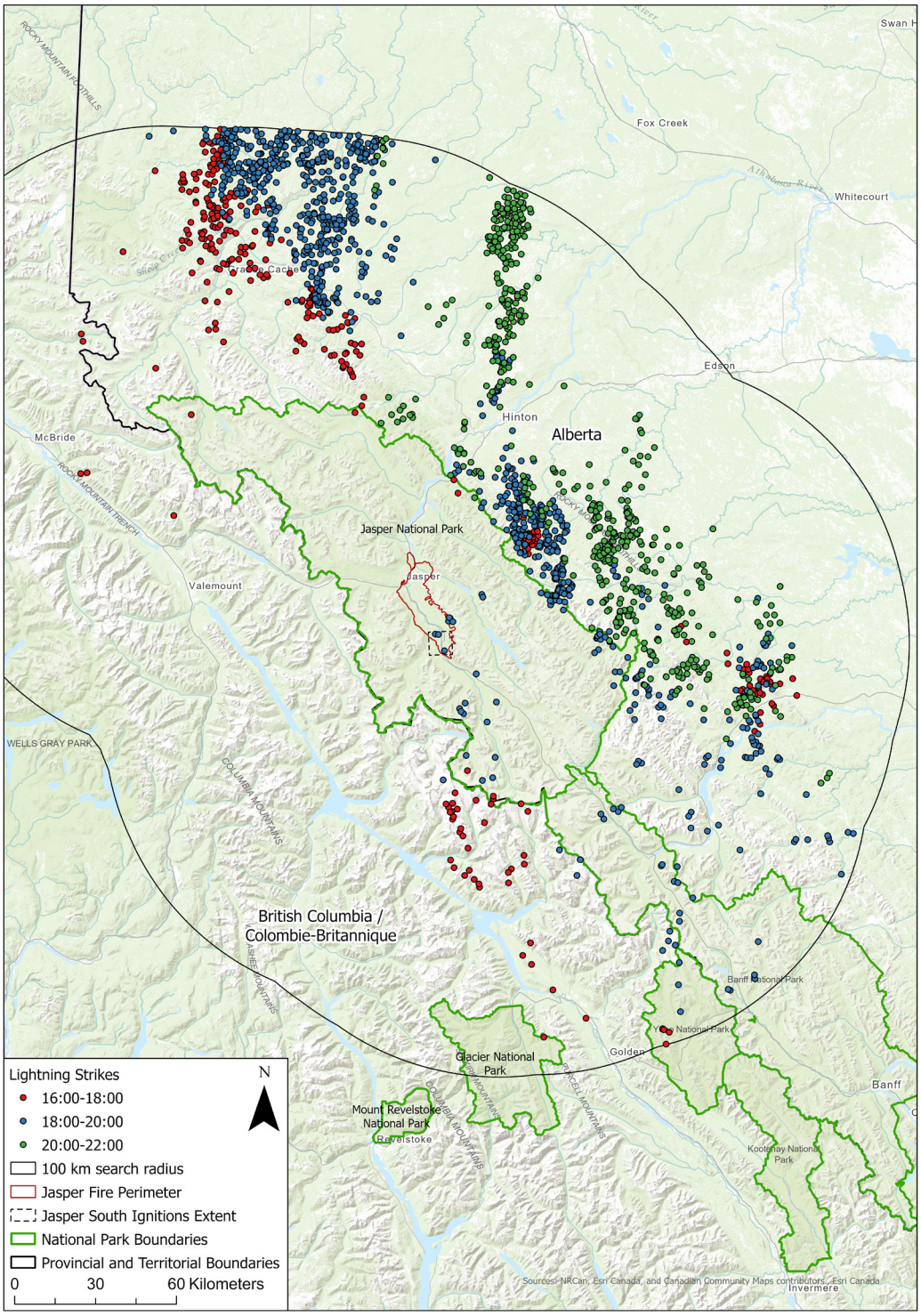

Figure S-5. Cloud-to-ground lightning strikes in the vicinity of Jasper National Park from 16:00–22:00, July 22. Red: 16:00–18:00; Blue: 18:00–20:00; Green: 20:00–22:00.

B3. Atmospheric stability

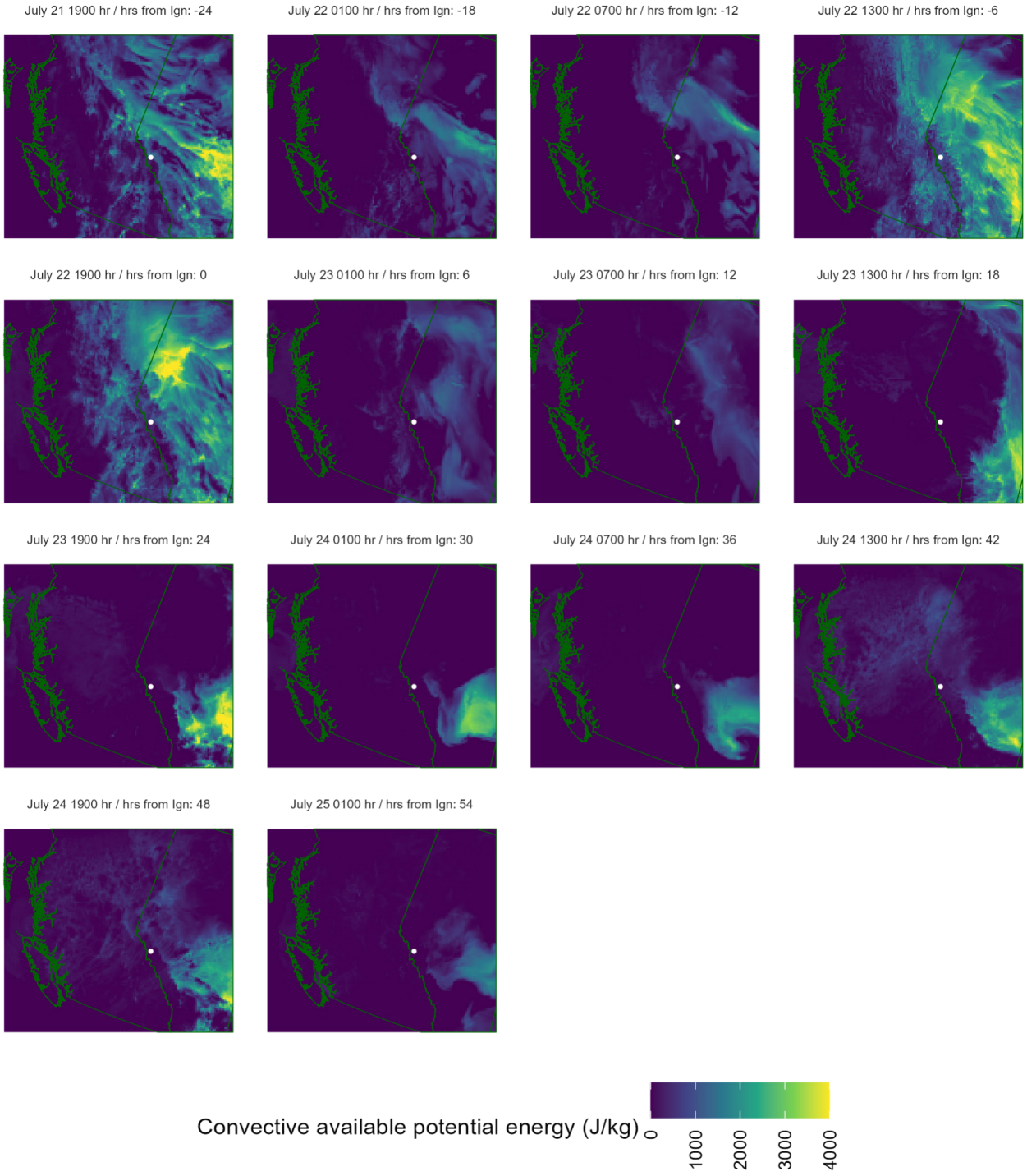

Figure S-6. Convective Available Potential Energy (CAPE) development across southern BC and Alberta. During the 12 h before and 54 h after ignition. Location of Jasper indicated by white point. Times are given in MDT.

B4. Modelled wind maps

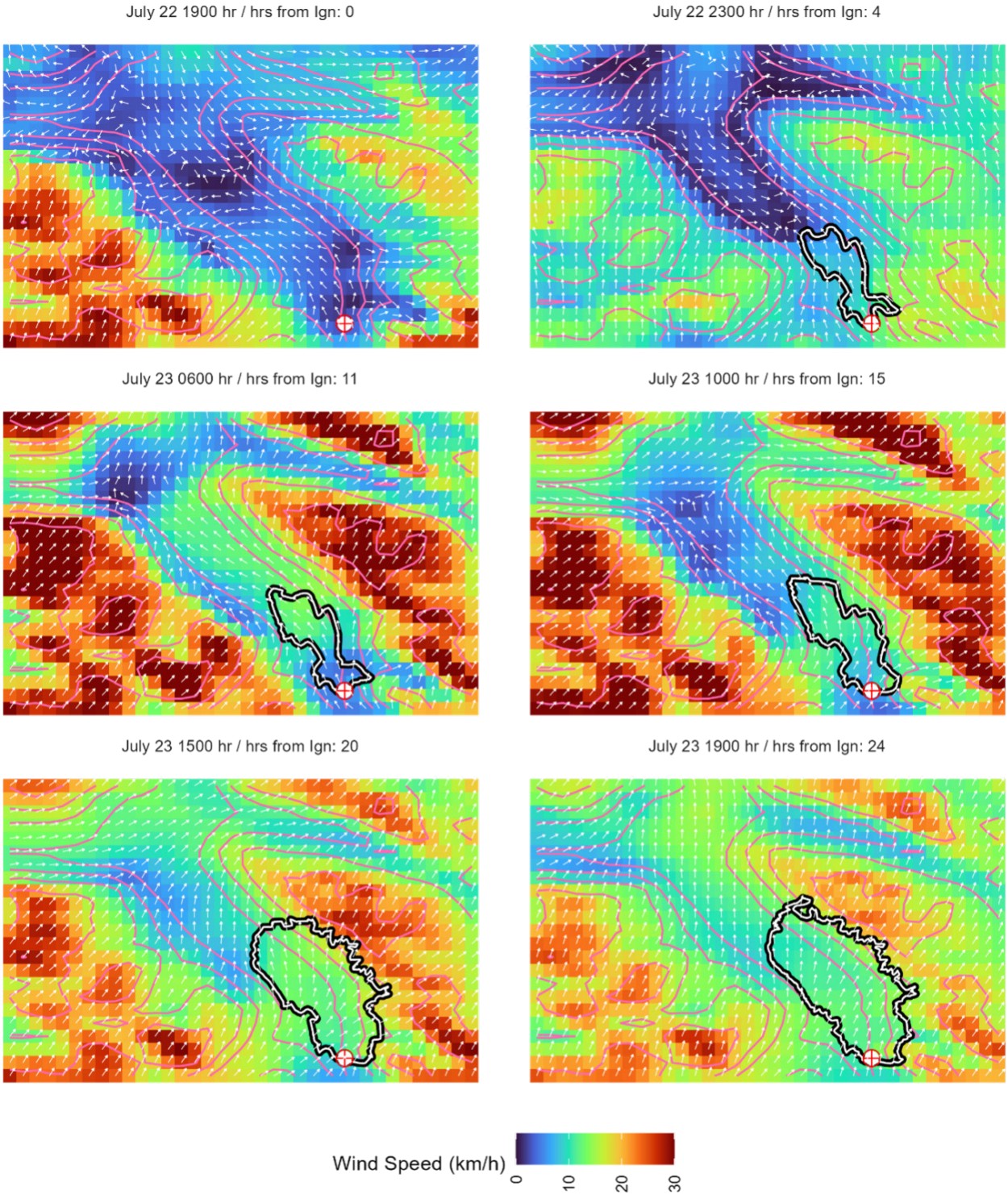

Figure S-7. Modelled HRDPS 10 m wind speed and direction for the region surrounding the fire. The wind vectors point in the direction of wind spread, which correspond to the main direction of fire spread. Elevational contour lines are provided as pink lines, the southern-most ignition point is shown as a red cross and the estimated fire progression is indicated by the white and black polygon. Times are given in MDT.

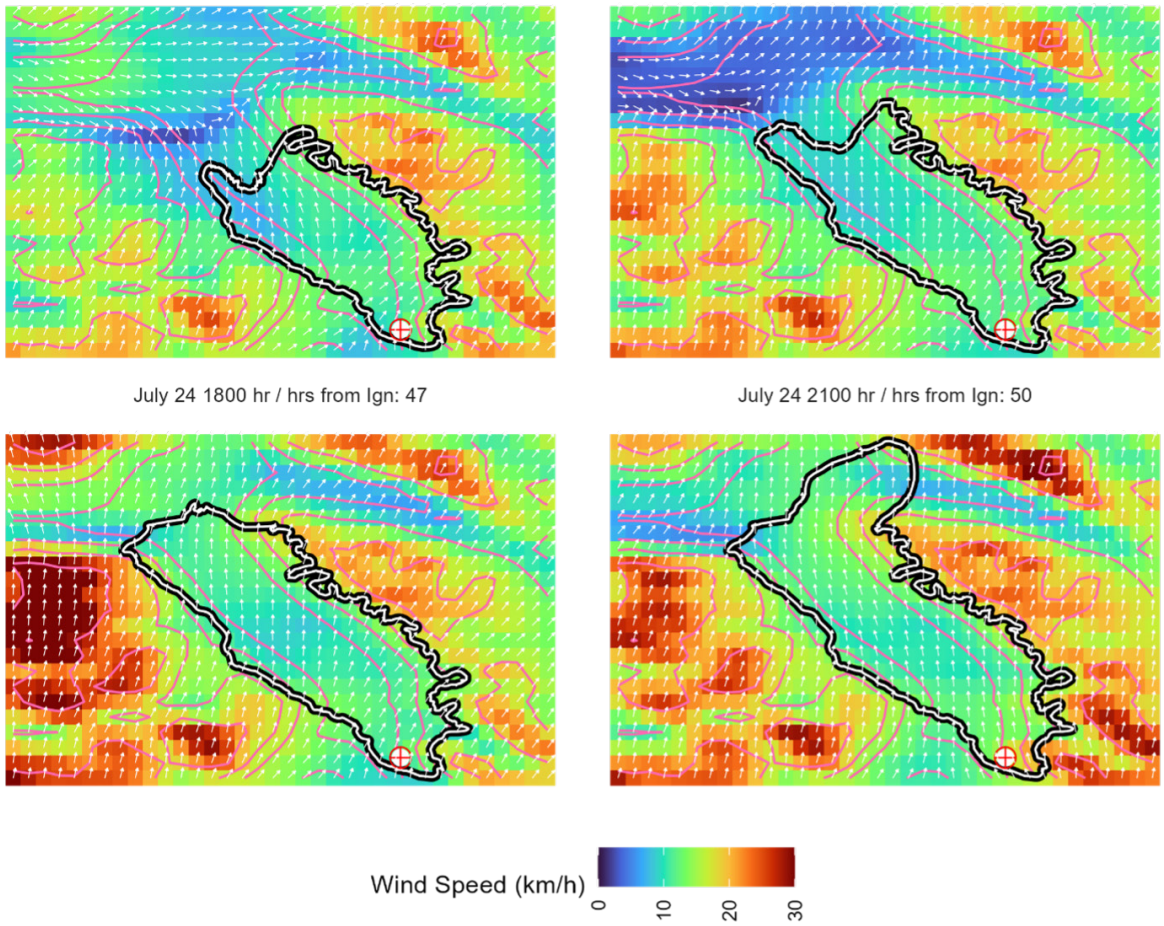

Figure S-7 (continued).

B5. Additional surface weather station observations

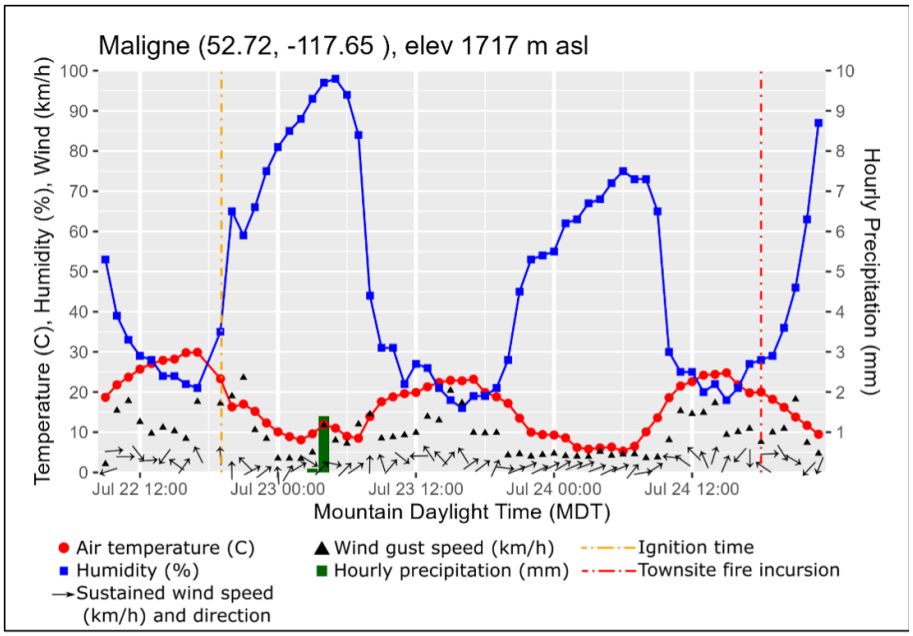

Figure S-8. Surface hourly weather observations at the Maligne weather station (**Figure 1**). The red and blue lines indicate temperature and relative humidity, respectively, while arrows show wind speed and direction. Triangles show max wind gust speed (based on 1 minute frequency observations). The dotted orange vertical line indicates the time of Ignition, while the dotted red vertical line shows the time of first structure ignition at the Jasper townsite.

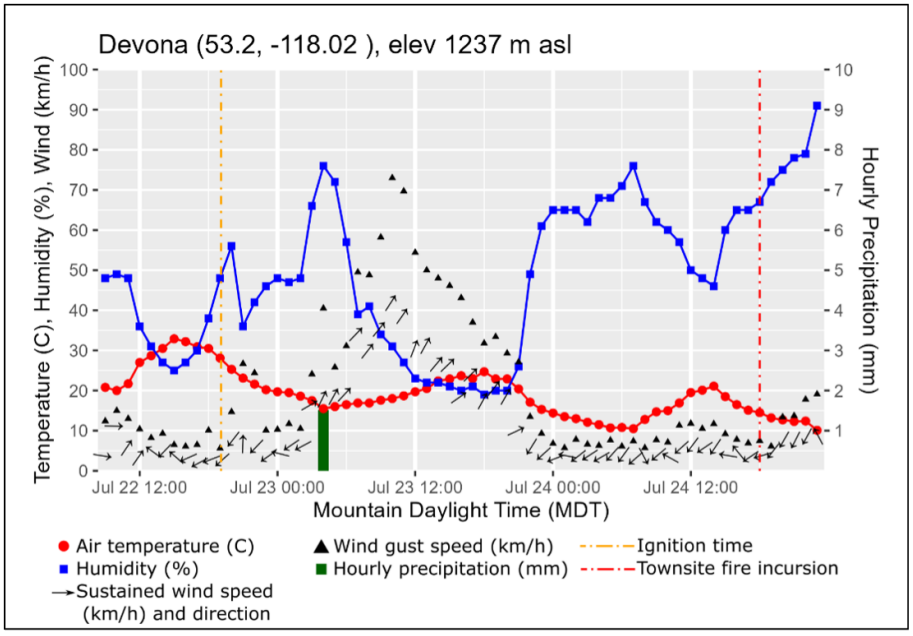

Figure S-9. Surface observations at the Devona weather station. See **Figure S-8** for symbol explanations.

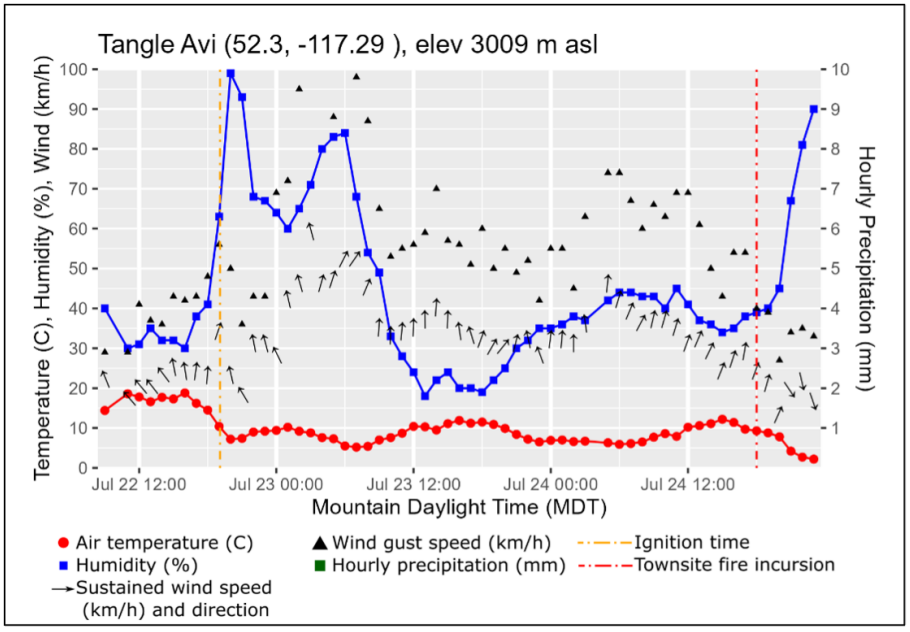

Figure S-10. Surface observations at the Tangle ridgetop avalanche weather station. See **Figure S-8** for symbol explanations.

B6. Satellite earth observation of the Jasper Complex Fire

Earth Observation (EO) satellites can provide an important data record of fire activity, and so called "hotspot" data products are widely used by fire management agencies as part of a suite of tools for fire monitoring and situational awareness. Hotspot products are a particularly valuable source of information when few resources are available for terrestrial or aerial monitoring, or during periods when dense smoke is grounding aerial reconnaissance assets.

Some of the most widely used hotspot products are generated from data collected by the Visible Infrared Imaging Radiometer Suite (VIIRS) instrument that is flown on the joint NOAA/NASA Suomi National Polar-orbiting Partnership (*SNPP*) satellite and NOAA's *NOAA-20*, *NOAA-21* satellites, and the Moderate Resolution Imaging Spectroradiometer (MODIS) instrument that is flown onboard NASA's *Aqua* and *Terra* satellites. These hotspot products are available online in near real time (within 3 h or less of satellite overpass) through web viewers [130] (e.g. NASA FIRMS) and application interfaces that allow data to be displayed within a user's information system.

In this appendix we reconstruct the EO data record provided by the VIIRS instruments by examining the Level-1B imagery and "fire mask" products from which the hotspot products are derived. Specifically, we use the Level-1B VJ103IMG (*NOAA-20*), VJ203IMG (*NOAA-21*), VNP03IMG (*SNPP*) Imagery Resolution Terrain-Corrected Geolocation 6-Min L1 Swath 375m products [131] and the VJ114IMG (*NOAA-20*), VJ214IMG (*NOAA-21*) and VNP14IMG (*SNPP*) Active Fires 6-Min L2 Swath 375m ("fire mask") products [132]. All data were downloaded from NASA's Earth data, and Level-1 and Atmosphere Archive & Distribution System Distributed Active Archive Center (LAADS DAAC), online portals.

Between the South Fire ignition (2024-07-22 19:05 MDT) and the evening of July 24 (2024-07-24 23:00 MDT), the Jasper area of interest was imaged 17 times by satellites carrying VIIRS (**Figure S-11**).

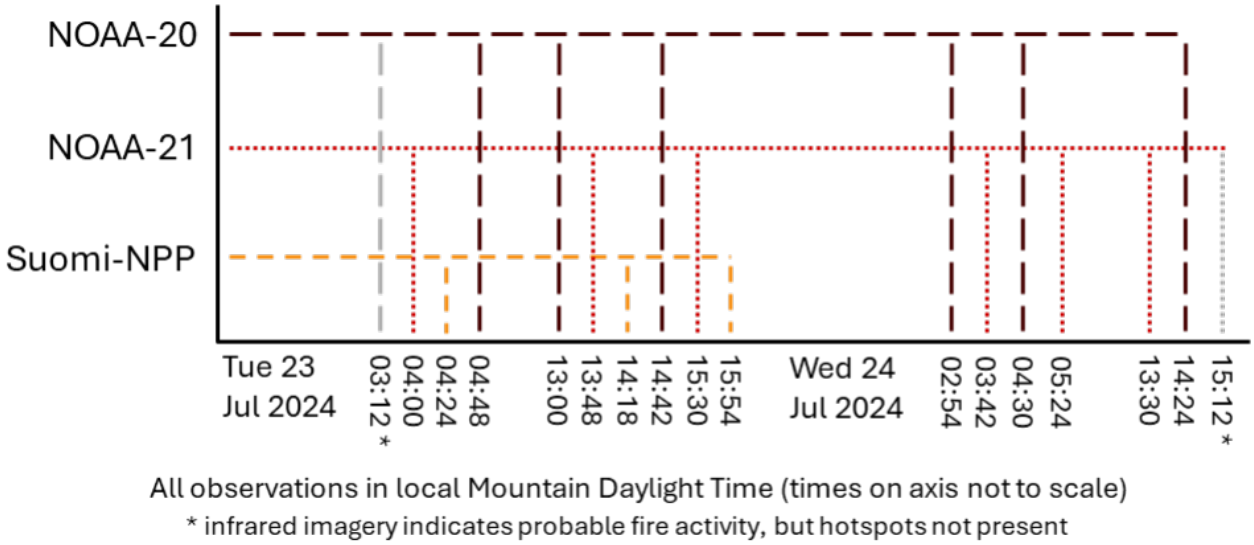

Figure S-11. A timeline of all available VIIRS overpasses of the Jasper Complex Wildfire, broken down by satellite. Images from *NOAA-20* are indicated by dark red long-dash vertical lines, *NOAA-21* images are indicated by red dotted vertical lines, Suomi-NPP images are indicated by orange dashed lines. Timestamps with asterisks (*) and corresponding grey vertical lines indicate satellite Images where no fire pixels ("hotspots") were detected by the VIIRS fire detection algorithm.

Fire masks generated from these satellite images (and from which the widely used hotspot products are derived) identified fire activity in 15 of 17 images. For each of these 15 images, we present three visualisations of the area of interest (**Figure S-12** to **Figure S-16**):

1. a false colour composite of red visible, near infrared, and shortwave infrared imagery (only shown for daytime scenes, due to the unavailability of the underlying data at night);
2. a reclassification of the fire mask data focusing on only the most pertinent elements of the scene (i.e. fire, cloud/smoke, other, no data); and
3. VIIRS I4 band (375m) midwave infrared (MWIR) imagery from the Level 1B product expressed as brightness temperatures in units of kelvin. Thermal features emit a strong signal in the MWIR rendering fires highly visible to the human eye in such imagery; MWIR data is also central to the fire detection[11] algorithm that is used to generate the fire masks. Generally, fire affected areas show up as much hotter than surrounding areas in the MWIR, however due to the VIIRS sensor design, very intense fire activity can show up as anomalously cold (208 K) in the I4 band. The VIIRS fire detection algorithm description document [142] provides more details of this MWIR I4 channel behaviour.

The first observation of the South and North Fires by VIIRS after ignition of the Jasper Complex Wildfire was made by *NOAA-20* at 03:12 MDT on July 23 (not shown). At this point in time no fire activity was detected but an elevated MWIR signal coincident with the North Fire is visible from manual data inspection.

The first VIIRS detected fire activity was of the South Fire at 04:00 MDT (*NOAA-21*, **Figure S-12A**); the North Fire was undetected at this point in time due to cloud obscuration. 24 min later (04:24 MDT) the North Fire was detected by *SNPP*-VIIRS, but the South Fire was undetected (**Figure S-12B**). While no cloud is apparent from the fire mask, the presence of relatively cool areas of the corresponding MWIR imagery over the location of the fire detection in the previous scene suggest that some cloud obscuration may have hindered detection here. At 04:48 MDT, substantial fire activity was detected by *NOAA-20* at both locations, most notably at the site of the South Fire, south of the Athabasca River (**Figure S-12C**).

The next series of VIIRS overpasses occurred in the afternoon of July 23; six images were collected in close succession between 13:00-15:54 MDT (**Figure S-13** and **Figure S-14**). By this point in time, the South Fire had grown considerably and was visibly spreading in a northeasterly direction to the north of the Athabasca River, though there is little visible fire growth during this 2-h time interval. Examination of the false colour composite imagery shows the presence of a thick condensing smoke plume spreading to the northeast due to strong upper southwesterly winds. While MWIR imagery allows fires to be detected through moderately thick smoke, this plume was likely of sufficient density as to be partially obscuring some of the fire activity occurring at the head of the fire from detection. As such, the head of the fire is likely further to the northeast at this point in time than the imagery and fire products here suggest.

By the early morning (02:54–05:24 MDT) of July 24, southeasterly growth of both the South and North Fires was apparent, with substantial fire activity occurring at the South Fire on the south side of the Athabasca River (**Figure S-15** and **Figure S-16A**). During this period, the VIIRS fire products generally capture the extent of the fire perimeter that is clearly visible in the MWIR imagery well.

By the early afternoon (13:30–14:24 MDT) VIIRS overpasses on July 24, no fire activity was detected at the location of the North Fire, and only a portion of the active fire perimeter for the South Fire was detected by the VIIRS fire products (**Figure S-16B** and **Figure S-16C**). This was likely due at least in part to the increasing smoke concentrations in the general area, and the arrival of a thick cloud bank to the northwest of the site (see **Figure S-17** for a broader view of the area and cloud bank shown in **Figure S-16C**). Despite the restricted ability of the VIIRS fire products to detect fire activity through thick smoke and cloud, examination of the MWIR imagery gives good situational awareness of the most active areas of the fire, even under cloud (e.g. MWIR image in **Figure S-13C**).

An additional image of the area was collected by *NOAA-21* VIIRS at 15:12 MDT (not shown here). While some elevated MWIR signals were observed coincident with the fires' locations, no fire detections were made by the VIIRS fire detection algorithm at this point in time, likely due to the presence of thick cloud.

[11] Note: Throughout this appendix we use the term "fire detection" in the sense that it is used within the fire earth observation community, where a pixel is algorithmically determined to be fire affected and a hotspot generated, rather than the more common usage of detection within the fire management community, where "detection" refers to the first confirmed report of a wildfire.

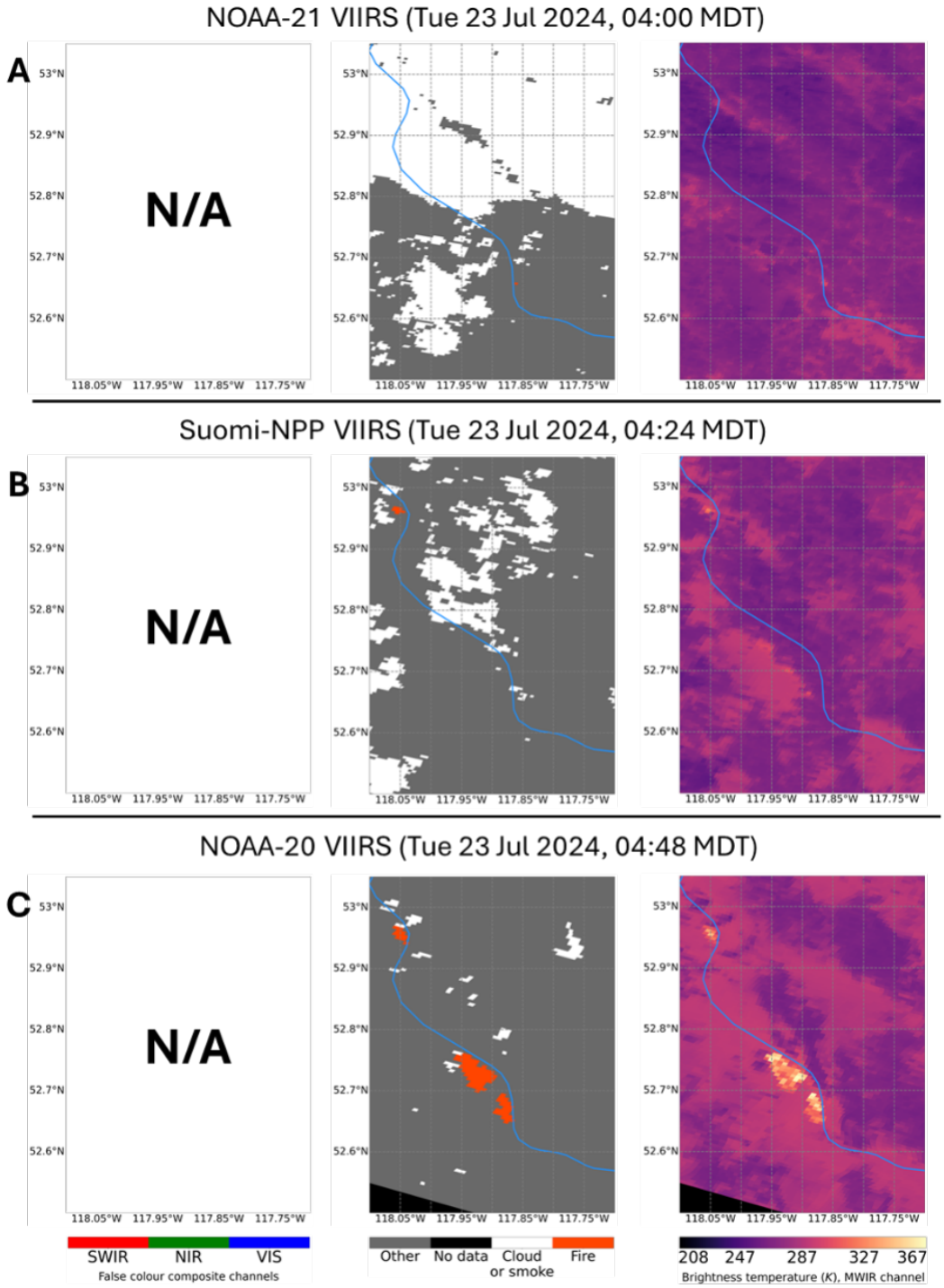

Figure S-12. VIIRS imagery and derived data for the Jasper Complex Wildfire. Each row shows data derived from a single satellite overpass as detailed in the corresponding subheadings. Left column: False colour composites of shortwave infrared (SWIR), near Infrared (NIR) and red wavelength visible (VIS) channel data. During the nighttime these data are not available (indicated by N/A. Middle column: A simplified reclassification of the VIIRS Active Fires 6-Min L2 Swath 375m ("fire mask") products, reclassified to emphasize areas of active fire (i.e. the locations where hotspots are reported) and cloud and/or smoke. Right column: VIIRS Level-1B I4 band (375m) midwave infrared (MWIR) data. In general, fire activity shows up in MWIR imagery as being hotter (yellows/oranges) than the surrounding areas (dark purple/pinks). However, due to the specific behaviour of the VIIRS sensor [132], very intense areas of fire activity can show up as being extremely cold (208 K). In all images the Athabasca River is shown as a blue line. Note: for ease of interpretation, all data are shown geographically projected into units of latitude/longitude. However, due to geographic overlap between some pixels in the VIIRS products, these renderings will not always represent the raw data products with full accuracy. If 100% accuracy is needed, the reader should refer to the raw data products.

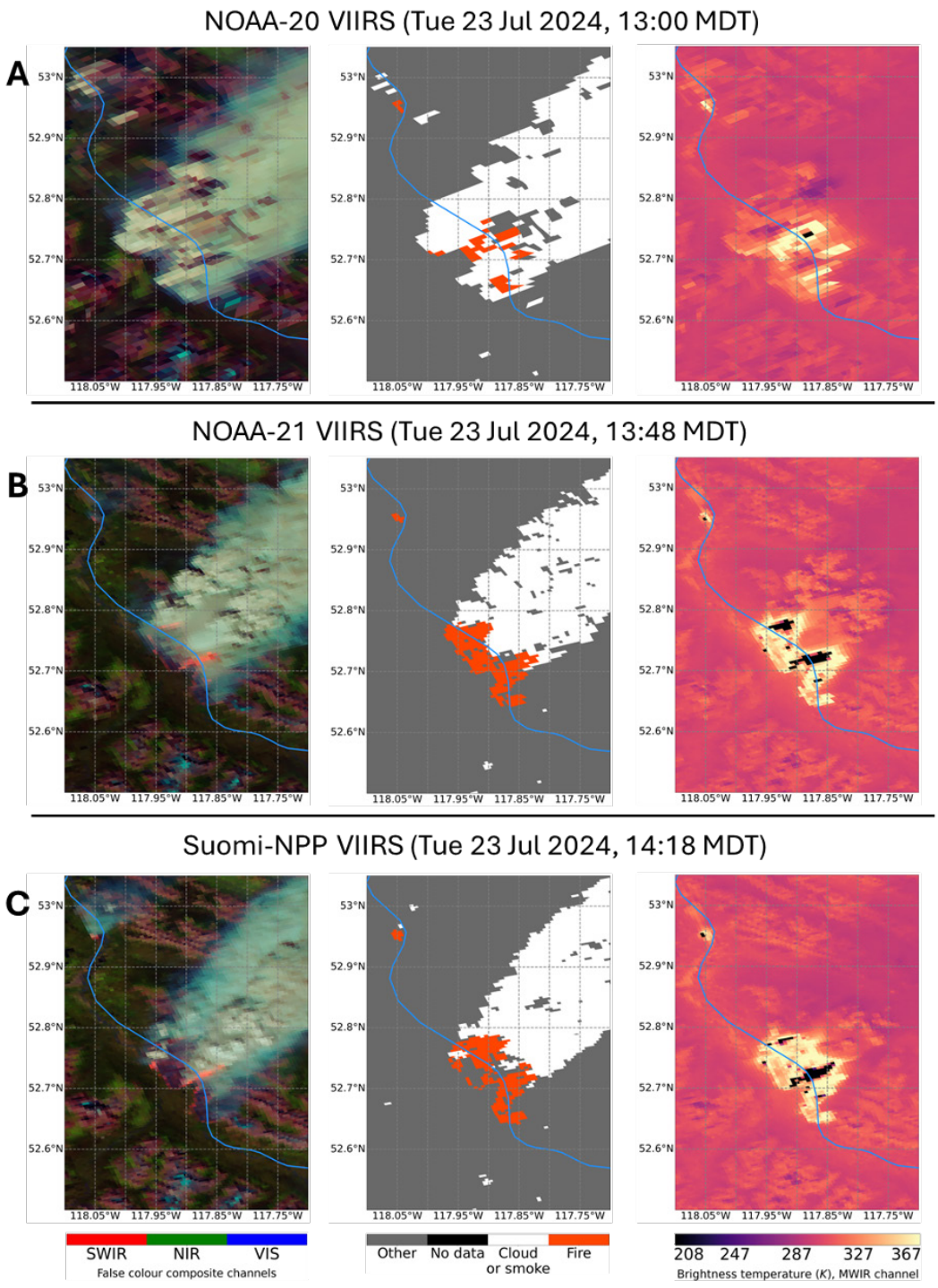

Figure S-13. VIIRS imagery and derived data for the Jasper Complex Wildfire (continued). See Figure S-12 for label details.

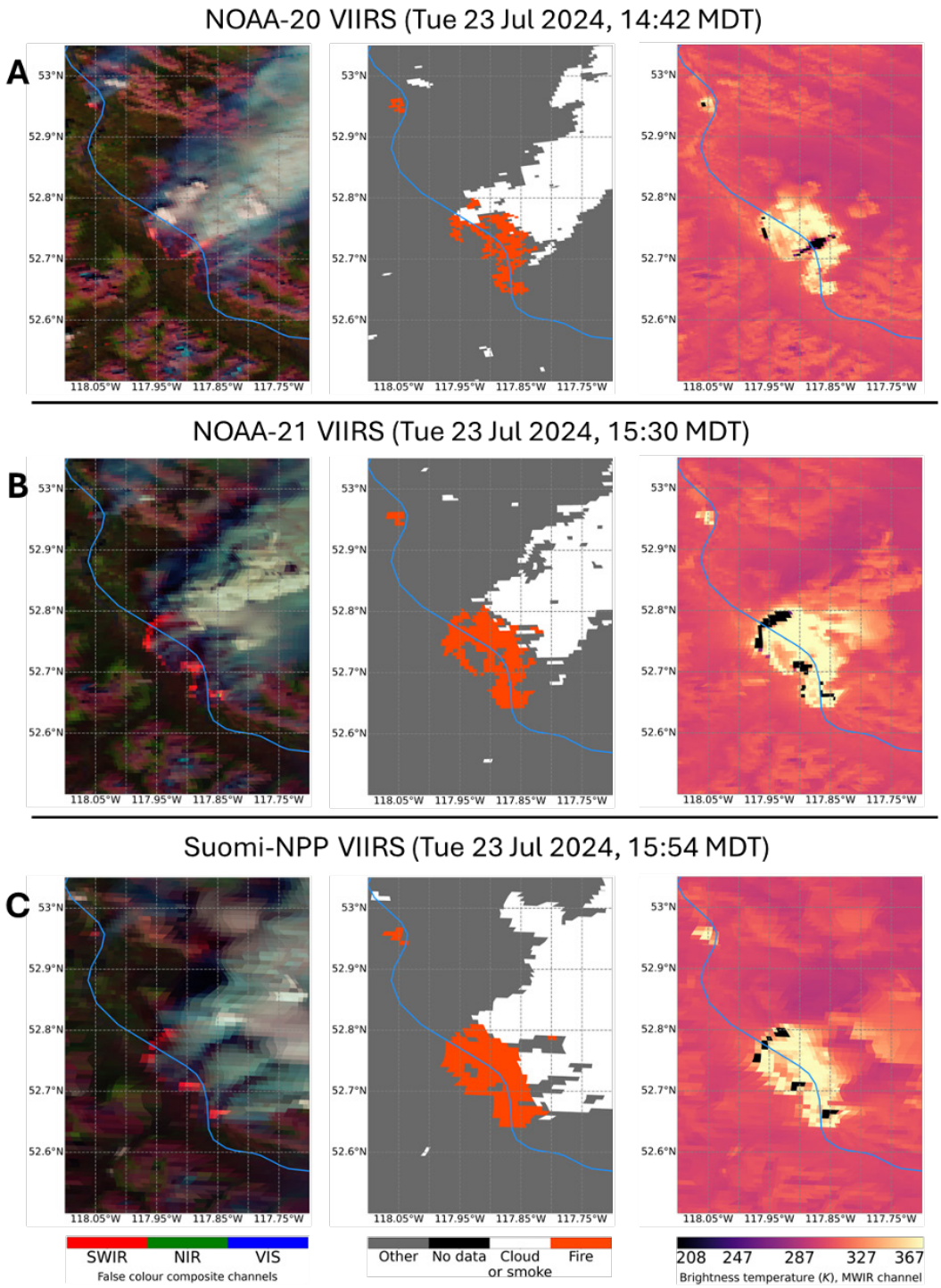

Figure S-14. VIIRS imagery and derived data for the Jasper Complex Wildfire (continued). See Figure S-12 for details.

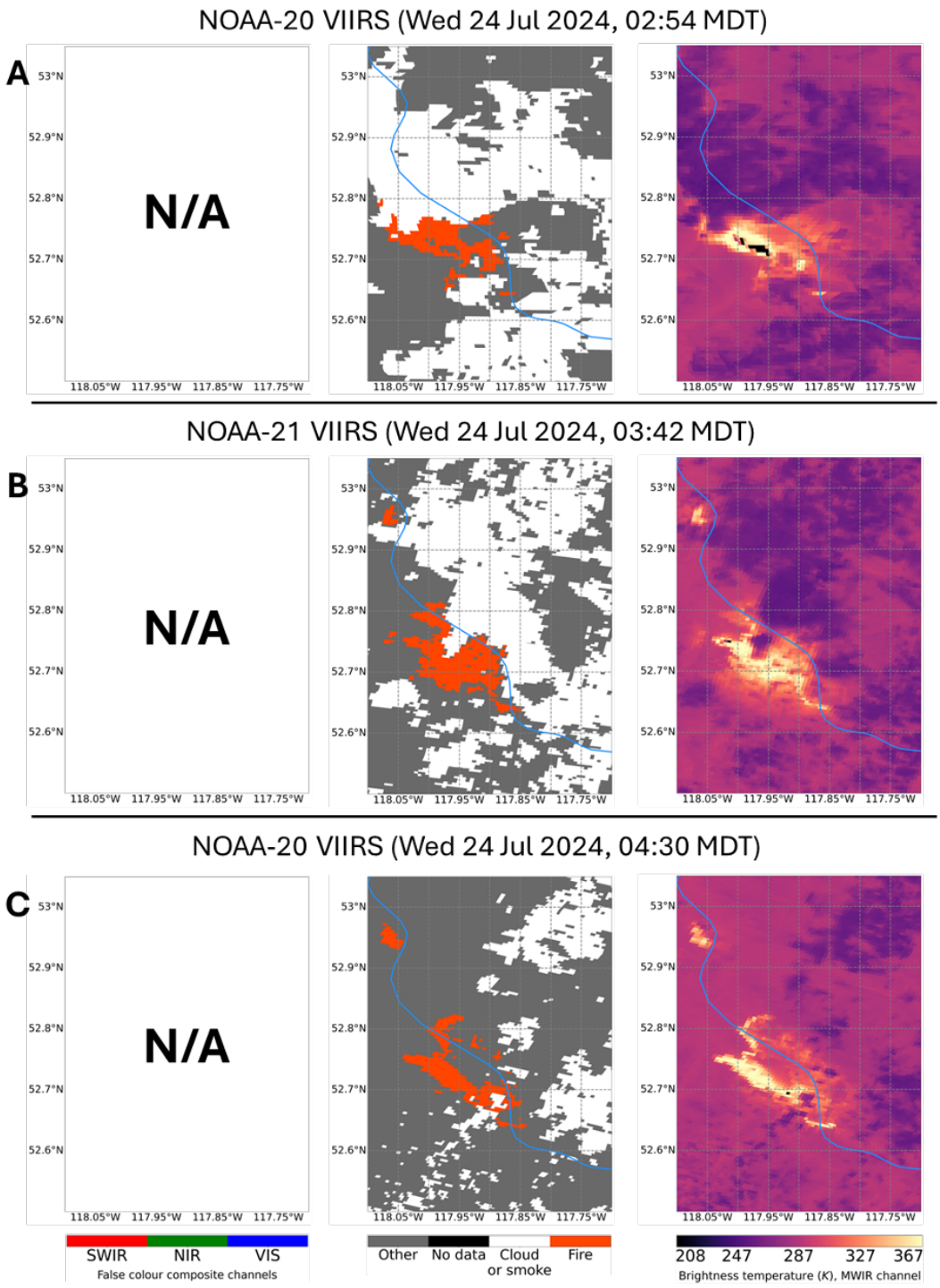

Figure S-15. VIIRS imagery and derived data for the Jasper Complex Wildfire (continued). See **Figure S-12** for details.

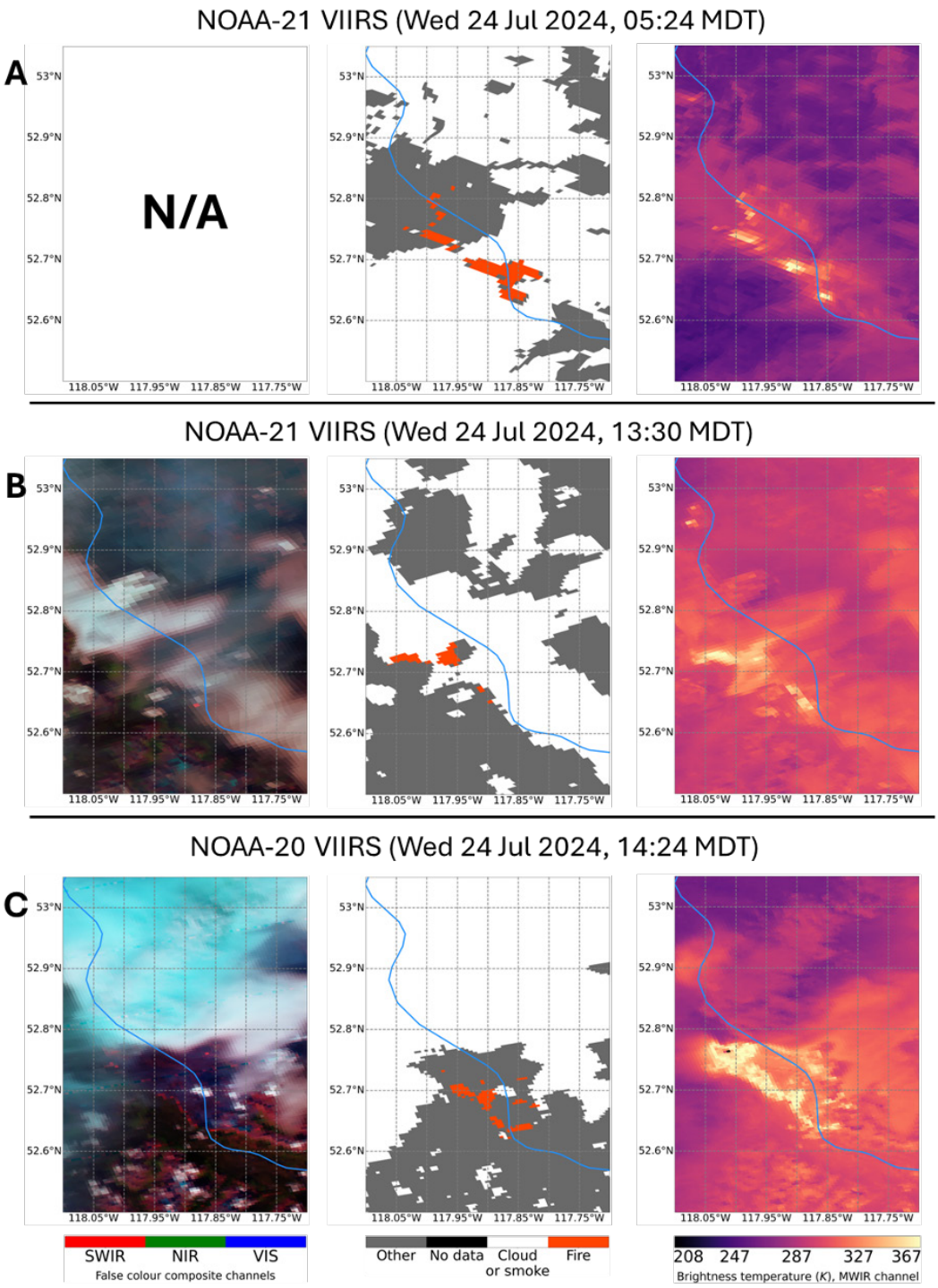

Figure S-16. VIIRS imagery and derived data for the Jasper Complex Wildfire (continued). See **Figure S-12** for details.

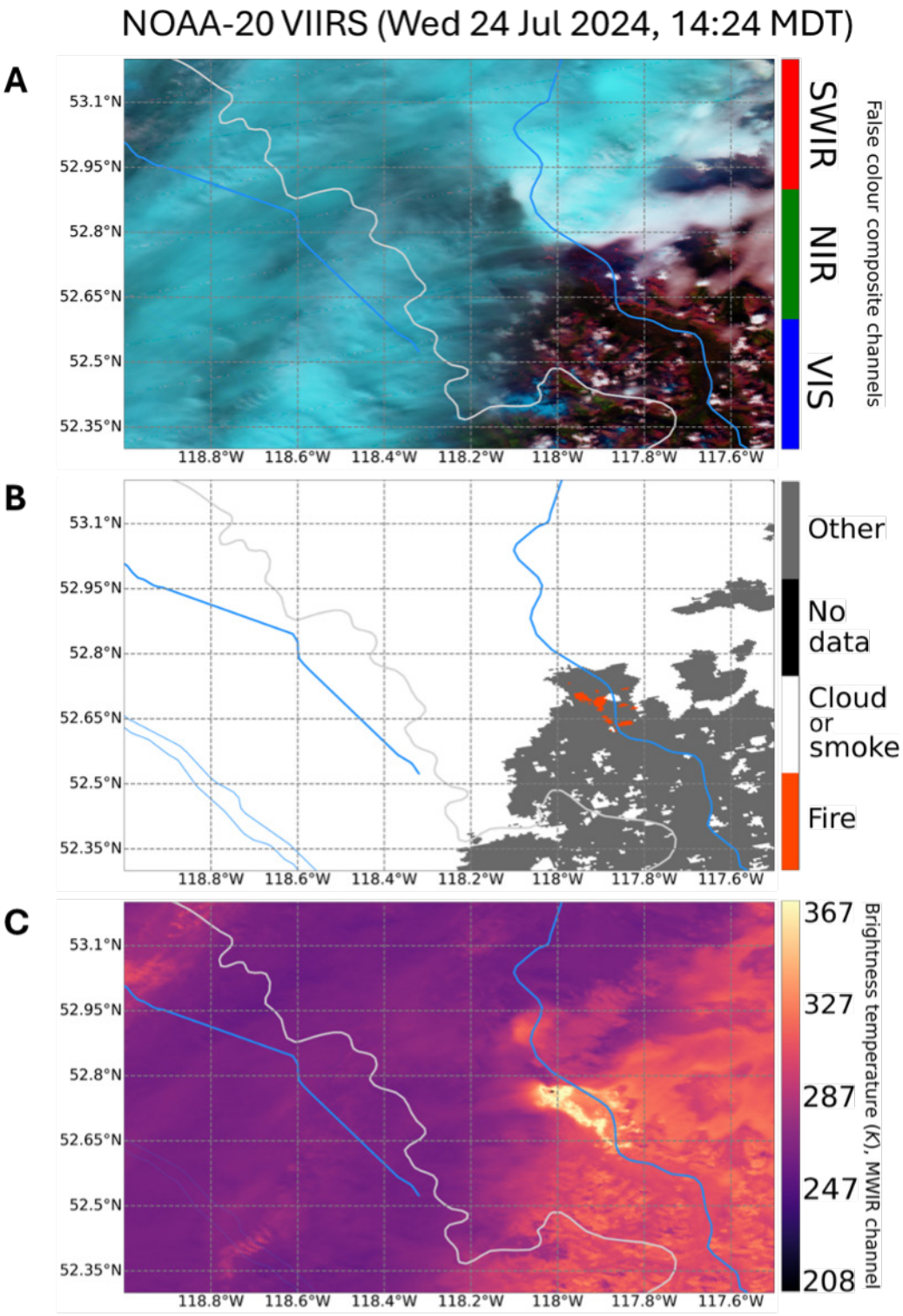

Figure S-17. A wide area view of the Jasper Complex Fire and the extensive cloud bank that moved into the area on the afternoon of July 24. This figure shows the same *NOAA-20* VIIRS overpass from 2024-07-24 14:24 MDT shown in **Figure S-16C**. The Athabasca and Fraser Rivers are shown as blue lines, and the Alberta-British Columbia border is indicated with a light grey line. See **Figure S-12** for additional details.

B7. Detailed ignition operations map

Figure S-18 shows the approximate location of aerial ignition by helicopter-mounted Plastic Sphere Device, conducted on the afternoon of July 24. Ignition lines were variously aimed at creating convection to draw fire uphill and away from the townsite and other values.

Ignition effects on fire behaviour and overall effectiveness of the ignition operations at meeting stated objectives cannot be determined at this time.

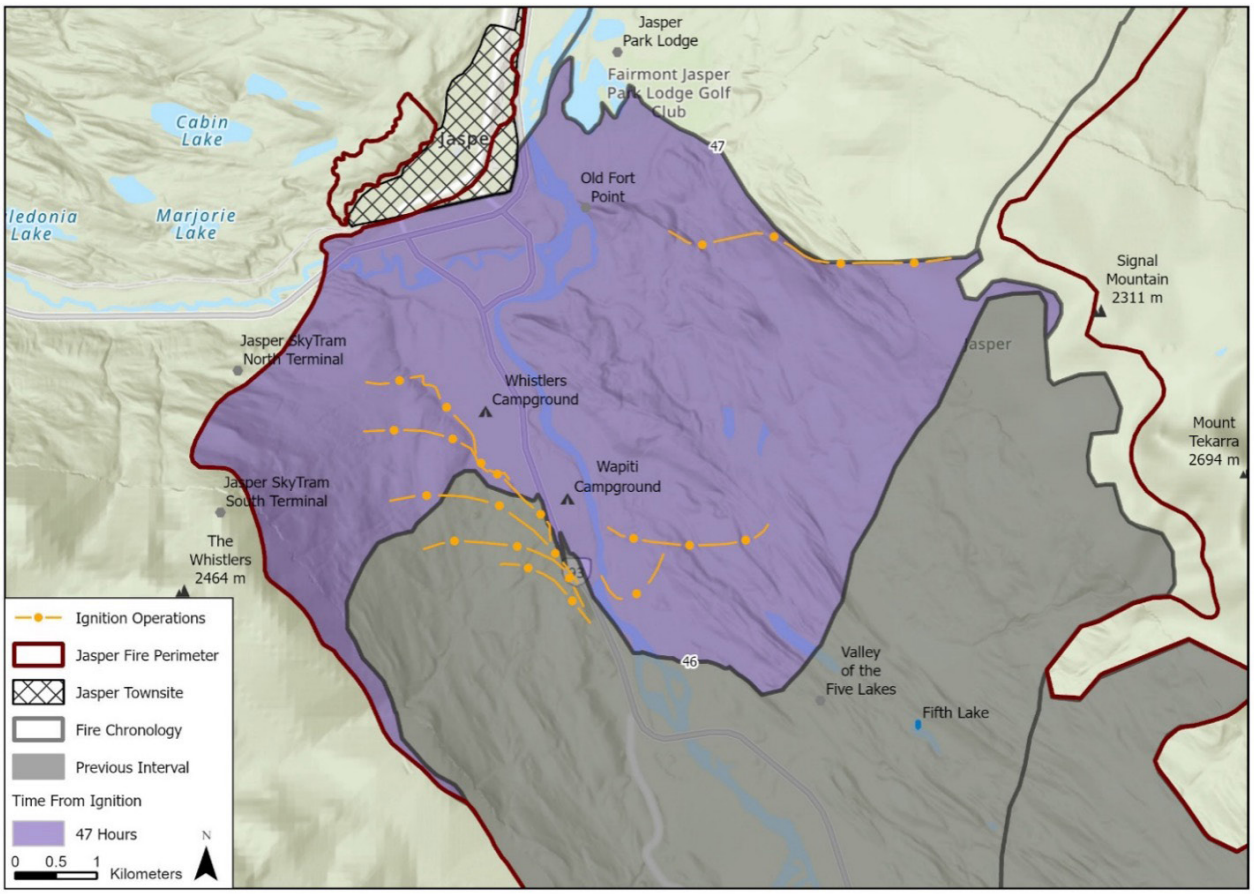

Figure S-18. Aerial ignition lines conducted on July 24, 16:42–17:15. Location of ignition lines is approximate, digitized from a hand-drawn map.

B8. Behaviour of previous wildfires in eastern cordillera

To further understand the novelty of the behaviour observed on the Jasper South Wildfire, nine other wildfires are presented for comparison. These fires occurred within the same geographical region (Rocky Mountains, eastern BC) and same ecozone (Montane Cordillera) and were the largest in the region since 2003. The location of these fires in relation to the Jasper wildfire can be observed in **Figure 19** below.

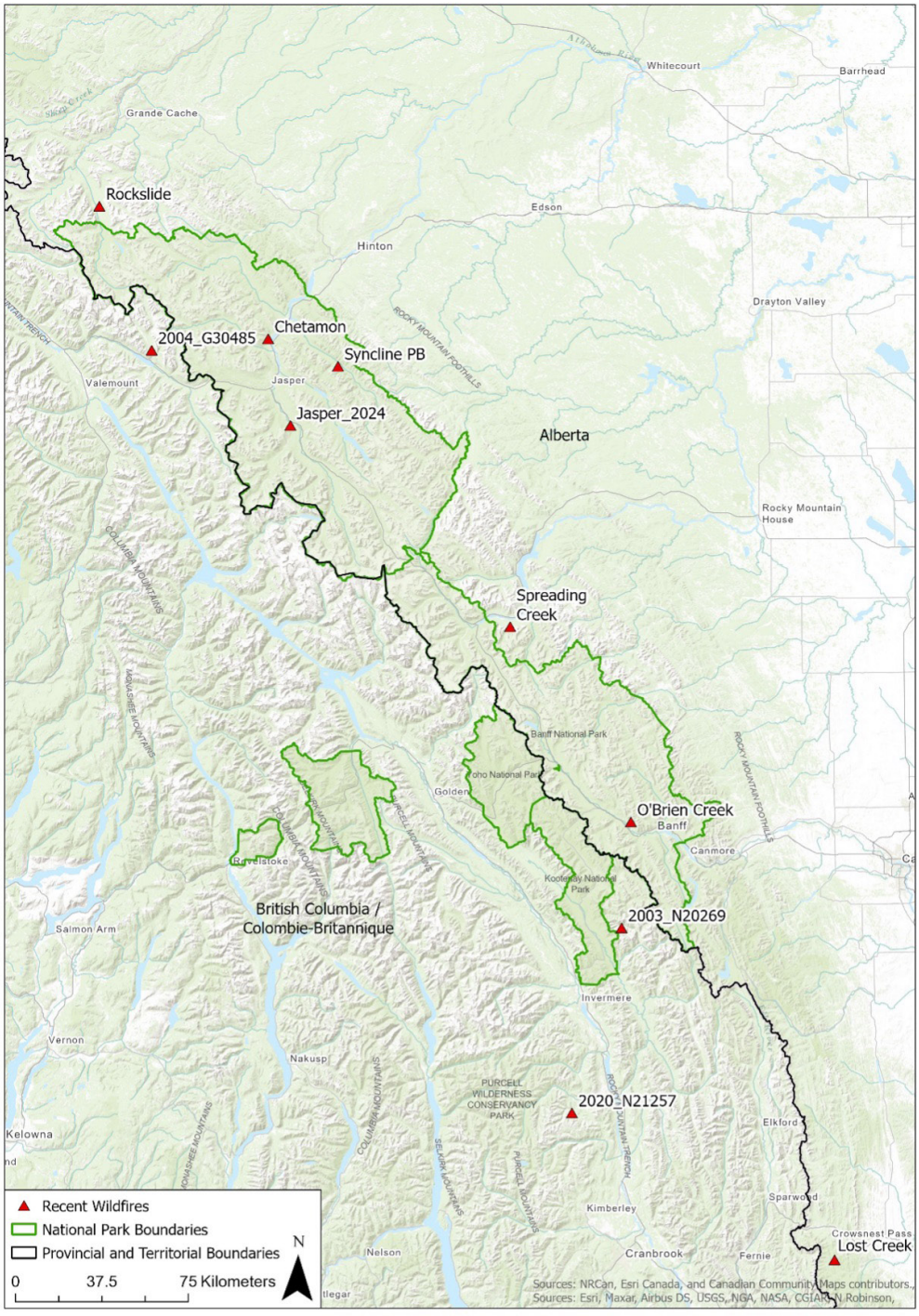

Figure S-19. Locations of other historical wildfires within the same geographical region (Rocky Mountains, eastern BC) and same ecozone (Montane Cordillera) as the 2024 Jasper Wildfire Complex.

The comparison focuses only the first three days of spread for each fire, as that period encompassed the vast majority of area burned and damage of the 2024 Jasper South fire. **Figure S-20** shows area burned for each fire, with the plot lines coloured in correspondence to the daily BUI of the region where/when these fires burned. In the figure, it is apparent that the Jasper wildfire grew much larger than the rest of the fires, where even in its first day of burning, grew to a size larger than seven of the other fires after two days.

Of these events, the most directly comparable to the 2024 Jasper fire is the 2022 Chetamon wildfire, which also burned within the Athabasca valley inside the National Park boundary. The Chetamon fire was also ignited by lightning and exhibited a period of rapid following ignition. It ignited during late summer during a period of lower fire danger, but grew to > 6,000 ha within the first week after ignition. It is apparent that these two wildfires occurred under similar weather (temperature and RH) conditions and fine fuel moisture content; however, the 2024 Jasper South fire burned during BUI conditions nearly twice as high as those of Chetamon, and perhaps as a result its size was much larger after 48 h. The occurrence of both of these fires highlights the region's susceptibility to large fires and the propensity for fires to spread rapidly along the major valleys during different periods of the fire season.

Compared to other fires in the region from the last 25 years, the Jasper wildfire spread faster on each of its three first growth days (including from ignition at 19:05 MDT on July 22 until the following morning at 06:00). Only the Lost Creek fire in southern Alberta near the Crowsnest Pass showed similar Buildup Index (BUI) values and ultimately grew to a similar size of 22,000 ha, but over the course of a much longer period.

Though lacking the topographic constraints of mountains as well as the pine-dominated forests, the 2024 Jasper Complex Wildfire showed initial growth more comparable to large fires in northern Alberta. The spring 2001 Chisholm fire south of Slave Lake Alberta was notable for its 35 km spread day on the seventh day of the fire under strong winds. But the first three days of growth on the Chisholm Fire totalled 11,000 ha and 20 km of total fire spread distance [133], which falls short of observed area and distance of fire growth in the Jasper South Fire. The notable 2016 Horse River Wildfire that impacted Fort McMurray reached 18,000 ha at the end of the third burning day, and similarly had the majority of the structure impacts occur on the third day of burning. On the fourth day of burning, strong winds at 30–50 km/h allowed for over 40 km of fire growth distance, accompanied by severe pyrocumulous activity [1]. There were no field observations of blowdown damage patterns similar to those observed in the Jasper Complex Wildfire.

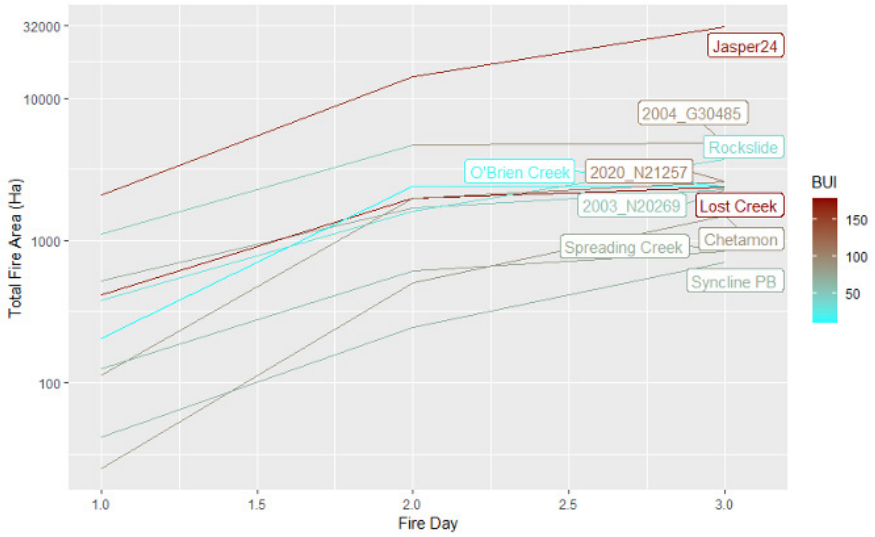

Figure S-20. Total area burned for the first three days of the 2024 Jasper Wildfire Complex and eight other regionally similar fires. Line colours represent best estimate of daily BUI for each fire day, where "fire day" is defined as starting at 06:00 local time, near maximum humidity and minimum fire activity conditions. The first "fire day" begins at the time of ignition and ends at 06:00 local time, no matter the hour of ignition. Note the logarithmic scale for area burned.

Beyond fires which occurred in the same region as the 2024 Jasper wildfire, the growth rate of the 2024 Jasper fire was compared to two notable recent fires in western Canada: the 2021 Lytton Creek and 2023 Hay River fires. These fires were compared not by looking at their growth during the initial three days, but instead in comparison to their three most active burn days.

Comparing the Jasper fire to the Lytton creek wildfire of 2021, the most active three sequential days of the Lytton fire were on the 22nd to 24th day of burning. In this burn window the Lytton fire grew 4,863 ha, 3,414 ha, and 5,349 ha growing from 17,000 ha to almost 31,000 ha. In comparison, the Jasper fire had grown to 31,000 ha within 48 h of ignition. Similar to the Jasper wildfire, the Lytton wildfire shared its rapid spread rate and growth immediately after ignition. During the first day of burning, the Lytton Creek wildfire grew to a size of roughly 4,000 ha, similar to the Jasper fire's growth during its initial burn day. Unlike the Lytton fire, the Jasper South fire near Athabasca Falls burning to 3,000 ha in the first day was the product of multiple ignitions that were approximately 6 km apart and merged within the first evening. However, the subsequent two days of the Lytton fire saw the fire increase by 1,500 ha, far less than what was observed during the Jasper wildfire.

During the Hay River wildfire of 2023, the largest sequential growth days occurred on August 13–16 where the fire saw growth days of 43,570 ha, 85,920 ha, 7,580 ha, and 59,716 ha. All but one of these growth days burned more than the final Jasper wildfire size. Some key differences exist however which must be addressed when comparing these fires. Key differences between these fires are the availability of fuels, and growth constriction due to Rocky Mountains, rivers, and road systems, as well as the fact that the Hay River fire experienced strong regional wind events which significantly aided in the fires growth, whereas the Jasper fire was more drought (BUI) driven with much lighter winds.

When examining the relative growth of the fires per day, meaning, given the fires size on a particular day, what percentage of that size was a result of the growth for that same day, the Jasper fire still grew at a faster rate even compared to these other large fires. However, as the burn window in question for the Jasper wildfire was early in the timeline of the burn, larger percentages are not as easier to acquire than once the fire has reached a large size, where even extreme growth days may not have a large percent influence. Given these results, the growth observed by the 2024 Jasper wildfire can be seen as being at the very limits of historical observed values, both regionally, and when compared to other large historical fires with large growth days.

Table S-3. Summary of weather, fuel indices, and fire growth for the 2024 Jasper wildfire and nine other regionally similar fires.

Name	Fire day	Temp (°C)	RH	WS	FFMC	DMC	DC	BUI	Total Area (ha)	Daily Growth (ha)	Final Size (ha)
Jasper 2024	1	31	22	6	95	135	520	164	2,100	2,100	32,722
	2	23	23	14	95	140	528	168	14,100	12,000	
	3	23.7	33	6	93	144	526	172	31,500	17,400	
Chetamon	1	26.4	24	9.9	93	54	494	85	25	25	6,450
	2	28.8	26	6.2	93	58	501	90	500	475	
	3	26.5	29	4.1	93	61	508	94	1,500	1,000	
2020_N21257	1	25.6	26	11	88	58	434	87	113	113	7,154
	2	25.3	24	13	94	70	479	102	1,982	1,869	
	3	23.5	36	7	92	73	504	110	2,582	712	
Rockslide	1	13.5	20	8	93	28	95	32	379	379	9,885
	2	12	20	8	93	32	99	36	1,613	1,234	
	3	13	20	8	93	38	123	43	3,713	2,478	
Spreading Creek	1	19.5	27	11	91	42	296	62	126	126	8,972
	2	17	46	10	90	53	362	78	612	486	
	3	15.5	43	9	89	52	341	75	835	349	
O'Brien Creek	1	7	27	13	91	10	14	10	204	204	2,381
	2	10	27	13	91	14	20	14	2,381	2,177	
	3	4	27	13	91	18	26	17	2,381	204	
2004_G30485	1	22	32	4	91	32	355	52	1,098	1,098	5,109
	2	23	27	5	93	67	413	93	4,694	3,596	
	3	24.5	57	12	89	71	425	99	4,795	1,198	
2003_N20269	1	25.7	26	6	83	49	334	72	518	518	2,702
	2	26	22	13	83	33	320	52	1,678	1,159	
	3	26	18	18	94	38	328	59	2,264	1,104	
Lost Creek	1	29.5	23	26	94	121	758	173	417	417	22,000
	2	29.5	40	20	92	125	766	177	1,969	1,551	
	3	27.5	46	15	90	127	773	180	2,339	787	
Syncline PB	1	24.5	14	22	94	54	192	64	42	42	19,806
	2	25.7	19	7	93	60	205	69	246	204	
	3	25	35	13	92	64	208	72	706	502	

B9. Firebrand production and transport characteristics

Firebrand deposition ahead of the main fire front is the primary cause of structure ignition in WUI fires. While coupled fire-atmospheric models like FIRETEC can simulate firebrand transport, critical data on firebrand quantity and size (e.g. mass, surface area, and volume) needed for these models remains lacking.

During an initial reconnaissance of fire impacts at the Fairmont Jasper Park Lodge (JPL), a large number of firebrands were observed on the golf course fairways and in sand traps, presenting a unique opportunity to sample wildfire-generated firebrands. Following further assessment, we focused on sampling firebrands in sand traps, where they were easily identifiable. All firebrand particles were collected from 30 sand traps across the course, and fire impact assessments were conducted in the forest stands upwind of the traps. The surface area of the sand traps and their distances from the forest edge were determined using high-resolution satellite imagery in ArcGIS Pro.

The collected firebrand samples were oven-dried and sorted into four main morphological types—spheroids (cones), cylinders (branches and twigs), plates (bark flakes), and pellets (charred wood fragments), and further subdivided into 2 cm diameter classes. Each sample was photographed, and image analysis was used to determine the number and surface area of the particles. A subset of up to 30 particles from each sample was measured for diameter and mass. At the time of writing, three-quarters of the samples have been processed. Some interim results are summarized below.

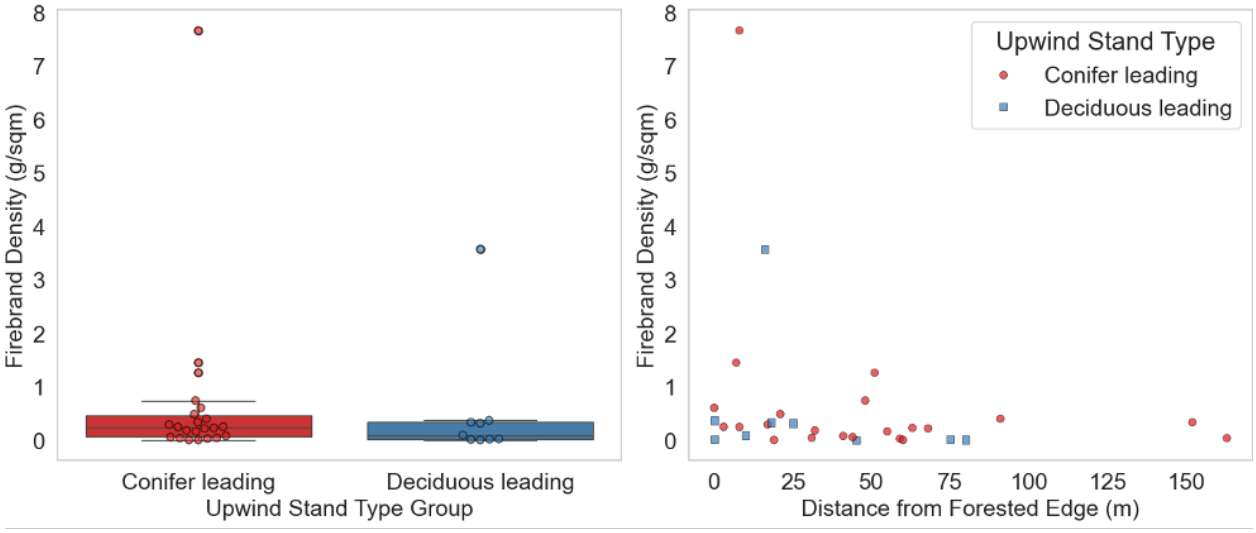

Figure S-21. Firebrand observations on the 2024 Jasper Wildfire Complex. Left, Firebrand density measured in grams per square meter as a function of stand type upwind of catchment area. This data is from a preliminary analysis of 3/4 of the sampled locations near Jasper Park Lodge. Conifer stands include Lodgepole pine, Spruce or Douglas-fir leading stands, while deciduous stands are Aspen-leading. Right, Density of material as a function of distance from forested edge. Bulk weight measurements of material include partially charred material.

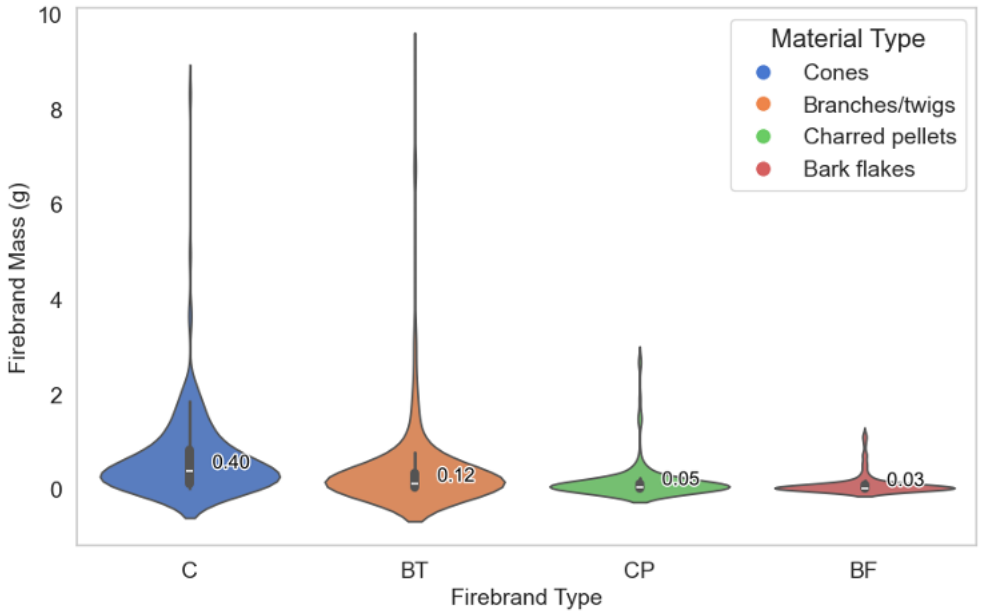

Figure S-22. Mass distribution by select firebrand types, including median values, sampled post-fire at Jasper Park Lodge. This data is from a preliminary analysis of 3/4 of the sampled locations. The top four most sampled firebrand types are cones (C), branches and twigs (BT), charred pellets (CP) and bark flakes (BF).

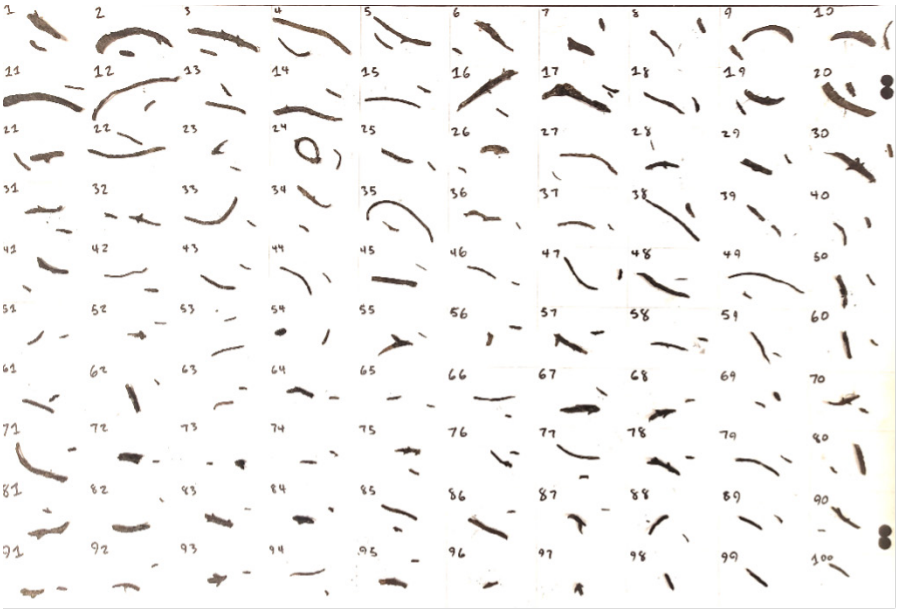

Figure S-23. Sample of branches and twigs from one ember site pre-processing and subsampling.

B10. Reconstruction of extreme winds within the fire convective column

To reconstruct the wind speeds produced during the rotating convective column observed on the afternoon of July 24, the minimum wind speed required to tip over two observed steel containers was calculated. These calculations for regularly sized rigid objects are meant to complement other damage observations in the vicinity such as widespread uprooted but otherwise unburned mature spruce trees at the Wabasso campground. The first object of interest is a recycling bin in the Wabasso Campground (**Figure S-24**) that was blown over by strong fire induced winds ahead of the fire front. The scorch pattern on the blue paint suggests the bin was first pushed over by winds ahead of the actual fire front, followed shortly after by a surface fire in the grass. If it is assumed the recycling bin is a simple box with enough force acting on the crosswind side to rotate the entire box about the bottom right edge point *P* (**Figure S-25**), we then know the torque generated by the wind must exceed the opposing torque generated by gravity in order for the box to tip over. Torque is calculated using the component of force perpendicular to the rotation point, and the distance of that force to the rotation point.

Figure S-24. Recycling box blown over ahead of the fire in Wabasso Campground

For example (**Figure S-25**), if it is assumed the force of the wind is evenly distributed along the entire left side of the box and the weight is equal throughout the box, the forces can be simplified to an average force passing through the centre of gravity (red centre point). Thus, the torque due to the wind and gravity (about point P) are simply $\tau_w = 0.5H\,F_w$ *and* $\tau_g = 0.5W\,F_g$, respectively, where *H* is the height of the box and *W* is the width.

$$F_w = C_D A \rho \frac{v^2}{2} \qquad \text{Equation 1}$$

$$F_g = mg \qquad \text{Equation 2}$$

$$C_D A \rho \frac{v^2}{2}\frac{H}{2} = mg\frac{W}{2} \qquad \text{Equation 3}$$

The force of the wind (F_w) and the force of gravity (F_g) can be approximated using Equations 1 and 2, where C_D is the drag coefficient for a box, *A* is the cross sectional area of the box exposed to the wind, ρ is the air density, *v* is the unknown windspeed, *m* is the mass of the box, and *g* is the gravitational constant. Therefore, returning to $\tau_w > \tau_g$ we can substitute Equations 1 and 2, and rearrange Equation 3 to solve for the velocity using estimates of the drag coefficient, box dimensions, air density, and mass of the box. Using values found in **Table 3**, we estimate the velocity of the wind required to tip over the box illustrated in **Figure S-25**, which applies to both the recycling container and the large shipping container that was pulled out of the Athabasca River.

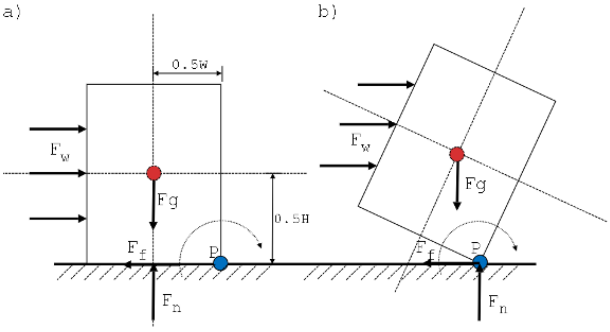

Figure S-25. Free body diagram of a box illustrating the forces, F, and rotational point, P. a) before tipping and b) during tipping. F_w, F_f, F_n, and F_g are the forces due to the wind, frictional force, normal force, and gravitational force, respectively. The frictional force opposes the wind force and is the sliding resistance along the ground. The normal force is the force of the ground opposing the force of the gravity from the mass of the box. Neither the normal force or the frictional forces are factored into the analysis here but are included for completeness.

Table S-4. Values used to compute the minimum velocity required to tip the shipping container and blue recycling box

Container	**Coefficient of drag,** C_D	**Area,** *A*	**Density,** ρ	**Height,** *H*	**Mass,** *m*	***Gravity,*** *g*	**Width,** *W*	**Minimum velocity,** *v*
Blue Box	≅1	1 m × 1.5 m	≅1 kg m^{-3}	1.5 m	200 kg	9.8 m s^{-2}	1.3 m	48 m s^{-1} (173 km h^{-1})
Shipping Container	≅1	6 m × 2.6 m	≅1 kg m^{-3}	2.6 m	3000 kg	9.8 m s^{-2}	2.4 m	59 m s^{-1} (212 km h^{-1})

There are several caveats to consider. First, the wind forces required to pick up and loft the shipping container are greater than the force described here and are beyond the scope of this simple analysis. Second, we assume the containers are both smooth and rectangular shaped and sitting flat on level ground. Third, the local gustiness, sustained winds, and the air temperature (which affects air density) are largely unknown at the time these containers were moved. As such, we make assumptions about the drag coefficient, ≅1, the air density ≅1 kg m^{-3}, and assume the calculated minimum windspeed must be sustained for at least several seconds to tip the containers over. And finally, the recycling container weight was not measured, but a calculation of mass (200 kg) was done using the measured thickness of steel (1/16 inch or 1.59 mm), the dimensions of the box (1.5 m × 1.0 m × 1.3 m) and the assumption that the interior frame was square steel tubing. The container was observed as being 25% full of mostly aluminum cans, so the weight of the beverage containers themselves is considered minimal.

B11. List of abbreviations

Abbreviation	Definition and comments
AB	Aberta (Canada)
AGL	Above Ground Level (elevation, m)
ASL	Above Sea Level (elevation, m)
BA	Basal Area (cross-sectional area of live trees, usually in m^2/ha)
BC	British Columbia (Canada)
BUI	Buildup Index (Fire Weather Index System; unitless)
CFC	Canopy (or crown) Fuel Consumption (kg/m^2)
CFB	Crown Fraction Burned (%)
CFFDRS	Canadian Forest Fire Danger Rating System
CFS	Canadian Forest Service (Department within Natural Resources Canada)
CLDN	Canadian Lightning Detection Network
DMC	Duff Moisture Code (Fire Weather Index System, unitless)
DRATT	Documentation, Reconstruction, and Analysis Task Team (corporate author of this report)
ECCC	Environment and Climate Change Canada
FBP	Canadian Fire Behavior Prediction (System)
FFMC	Fine Fuel Moisture Code (Fire Weather Index System, unitless)
FFFC	Forest Floor Fuel Consumption (kg/m^2)
FRI	Fire Return Interval, number of years
FWI	Fire Weather Index (unitless index or System); standard daily or hourly value
ha	Hectares
HFI	Head fire Intensity (measure of fire output power; kW/m)
HRDPS	High Resolution Deterministic Prediction System (weather model)
IC	Intensity Class
ISI	Initial Spread Index (Fire Weather Index System, unitless); standard daily or hourly value
JNP	Jasper National Park
JPL	Jasper Park Lodge
MDT	Mountain Daylight Time (time zone that contains Jasper National Park)
MODIS	Moderate resolution Imaging Spectroradiometer (satellite imaging sensor)
MPB	Mountain Pine Beetle
NOAA	National Oceanographic and Atmospheric Administration (USA)
RA	Rapid Assessment (plots used to estimate fire direction and crown involvement)
RH	Relative Humidity (weather)
ROS	Rate of Spread, m/min
S-B	Spruce-balsam forest (Engelmann spruce – subalpine fir; *Picea engelmanii* and *Abies lasiocarpa*)
TFC	Total Fuel Consumption (kg/m^2)
VIIRS	Visible Infrared Imaging Radiometer Suite (satellite imaging sensor)
VRI	Vegetation Resource Inventory (forest classification system)
WFC	Woody Fuel Consumption (kg/m^2)
WIPS	Wildfire Intelligence and Predictive Services (team within CFS)
WUI	Wildland-Urban Interface (region representing outskirts of a community, where residential structures and infrastructure meet wildland fuel complexes; also a type of fire occurring in these areas)


Valley of the
Five Lakes
Vallée des
Cinq Lacs